

STRESS AND IMMUNOTHERAPY IN OVARIAN CANCER

***Investigating the adrenergic immune regulation
affecting PD-(L)1 checkpoint inhibitors***

Marta Falcinelli

A thesis submitted in partial fulfilment of the
requirements of the University of Brighton for the
degree of Doctor of Philosophy

October 2019

Abstract

Although there have been major advances in cancer therapeutics, ovarian cancer remains the fifth deadliest malignancy among women. Patients with ovarian cancer experience increased levels of psychological stress with pre-clinical evidence suggesting that adrenergic stress influences tumour progression with an increased tumour burden, metastasis and angiogenesis. The immune regulation plays an important role in ovarian cancer. In the interface between cancer and immune cells, a crucial role has the interaction between the programmed cell death protein 1 (PD-1) on immune cells and the programmed cell death protein ligand (PD-L1) on cancer cells. This interaction creates an immunosuppressive microenvironment in which the tumour can escape the immune response. This research aims to explore the effects of adrenergic stress, mediated by Noradrenaline (NA), on the immune regulation of PD-L1 and how this influences the immunotherapy targeting the PD-(L)1 axis. PD-L1 expression was evaluated on ovarian cancer cell lines and on tissues derived from ovarian cancer patients. The adrenergic regulation was examined *in vitro* by treating either ovarian cancer or immune cells with NA and using Propranolol (PRO), a non-selective beta-blocker, to inhibit the adrenergic signalling. To investigate the molecular mechanism regulating the immune-cancer interactions, *in vitro* experiments included co-culture of immune and cancer cells in a 2D trans-well model and in a 3D spheroid model. A syngeneic mouse model of ovarian cancer was used to test a combined therapy of PRO and a PD-(L)1 inhibitor. C57BL/6 mice were injected with ovarian cancer cells and underwent chronic restraint stress. Tumour burden, metastatic nodules, and the immune signature were evaluated.

Adrenergic stress was shown to have a role in the regulation of the immune response to cancer. In particular, the adrenergic stress blockade with PRO reduced the levels of IFN- γ , a pro-inflammatory cytokine which upregulates PD-L1 expression on ovarian cancer cells. In the 3D spheroid model of ovarian cancer, PRO increased the immune infiltration into the tumour mass. The syngeneic *in vivo* mouse model showed that a combined therapy of PRO and PD-(L)1 inhibitor decreased tumour burden, metastatic nodules and increased the anti-tumour immune signature.

In summary, this study demonstrates that the adrenergic stress has a negative impact on ovarian cancer and this is mediated – among other processes - by the regulation of the immune response. Furthermore, a combined therapy of PRO and PD-(L)1 inhibitor could represent a potential therapeutic strategy for ovarian cancer patients.

Abstract	I
List of figures	VII
List of tables	IX
List of the main abbreviations	X
Acknowledgments	XII
Chapter overview	XIV
1. Chapter 1 – Introduction	1
1.1 Ovarian cancer	2
1.1.1 Epidemiology.....	2
1.1.2 Treatments	2
1.1.3 Ovarian cancer classification	2
1.2 Psychological stress	6
1.2.1 Introduction to psychological stress.....	6
1.2.2 Adrenergic stress	6
1.2.3 Stress and cancer.....	8
1.2.4 Adrenergic stress and ovarian cancer	10
1.2.5 Beta-blockers as potential anticancer agents	11
1.2.6 Adrenergic stress effect on immune metabolism	12
1.3 The immune system	13
1.3.1 Introduction to the immune system	13
1.3.2 The innate immune response.....	14
1.3.3 The adaptive immune response	15
1.3.4 T cell biology and activation process.....	16
1.3.5 Immune response to cancer.....	18
1.3.6 The role of PD-(L)1 axis in physiology and cancer	20
1.3.7 Programmed cell Death Ligand 1 (PD-L1) expression in cancer	21
1.3.8 IFN- γ and PD-L1 expression.....	22
1.3.9 Cancer immunotherapy: PD-1 and PD-L1 immune checkpoint inhibitors.....	23
1.3.10 PD-(L)1 blockade in ovarian cancer	24
1.3.11 Cancer immunogram	25
1.4 3D tumour spheroid model	28
1.4.1 Advantages of 3D tumour spheroids.....	28
1.4.2 Techniques to generate spheroids	29
1.4.3 A 3D spheroid model of ovarian cancer and multicellular spheroids	30
1.4.4 Response to hypoxia in 3D spheroids.....	30
1.4.5 Metabolic competition in the tumour microenvironment.....	31
1.5 Hypothesis	32
1.6 Aims of the thesis	32

1.7	Original contribution to knowledge	- 32 -
2.	Chapter 2 - Materials and methods	- 34 -
2.1	In vitro models	- 35 -
2.1.1	Ovarian cancer cell culture	- 35 -
2.1.2	Hormones treatments	- 35 -
2.1.3	Cytokine treatments	- 36 -
2.1.4	Splenocytes culture	- 36 -
2.1.5	Splenocytes activation <i>ex vivo</i>	- 36 -
2.1.6	Trans-well co-culture: cancer cells and splenocytes	- 37 -
2.1.7	3D spheroids model	- 38 -
2.1.8	3D spheroid co-culture: cancer cells and splenocytes	- 38 -
2.1.9	3D spheroid imaging	- 38 -
2.1.10	3D spheroid imaging: acquisition of data	- 39 -
2.1.11	3D spheroid imaging: analysis	- 39 -
2.2	Orthotopic <i>in vivo</i> model of ovarian cancer	- 41 -
2.2.1	Syngeneic mouse model of ovarian cancer	- 41 -
2.2.2	Osmotic pump implantation for Propranolol release	- 42 -
2.2.3	PD-(L)1 inhibitor treatment	- 43 -
2.2.4	Restraint stress procedure	- 43 -
2.3	Human samples collection	- 45 -
2.3.1	Immunohistochemistry	- 45 -
2.3.2	Analysis	- 45 -
2.4	Gene expression analysis	- 47 -
2.4.1	Principles	- 47 -
2.4.2	RNA extraction from cells	- 47 -
2.4.3	RNA extraction from mouse tissues	- 47 -
2.4.4	cDNA synthesis	- 47 -
2.4.5	Real Time PCR	- 48 -
2.4.6	Data analysis	- 48 -
2.5	siRNA transfection	- 49 -
2.5.1	Principles	- 49 -
2.5.2	Protocol	- 49 -
2.5.3	Immunofluorescence (IF) on transfected cancer cells	- 49 -
2.6	Flow cytometry	- 50 -
2.6.1	General principles	- 50 -
2.6.2	Fluorescence principles	- 50 -
2.6.3	Cell staining	- 50 -
2.6.4	Compensation	- 51 -

2.6.5	Analysis with FlowJo.....	- 51 -
2.7	Enzyme-Linked Immunosorbent Assay (ELISA)	- 52 -
2.7.1	Principles	- 52 -
2.7.2	Protocol	- 52 -
2.8	Mass Spectrometry.....	- 53 -
2.8.1	Principles	- 53 -
2.8.2	Extraction of proteins.....	- 53 -
2.8.3	SDS-PAGE principles	- 53 -
2.8.4	SDS-PAGE Protocol	- 53 -
2.8.5	Peptide preparation: destain, reduction-alkylation, digestion and extraction of peptides - 54 -	
2.8.6	Acquisition of data	- 54 -
2.8.7	Mass spectrometry data analysis	- 54 -
2.9	Data Analysis.....	- 56 -
3.	Chapter 3 - Adrenergic blockade with Propranolol downregulates IFN-γ production by immune cells and PD-L1 expression on cancer cells	- 57 -
3.1	Introduction	- 58 -
3.1.1	Molecular effects of adrenergic stress on the immune response to cancer	- 58 -
3.2	Aims	- 59 -
3.3	Results.....	- 60 -
3.3.1	PD-L1 is expressed in tissues derived from ovarian cancer patients.....	- 60 -
3.3.2	PD-L1 was expressed in ovarian cancer cell lines treated with IFN- γ alone or in combination with NA or PRO plus NA	- 63 -
3.3.3	Immune cells activated <i>ex vivo</i> produced IFN- γ	- 65 -
3.3.4	PD-L1 is expressed on ID8 cells after treatment with IFN- γ at different concentrations.. 67 -	
3.3.5	NA and PRO modulate IFN- γ production in immune cells.....	- 69 -
3.3.6	PMA and Ionomycin affect PD-L1 expression: optimization of the co-culture experiment	- 71 -
3.3.7	PD-L1 expression in ovarian cancer cells is modulated by the presence of activated immune cells treated with NA and PRO plus NA.....	- 73 -
3.3.8	Immune cells co-cultured with ovarian cancer cells increase IL-10 levels	- 75 -
3.3.9	IFNR1 was transiently silenced in ID8 cells but not in ID8 in co-cultured with immune cells activated <i>ex vivo</i>	- 77 -
3.4	Discussion.....	- 79 -
4.	Chapter 4 – Development of a 3D spheroid model of ovarian cancer to define NA, PRO, and stress-induced immune-tumour interactions	- 83 -
4.1	Introduction	- 84 -

4.1.1	Adrenergic stress and immune-tumour interaction.....	- 84 -
4.2	Aims	- 85 -
4.3	Results.....	- 86 -
4.3.1	The immune cell infiltration in a 3D model of ovarian cancer is affected by immune cells activation, treatment and time in co-culture	- 86 -
4.3.2	Adrenergic stress does not influence structural parameters of a 3D spheroids of ovarian cancer	- 88 -
4.3.3	NA and PRO affect the proteomic profile of 3D spheroids of ovarian cancer.....	- 90 -
4.3.4	Stress influences the metabolic program in multicellular ovarian cancer spheroids..	- 96 -
4.3.5	The proteomic profile of multicellular immune/cancer spheroids converted into human homologous match pathways involved in metabolism	- 99 -
4.4	Discussion.....	- 101 -
5.	Chapter 5 – Combined therapy with propranolol and PD-(L)1 inhibitor decreases tumour burden, metastasis, and promotes an anti-tumour immune signature in ovarian cancer.....	- 108 -
5.1	Introduction	- 109 -
5.1.1	Cancer immune signature	- 109 -
5.1.2	Adrenergic stress and Beta-blockers effects on the immune response to cancer ...	- 109 -
5.2	Aims	- 112 -
5.3	Results.....	- 113 -
5.3.1	Combined therapy with PRO and PD-(L)1 inhibitor reduces tumour burden and metastatic nodules	- 113 -
5.3.2	Combined therapy with PRO and PD-(L)1 inhibitor affects CD8+ cell population in the spleen of ovarian cancer bearing mice	- 115 -
5.3.3	Restraint stress upregulates <i>CD3</i> and <i>CD4</i> expression, but not <i>CD8</i> in mouse tumour tissues	- 117 -
5.3.4	Combined therapy with PRO and PD-(L)1 inhibitor upregulates the expression of <i>CD8</i> in mouse tumour tissues	- 119 -
5.3.5	Therapy with PRO and/or PD-(L)1 inhibitor affects <i>VEGF</i> expression in mouse tumour tissues	- 121 -
5.3.6	Combined therapy with PRO and PD-(L)1 inhibitor affects <i>Granzyme B</i> expression in mouse tumour tissues	- 123 -
5.3.7	Therapy with PRO affects <i>CXCL10</i> expression in mouse tumour tissues	- 125 -
5.3.8	Therapy with PRO affects <i>IDO1</i> expression in mouse tumour tissues	- 127 -
5.3.9	Therapy with PRO and/or PD-(L)1 inhibitor affects <i>PD-L1</i> expression in mouse tumour tissues	- 129 -
5.3.10	PD-L1 and IFN- γ protein expression are not informative in the evaluation of the ovarian cancer immune signature.....	- 131 -
5.4	Discussion.....	- 133 -

6.	Chapter 6 - General Discussion and conclusions	- 137 -
6.1	Conclusions	- 138 -
6.2	Limitations of the study	- 141 -
6.2.1	Limitations of the cell culture model.....	- 141 -
6.2.2	Limitation of the 3D spheroid model	- 142 -
6.2.3	Limitations of the in vivo model	- 143 -
6.3	Future perspectives	- 145 -
6.4	Novel contribution to knowledge	- 147 -

List of figures

Figure 1 Histopathological classification of ovarian cancers	5 -
Figure 2 Beta-adrenergic signalling pathway.....	8 -
Figure 3 Antigen presentation	16 -
Figure 4 PD-1 and PD-L1 interaction and checkpoint inhibitors.....	21 -
Figure 5 T-cell activation signalling pathway.....	37 -
Figure 6 General schematic timeline for the in vivo procedures.....	44 -
Figure 7 PD-L1 expression in tissues from patients with ovarian cancer	62 -
Figure 8 PD-L1 is expressed in ovarian cancer cells treated with IFN- γ	64 -
Figure 9 IFN- γ is produced by activated immune cells	66 -
Figure 10 PD-L1 is expressed on ID8 cells treated with IFN- γ	68 -
Figure 11 NA accelerates and PRO+NA inhibits IFN- γ production in activated immune cells.-	70 -
Figure 12 PMA and Ionomycin treatment up-regulate PD-L1 expression in ID8.....	72 -
Figure 13 ID8 cells co-cultured with immune cells that failed to produce IFN- γ present different expression of PD-L1	74 -
Figure 14 IL-10 levels increase in co-culture of ID8 and activated splenocytes (with or without NA treatment).....	76 -
Figure 15 IFNGR1 was transiently knock down using siRNA.....	78 -
Figure 16 Proposed mechanism of PRO-mediated PD-L1 downregulation.....	82 -
Figure 17 Immune cell infiltration in a 3D model of ovarian cancer is affected by immune cells activation, treatment and time in co-culture	87 -
Figure 18 Adrenergic stress does not influence structural parameters of a 3D spheroids of ovarian cancer.....	89 -
Figure 19 Spheroid (treated with PRO+NA) protein-protein interaction network map....	91 -
Figure 20 Spheroid (treated with NA) protein-protein interaction network map.....	92 -
Figure 21 Multicellular spheroids protein-protein interaction (PPI) network map.....	97 -
Figure 22 Combined therapy with PRO+PD-(L)1i decrease tumour burden and metastatic nodules.....	114 -
Figure 23 Combined therapy with PRO+PD-(L)1i decrease CD8 ⁺ cells resident in the spleen..	116 -
Figure 24 Restraint stress upregulates CD3 and CD4 expression, but not CD8 in mouse primary tumour tissues.....	118 -
Figure 25 CD3, CD4 and CD8 expression in mouse primary tumour tissues	120 -

Figure 26 <i>VEGF</i> expression in mouse primary tumour tissues	- 122 -
Figure 27 Expression of granzyme B in mouse primary tumour tissues	- 124 -
Figure 28 <i>CXCL10</i> expression in primary tumour tissues.....	- 126 -
Figure 29 <i>IDO1</i> expression in primary tumour tissues.....	- 128 -
Figure 30 PD-L1 expression in primary tumour tissues	- 130 -
Figure 31 PD-L1 and IFN- γ protein levels in tumour tissues	- 132 -
Figure 32 Proposed mechanism of PRO-mediated PD-L1 downregulation	- 139 -

List of tables

Table 1 Adrenergic receptors.....	- 7 -
Table 2 T helper cell subtypes.....	- 17 -
Table 3 CellProfiler pipeline for spheroid analysis.....	- 40 -
Table 4 Scheme of mice groups and treatments	- 42 -
Table 5 Mass spectrometry buffers and reagent with correspondent recipe.....	- 55 -
Table 6 Patients' QoL and PD-L1 expression.....	- 61 -
Table 7 Protein enriched in spheroids treated with PRO+NA (Gene Ontology analysis) ..	- 93 -
Table 8 Protein enriched in spheroids treated with NA (Gene Ontology and KEGG analysis) .	- 94 -
Table 9 Protein list of multicellular spheroids (Gene Ontology).....	- 98 -
Table 10 Reactome analysis of multicellular spheroids proteins converted into human homologues	- 100 -

List of the main abbreviations

A: Adrenaline
ADRB: beta-adrenergic receptor(s)
ANOVA: Analysis of Variance
APC: Antigen presenting cells
ACTH: Adrenocorticotrophic hormone
Ag: Antigen
BRCA: Breast cancer related gene
CNS: Central Nervous System
CTLA-4: Cytotoxic T-lymphocyte Antigen 4
DC: Dendritic cell
DNA: Deoxyribonucleic Acid
ECM: Extracellular matrix
EOC: Epithelial ovarian cancer
HGSC: High grade serous (ovarian) carcinoma
IFN: Interferon
IL: Interleukin
LGSC: Low grade serous (ovarian) carcinoma
MHC I: Major histocompatibility complex class I
MHC II: Major histocompatibility complex class II
MMP: Matrix metalloproteinase
NA: Noradrenaline
NK: Natural killer cell
NSCLC: Non-small cell lung carcinoma
OSE: Ovarian surface epithelium
PARP: Poly ADP ribose polymerase
PCR: Polymerase chain reaction
PD-1: Programmed cell death protein 1
PD-L1: Programmed cell death protein-ligand 1
PI3K: Phosphoinositide 3 kinase
PLC: Phospholipase C
PRO: Propranolol hydrochloride
PTEN: Phosphatase and tensin homolog
RNA: Ribonucleic acid

SEIC: Serous endometrial intraepithelial carcinoma

TAM: Tumour associated macrophages

TIL: Tumour infiltrating lymphocytes

TGF: Transforming growth factor

TP53: tumour protein 53

VEGF: Vascular endothelial growth factor

Acknowledgments

I would like to express my profound gratitude to my supervisor Dr Melanie Flint who believed in me, my work, and this project more than anyone else. I truly appreciate her as a mentor who encourages original thinking and embraces challenging ideas in respect of the scientific rigour. I am also very grateful for her advice to rest and enjoy my time once the work was done. This made me a happier and more productive scientist.

I would like to thank Dr Marcus Allen for his valid contribution to this project with competence and scientific criticism. I also thank him for sharing - with a taste of British humour - his exceptional knowledge about science and pharmacology.

I express my appreciation to Professor Premal Thaker whose remarkable work inspired this project. I would also like to acknowledge her for providing intellectual and scientific contribute to this research.

I thank the University of Brighton for giving me the opportunity of carrying out this research. A special thanks to my lab team and my colleagues for their incredible support. This thesis would not be the same without your passionate brainstorming and practical help.

I would like to express my deepest gratitude to the friends I met in this journey. I have shared with you tears and laughs; special moments that will always be wonderful memories. I also thank my best friends that still have the patience to support me. Even if the world keeps us apart, we will always find a way to be next to each other.

I would like to thank my colleagues in the PhD office for supporting each other and creating an enthusiastic work environment. Being in contact everyday with people from many different countries is a wonderful opportunity to learn more about cultures and develop a profound sense of respect and empathy.

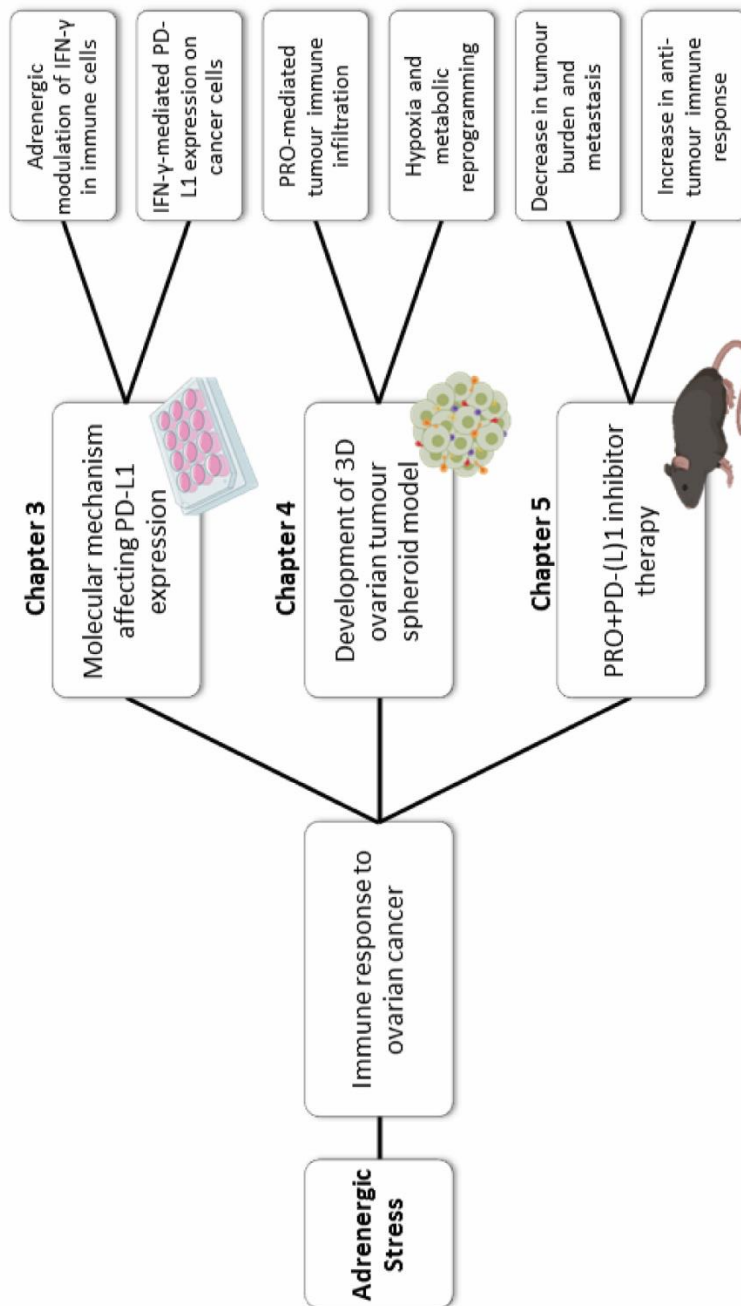
Finally, I thank my family and my parents who always believe in my qualities and support me with pride.

Declaration I declare that the research contained in this thesis, unless otherwise formally indicated within the text, is the original work of the author. The thesis has not been previously submitted to this or any other university for a degree, and does not incorporate any material already submitted for a degree.

Signed

Dated

Chapter overview



1. Chapter 1 – Introduction

1.1 Ovarian cancer

1.1.1 Epidemiology

Ovarian cancer is the sixth most common malignancy type in women and the second among gynaecological cancers with the highest mortality rate [1]. According to Cancer Research UK, there is a high proportion of deaths in relation to new cases with 4,200 ovarian cancer deaths out of 7,500 new cases in the UK in 2016. The incidence of ovarian cancer is higher in developed countries where the majority of the tumours are epithelial (90%) and they are diagnosed after menopause [2]. The 5 years survival rate is just 46% and the poor prognosis is related to the fact that patients are generally diagnosed at an advanced stage of the disease [1]. Clinicians normally refer to ovarian cancer as “the silent killer” because non-specific symptoms (e.g. bloating, weight gain etc.) are usually interpreted by patients as related to ageing or other diseases. Until definitive diagnostic factors and valid screening procedures are entirely identified, the early detection will be one of the most important challenges in the ovarian cancer diagnosis process [3].

1.1.2 Treatments

The current treatment of advanced ovarian cancer consists of cytoreductive surgery followed by chemotherapy, which is mainly the combination of taxanes (e.g. paclitaxel) and platinum agents. Although the majority of the patients initially respond to the above first line therapy, around 70% of them relapse and eventually become resistant to treatment [4]. New therapies are currently studied and used in combination with other common treatments to improve ovarian cancer outcomes [5]. These new approaches include monoclonal antibodies targeting the vascular endothelial growth factor (VEGF) such as Bevacizumab [6]. Other monoclonal antibodies are specific for immune checkpoints (discussed in section 1.3.7) such as Nivolumab that targets PD-1 or Ipilimumab (anti-CTLA4). Other treatments include the ones focused on Poly-ADP-ribose polymerases (PARP) inhibitors. These compounds block a family of proteins (PARP) involved in the DNA repair and genomic stability. These compounds have shown to be effective on ovarian cancers that harbour mutations in the breast cancer (BRCA) genes [7].

1.1.3 Ovarian cancer classification

Ovarian cancer is a complex and heterogeneous disease with a wide range of molecular and histological features. Even if the classification has been improved over time, differences between tumour types are in some cases subtle and the diagnosis is still challenging for pathologists [8, 9].

The current classification of ovarian cancers is based on the histological characteristics and it evaluates the cellular morphology and differentiation with a prediction of how much the tumour is likely to grow and spread. This method categorizes tumours in different stages. There are two different staging classifications: the TNM staging system (classification of malignant tumours) and the International Federation of Gynaecology and Obstetrics (FIGO) classification. The former uses three parameters of classification: T describes the primary tumour size; N indicates the regional lymph nodes involvement; M gives details on distant metastasis [20]. The FIGO classification takes into consideration histopathological, molecular and genetic features of ovarian, fallopian tube and peritoneal cancers. The 2014 FIGO guidelines delineate a classification into 4 stages: stage 1 tumours are confined to ovaries or fallopian tubes; stage 2 cancers involve pelvic extension or primary peritoneal cancer; stage 3 tumours spread to the peritoneum outside the pelvis and/or metastasise to the retroperitoneal lymph nodes; stage 4 includes distant metastasis [21].

Considering the histopathological classification, more than 90% of ovarian cancers are classified as “epithelial” and the most common type is the epithelial serous carcinoma which can present well differentiated (low grade serous carcinoma, LGSC) or undifferentiated (high grade serous carcinoma, HGSC) cells (Figure 1).

In the past, the classification was based on the origin of ovarian cancers and carcinogenesis was considered as an epithelial transformation, supporting the idea that tumours derive from the epithelial cells on the ovarian surface. This hypothesis - known as “mesothelial origin theory” or “incessant ovulation theory” - asserts that the ovarian epithelium surface (OSE) is exposed to continuous trauma during oocytes release and it is surrounded by an ovulation-related inflammatory and hormone rich environment. Physical and molecular stress leads to the epithelium metaplasia and cell proliferation with the result of tumour growth [10]. The mesothelial theory has been modified after the evidence that the most common ovarian malignancies such as high grade serous (HGSC) and endometrioid carcinomas (EC) arise from non-ovarian tissues [11, 12]. Fallopian tubes and the secondary Müllerian system are the tumour initiation sites of non-ovarian origins. Several studies have shown that HGSC arises from fallopian tubes as serous intra-epithelial carcinoma (SEIC) [11]. SEICs occur in the majority of cancers designated as HGSC and they are predominantly localized in the fimbrial region, which is the closest to the ovary [10, 13]. The Müllerian origin for ovarian-like cancers (serous, endometrioid, clear cell) involves the secondary Müllerian system composed of para-ovarian cystic structures that are the cell source of the tumours [14, 15]. Endometriosis-associated cancers and peritoneal cancers are considered as ovarian-

like cancers with non-ovarian origin [11]. The classification of ovarian cancers on the basis of its origin presents some limitations and it is not sufficient to predict the evolution and the progression of the disease. For instance, cancers with the same origin can evolve differently and most ovarian cancer cells do not show phenotypic similarity with any normal cells. Furthermore, malignancies clinically or histologically similar to ovarian cancers can develop in non-ovarian sites [15].

In 2004, Kurman and Shih proposed a dualistic model to categorize ovarian cancers. The “two-pathway model” integrates the pathology of the tumour type with the clinical aspect adding molecular and genetic features [10]. Following this classification, ovarian cancers are divided into two types. Type 1 tumours include LGSC, low grade endometrioid, clear cell, mucinous and Brenner carcinoma. These malignancies are usually at a low stage, clinically indolent and characterized by genetic stability and standard mutations. Their genetic profile involves KRAS, BRAF mutations (mitogen-activated protein kinase, MAPK signalling pathway), phosphatase and tensin homolog (PTEN) mutations (phosphoinositide 3-kinase, PI3K signalling pathway), β -catenin and transforming growth factor (TGF- β mutations). Type 2 carcinomas are HGSC, undifferentiated carcinoma and malignant mixed mesodermal tumours. These cancers are highly aggressive, at an advanced stage and present genetic instability with very frequent (more than 80% of the cases) tumour protein (TP53) mutations [14, 16].

Ovarian cancers can be linked to the hereditary breast and ovarian cancer syndrome with germline mutations in Breast Related Cancer Antigen (BRCA1 and BRCA2) genes. It has been shown that BRCA1/2 mutations increase the risk of breast and ovarian cancer and a genetic screening in families with history of breast and ovarian cancers is nowadays common practise [17]. Although the risk of ovarian cancer is mostly correlated with the family history, mutations in BRCA genes play a significant role. BRCA1 and BRCA2 are tumour suppression genes with different functions such as the preservation of the genomic stability, the DNA repair and the regulation of cell-cycle checkpoints. The fact that BRCA mutations increase the risk of tissue-specific cancers (breast and ovarian) is presumably due to DNA damage and genomic instability caused by the exposure to menstrual cycle oxidative stress and hormones, in particular oestrogens [17, 18]. Hereditary ovarian cancers are mostly due to BRCA1 mutations (83%). Also, BRCA1 mutations are more common in ovarian cancer diagnosed before 50 years old, while BRCA2 mutations occur in late-onset ovarian cancers [19].

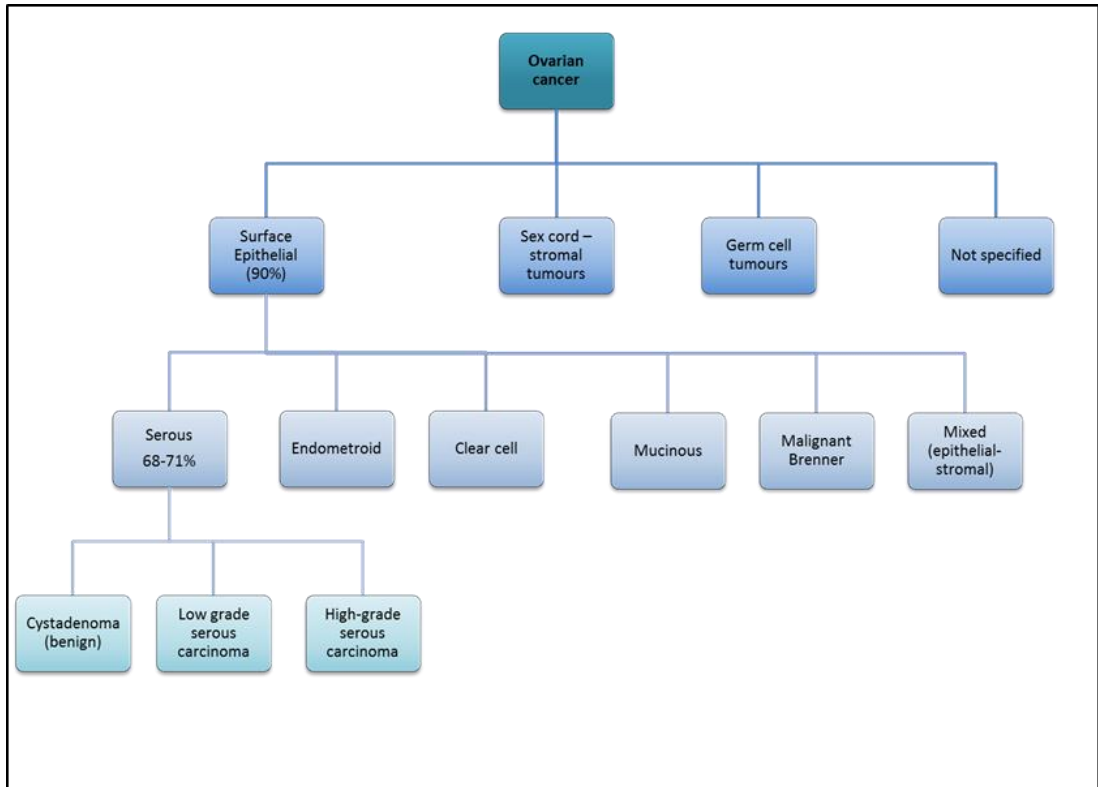


Figure 1 Histopathological classification of ovarian cancers

More than 90% of ovarian cancers are classified as “epithelial”. The most common type is the epithelial serous carcinoma (68-71%) which can present well differentiated (low-grade serous carcinoma, LGSC) or undifferentiated (high-grade serous carcinoma, HGSC) cells. Data are taken from the World Health Organization (WHO) [20].

1.2 Psychological stress

1.2.1 Introduction to psychological stress

The concept of stress was introduced by Hans Selye; he defined stress as “the non-specific response of the body to any demand for change” [21, 22]. Any living organism has the tendency to maintain equilibrium for optimal functioning. This stable state, known as homeostasis, is constantly disturbed by external or internal stimuli called “stressors”. In 1992, the definition of “stress” was revised. Stress was described as the threat to homeostasis or the perception of a threatening state against the psychological balance [23]. Stress stimuli produce a complex biological response which involves the central nervous system (CNS) and the periphery. Stress activates the hypothalamic pituitary adrenal (HPA) axis and autonomous nervous system (ANS) pathway. The central components include the paraventricular nuclei (PVN) of the hypothalamus and the noradrenergic loci cerulei (LC-NA). The PVN release the corticotrophin-releasing hormone (CRH) which stimulates the pituitary gland to produce adrenocorticotrophic hormone (ACTH). ACTH stimulates adrenal glands to produce cortisol and NA. In the ANS, neurons use Adrenaline (A) and Noradrenaline (NA) as neurotransmitters. Increased NA secretion enhances the stimulation of the adrenal glands and activates the adrenergic stress response [24, 25].

The neuroendocrine components of the stress system include not just stress hormones, but also neurotransmitters, cytokines, and growth factors that cooperate to produce a stress response [25]. Stress is also defined by the length of the response. Acute stress is a short-term stress which activates the “fight or flight” response increasing alertness, vigilance, attention, and aggression with the inhibition of vegetative functions such as feeding or reproduction [26]. To achieve this state, stress mediators increase the oxygenation of the brain and muscles accelerating the heart and respiratory rate. The body easily adapts to acute stress, but it has been shown by several studies that a prolonged exposure to stress due to an inappropriate basal activity or hyper-responsiveness to stressors can cause long-term damage [27-29]. Chronic stress and stress alteration can lead to depressive behaviour or anxiety disorders. Chronic stress can also be the cause of allergic manifestations and gastrointestinal symptoms [25].

1.2.2 Adrenergic stress

The term “adrenergic” refers to adrenaline (A) and noradrenaline (NA) that mediate stress response in the sympathetic nervous system. The physiological effects of NA include an activity as neurotransmitter and as hormone released during exercise or emotional response.

As mentioned before, adrenergic stimulation increases blood flow to muscles, heart output and respiration rate with downregulation of the metabolic activity [25].

NA binds and stimulates adrenergic receptors divided into α and β subtypes. Alpha-receptors are associated with vasoconstriction and relaxation of the gastrointestinal muscles; there are two different α receptors: α_1 associated with G_q proteins activating phospholipase C (PLC) and α_2 coupled with G_i heterodimeric proteins that reduce cAMP production. The group of β receptors has positive chronotropic dromotropic and inotropic effect and promotes relaxation of the muscles. The 3 different types of β receptors (β_1 , β_2 and β_3) are coupled to G_s proteins that upregulate cAMP produced by the adenylate cyclase [30, 31] (Table 1).

Receptor type	Localization	Mechanism	Effect
α_1 (A,B)	Ureter, hair, uterus, blood vessels	G_q	Muscle contraction, mydriasis, vasoconstriction
α_2 (A,B,C)	Gastrointestinal tract, CNS	G_i	Smooth muscles mixed affects
β_1	Cardiac muscles, kidneys, stomach	G_s	Positive dromotropic, chronotropic, inotropic effect
β_2	Smooth muscles, adipose tissue, skeletal muscles, ovary	G_s	Muscle relaxation
β_3	Adipose tissue	G_s	Lipolysis

Table 1 Adrenergic receptors

Adrenergic receptors are divided into α and β subtypes. Alpha-receptors are associated with vasoconstriction and relaxation of the gastrointestinal muscles; there are two different α receptors: α_1 associated with G_q proteins activating PLC and α_2 coupled with G_i heterodimeric proteins that reduce cAMP production. The group of β receptors has positive chronotropic dromotropic and inotropic effect and promotes relaxation of the muscles. The 3 different types of β receptors (β_1 , β_2 and β_3) are coupled to G_s proteins that upregulate cAMP produced by the adenylate cyclase [30, 31].

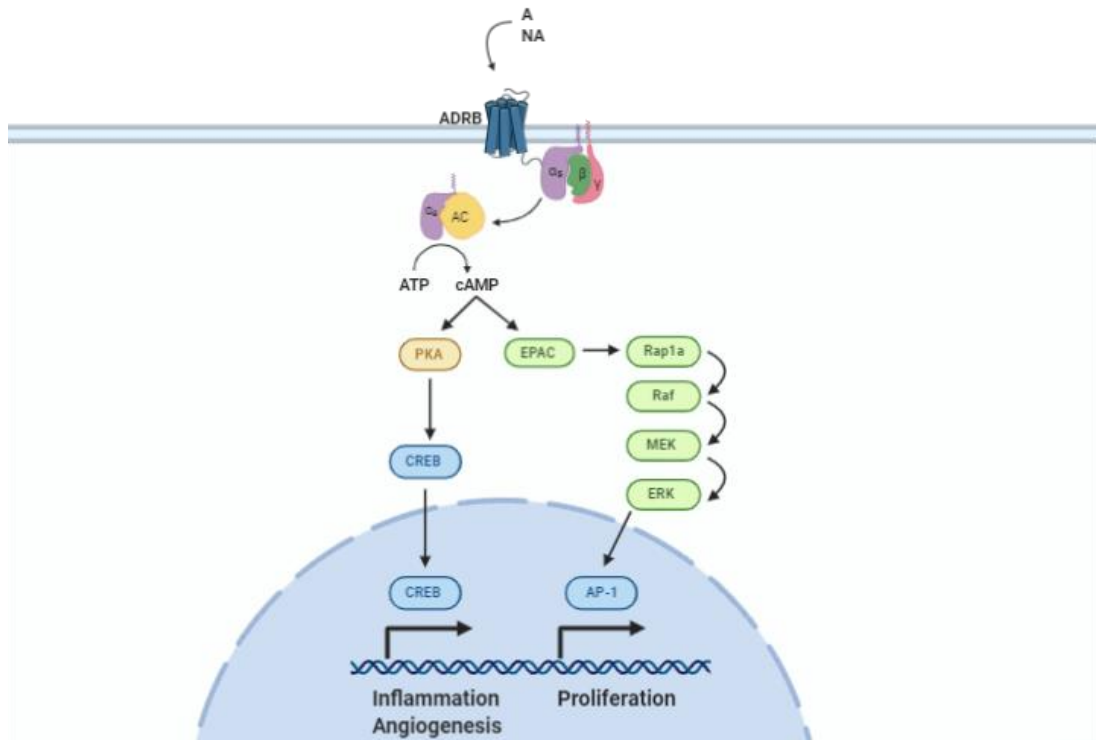


Figure 2 Beta-adrenergic signalling pathway

Adrenaline and Noradrenaline bind the ADRB, activate the adenylyl cyclase and, by converting ATP in cAMP, initiates two different signalling pathways mediated by PKA or EPAC. The PKA pathway activates CREB which upregulates the transcription of genes involved in inflammation and angiogenesis. EPAC activates the MAPK cascade terminating with ERK which allows the transcription of genes controlled by AP-1 and involved in proliferation [30, 31].

1.2.3 Stress and cancer

Chronic exposure to stress hormones (catecholamines and cortisol) can evolve in pathologic processes and stressed-related diseases [32]. The idea that psychological and emotional well-being can affect the outcome of certain diseases is linked to the biological effect of psychological stress. There is a wealth of evidence in the literature exploring the connection between stress and cancer. Studies can be divided into two categories listed below.

Stress and cancer initiation

Studies correlating stress to cancer initiation have shown opposite results; studies that correlate stress to cancer onset and studies that refuse a cause-effect relation. A study on (3T3) fibroblast cell line is representative of the first category. It showed that A and NA exposure induced DNA damage and promoted transformation. 3T3 cells exposed to NA and injected in the flank of nude mice induced a more aggressive tumour growth compared to non-stimulated cells [39]. Although this work demonstrates that the exposure to NA increases cancer development, it does not confirm a cause-effect association between psychological stress and tumour initiation. Biochemical stress mediator levels, in particular

NA and cortisol, are used as an appropriate clinical marker for stress [23]. However, the biological measurement has some limitations due to the stress hormones circadian fluctuation and the short half-life. At normal plasmatic levels, cortisol has a half-life of 66 minutes (increasing to 120 minutes with higher steroids concentrations) and NA's half-life is only few minutes [33, 34]. The quantification of stress levels is still challenging, and the psychological condition is evaluated by completion of questionnaires. Many epidemiological studies aimed to discover a link between stress and cancer evaluating psychological stress by examine a questionnaire completed by patients. In a case-control study, life events perceived as stressful seem to increase the risk of breast cancer [35]. Another case-control study in Poland showed an association between the stressful events and cancer risk [36]. These questionnaires included sociodemographic information, general lifestyle habits and patients were also asked to report stressing life events such as a loss of a family member, loss of job, divorce etc. [36]. Limitations of these investigations are related to the recall of bias in a retrospective study and the perception of stressful events in different patients.

Other evidence supports the hypothesis that cancer risk is not associated with stress. A study on breast cancer patients in UK used the Health and Life Experience Questionnaire (HLEQ) to assess the stress level of patients considering physical status and the experience of traumatic events. This work showed no evidence of association between social stress and cancer incidence [37]. Another population-based study supports the idea that cancer is not caused by stress, but rather stress is derived from the actual cancer diagnosis. In this nationwide population-based study among ovarian cancer survivors in South Korea, mental disorders such as depression and anxiety increased two months after cancer diagnosis [38].

Although the previous findings on stress and cancer association allow an insight into multiple and opposite points of view, evidence to support a correlation between stress and cancer development is inconsistent and further considerations are needed. Despite the controversy on the relationship between psychological stress and cancer risk, the increase of stress hormone levels and the endocrine stress response has a stronger association to cancer progression rather than cancer incidence [39].

Stress and cancer progression

Both the biological measurement of stress hormones and the use of questionnaires can present limitations in the evaluation of stress levels. To overcome these problems, recent studies have used animal models in which psychological stress can be reproduced by exposing animals to different types of stress including restraint stress, social isolation, cold, or surgical stress. Animal exposed to stress have a biological stress response which can be

evaluated by measuring the levels of stress hormones in plasma. Although animal models represent a valid approach to accurately study the biological stress response, the literature showing a cause-effect correlation between high levels of stress hormones and cancer initiation is still deficient and most the researchers focus on the interdependence between stress and cancer progression. In 2006, Thaker et al demonstrated that the adrenergic stress and, in particular NA stimulating the beta-adrenergic receptor (ADRB), promotes tumour progression in an orthotopic mouse model of ovarian cancer [40]. This *in vivo* model has also shown that stress increases angiogenesis and metastatic spread [40, 41]. Another study on skin cancer, restraint stressed mice presented a higher number of tumours compared to non-stressed mice. A study on surgical stress also demonstrated that stress enhances tumour growth and weight [42, 43].

Important advances have been made to understand the complex effects of stress on cancer taking into consideration the tumour evolution and progression. However, further analysis on stress and cancer is needed and it would offer an opportunity to improve cancer therapy.

1.2.4 Adrenergic stress and ovarian cancer

NA is naturally present in the ovary at biologically significant levels and is correlated with the overexpression of ADRB in growing follicles [44, 45]. The adrenergic signalling mediated by NA is also implicated in the stress-dependent increase of tumour growth and progression. It has been shown the presence of beta-adrenoreceptors on ovarian cancer cells and *in vivo* studies demonstrated that stimulation of these receptors enhances the tumour growth [46]. In particular, mice treated with a non-specific beta-receptor agonist (Isoproterenol) showed an increase in the number of tumour nodules and in tumour weight [46]. Treatments with a non-specific beta-antagonist (Propranolol) reverse the agonist-induced effect. Furthermore, a siRNA specific for beta2-adrenergic receptor (ADRB2) efficiently blocked the stress-mediated tumour augmentation [40]. The importance of NA and beta-adrenergic stimulation in the ovarian cancer progression have led to focus the attention of this research on NA signalling pathway.

The adrenergic-mediated promotion of tumour growth is sustained by an increased angiogenesis. Numerous findings show that NA promotes tumour vascularization, with an increase in vascular endothelial growth factor (VEGF) levels in stressed animals [46, 47]. Also, NA upregulates VEGF and matrix metalloproteinase (MMP)-2 and (MMP)-9 in tumour cells [47].

1.2.5 Beta-blockers as potential anticancer agents

Beta-blockers are pharmacological compounds ordinarily used in heart arrhythmia and hypertension. They can be described as non-selective beta-blockers, displaying affinity for all beta-adrenergic receptors (ADRBs) subtypes and selective beta-blockers, with specific affinity to ADRB1, ADRB2, or ADRB3. Beta-blockers are usually competitive antagonists for beta-receptors; they bind the same receptor site used by endogenous catecholamines (A and NA) and induce an opposite response to the adrenergic-mediated sympathetic stimulation. Some beta-blockers such as Propranolol (a non-selective beta-blocker) act as inverse agonists. In this case, they are associated with the receptor conformation, switching off the receptor activity [48].

Recent studies have given the proof that ADRBs are expressed on different cancer cell types and the idea to use beta-blockers as anti-cancer agents is emerging in several epidemiological studies [46, 49]. A retrospective study on patients with non-small-cell lung cancer (NSCLC) showed that the association of beta-blocker treatment before or during the radio therapy correlated with a lower stage disease. Also, patients under beta-blocker treatment showed an improved distant metastasis-free survival, disease-free survival and overall survival [50]. A retrospective meta-analysis on prostate cancer patients indicates a cancer-specific mortality reduction on patients taking beta-blockers [51]. A specific retrospective study on ovarian cancer was carried out in 2012 observing that beta-blocker use influences the survival rate. In particular, the progression-free survival was 27 months for beta-blocker users compared to 17 months for non-users [52]. However, Heitz et al. have shown no correlation between beta-blocker treatment and improved overall survival in ovarian cancer patients [53]. To better understand the impact of beta-blocker as potentially therapeutic in cancer, we need to consider that these compounds exert different effects. A step forward in this sense was made by Watkins et al. in 2015, when they demonstrate the clinical relevance of selective and non-selective beta-blockers in the survival rate of patients with ovarian cancer. This work suggests the idea that the heterogeneous subset of beta-blockers exerts disparate functions. Since tumours respond differently, beta-blockers have a diversified impact on the outcome of patients with cancer [54].

In conclusion, in the studies showing an improvement of cancer outcomes the molecular mechanisms that govern the beta-blockers activity are not clear. Nowadays, beta-blockers still represent a potential anti-cancer treatment, but the molecular processes involved in their response need a deeper understanding.

1.2.6 Adrenergic stress effect on immune metabolism

Immune cells derived from hematopoietic stem progenitors migrate to the lymphoid organs and the periphery to undergo a series of maturation processes. During these events, immune cells are subjected to a genetic and metabolic reprogramming [55]. One of the main events in the immune cells maturation is the activation. This process is particularly important for cells of the immune system that reside in the periphery in a quiescent state (naïve cells) and that can be triggered to massively proliferate and switch to effector cells. The rapid transition from naïve to activated cells induces a higher energy demand with a dramatic increase in the glucose metabolism [55, 56]. The relationship between the activation of effector functions and the switch of the metabolism is evident in many immune cells. DCs, neutrophils and macrophages initiate aerobic glycolysis after their activation [57]. T lymphocytes increase the expression of the glucose transporter 1 (GLUT1) on their surface and enhance the glycolytic pathway [58]. Aerobic glycolysis is a metabolic process converting glucose in lactate even when cells are exposed to normal levels of oxygen [59, 60]. Although it produces much less ATP than the classic oxidative process, the aerobic glycolysis is able to generate metabolic intermediates useful to sustain cell growth and proliferation [60]. Furthermore, the oxidative metabolism is not totally suppressed and it cooperates with the glycolysis to supply the higher energetic demand [56]. Glycolysis is rapidly induced in activated T cells by the TCR stimulation with an increase in specific enzymes and proteins involved in the process [56]. Several signalling pathways support and regulate this change in the immune cell metabolic program. Growth factors and cytokines support the T cell activation by promoting glycolysis via the activation of molecular regulators such as mTOR. The activity of mTOR is regulated by extrinsic and intrinsic signals reflecting the activation status, energy supply and stress response of the cell. The metabolic pathway supports the differentiation of the T cell towards a specific fate: CD4⁺ T cells, upon the activation of mTOR and the switch to glycolysis, differentiate in T helper cells; when mTOR activity is suppressed CD4⁺ T cell differentiate in regulatory T cells (T_{reg}) [61].

Glucose is an essential metabolic substrate for activated T cells. Deprivation of glucose resulted in impaired T cell activation, reduction of the clonal expansion and decrease in the production of effector molecules such as IFN- γ and granzyme B [55]. As mentioned above, GLUT1 is translocated on the membrane of activated T cells in response to TCR-induced activation and the stimulation of the phosphoinositol-3 kinase (PI3K)-Akt pathway [62, 63]. The translocation of GLUT1 increments the glucose intake in the cell and supports the increased metabolic demand. A recent study has shown that the ADRB signalling affects the

metabolic reprogramming and GLUT1 membrane expression in CD8⁺ T cells [64]. As widely discussed in this thesis, immune cells express ADRB and respond to adrenergic stimulus which affects their functions. CD8⁺ T cells activated *ex vivo* in the presence of isoproterenol, a ADRB agonist, inhibited the expression of GLUT1 on their surface and decreased their glucose uptake [64]. Since the glycolysis promotion in activated immune cells is dependent on the glucose uptake, it is expected that ADRB signalling inhibits the glycolytic capacity of T cells impairing their effector activity [64]. This evidence is supported by an *in vivo* study using tumour mouse models where animals were housed at 20-26°C instead of 30-31°C. Housing animals at sub-thermoneutral temperature is a method to induce mild chronic stress *in vivo* and activate the adrenergic signalling. The authors found that mice housed at a standard temperature showed a decreased tumour growth rate and metastasis compared to the ones housed at sub-thermoneutral temperature. These improvements were immune-dependent with increased CD8⁺ T cells in the tumours of mice housed at standard temperature compared to the ones housed at sub-thermoneutral temperature. Interestingly, CD8⁺ T cells isolated from tumours of mice housed at sub-thermoneutral temperature have shown a lower expression of GLUT1 on their surface compared to the ones isolated from tumours of mice housed at standard temperature [65]. These mechanisms reveal the capacity of adrenergic stress of suppressing the immune effector functions by modulating the metabolic pathway of immune cells. For these reasons, assessing the metabolic program can be indicative of the tumour immune modulation.

1.3 The immune system

1.3.1 Introduction to the immune system

The immune system includes a great variety of organs, cells and molecules that coordinate an effective response to fight pathogens. The human body is continuously exposed to micro-organisms that have the potential to be infectious. A first defence against infectious organisms is composed by physical and biochemical barriers. For instance, skin and mucosae represent the most effective physical barriers of our body. Any organism that can overcome this first line of defence encounters other two levels of protection: the innate and acquired immune response. Both of these responses have a double step process of recognition and elimination of the pathogen. The differences between the innate and adaptive (acquired) response are that the former is faster and the latter is more specific and trains the immune system to have an improved response during successive encounters with the same type of pathogen [66].

1.3.2 The innate immune response

In general, the innate immune system consists of cells called phagocytes that carry out both the recognition and the elimination stage. These cells belong to two lineages: monocytes/macrophages and polymorphonuclear granulocytes. Macrophages are specialized in two functions: phagocytosis of micro-organisms and cancer cells; and the antigen presentation to T cells. Granulocytes are classified into neutrophils, basophils and eosinophils according to their cytoplasmic stain with acidic dyes. Their function is mainly phagocytosis, but they also produce cytokines [67].

Natural killer (NK) cells, as suggested from the name, have a cytotoxic function; they have the ability to induce apoptosis to target cells without an activation process (typical of lymphocytes) allowing a fast response against infected or tumour cells. NK cells present on their surface different types of activating or inhibitory receptors and on the basis of which type of receptor is activated their cytotoxic activity is induced or inhibited [68].

Dendritic cells (DCs) are antigen presenting cells (APCs) that are involved in the activation of the adaptive response. They are activated by signals of danger such as the release of interferon- α from infected/tumour cells or the increase of heat-shock proteins. Other signals that activate DCs include the lipopolysaccharide (LPS) on the surface of gram positive bacteria, the mannose and the toll like receptors [66].

The innate immune response is composed of cellular and soluble factors. Soluble mediators of the innate immune response include complement proteins and cytokines. The complement system is a group of proteins that are involved in the inflammation process. The activation of the complement generates a signalling cascade that initiates a series of functions such as the opsonisation of micro-organisms, chemo-attraction of phagocytes in the site of inflammation, increased permeability of the blood vessels and the release of other inflammatory mediators. Soluble molecules implicated in the immune response, but also in the maturation of the immune cells are called cytokines. There are different types of cytokines, but generally they are glycoproteins that mediate the immune response through the recognition via specific receptors. The principal sets of cytokines include the interferons (IFN), the interleukins (IL) and chemokines. Different types of IFNs (IFN- α , IFN- β , IFN- γ) are secreted by different types of cells and they exert many functions. Usually, IFNs are produced in the early stage of infection and they flag the presence of an infected or tumorigenic cell. ILs are mainly produced by T cells and they are important for the immune cell development and maturation. Chemokines primary function is to attract other cytokines and immune cells in the site of infection [69].

1.3.3 The adaptive immune response

The adaptive immune response represents a pathogen-specific reaction in which specialized cells are subject to the antigen presentation, proliferation and differentiation.

The term antigen (Ag) indicates a series of molecules or parts of them (haptens) that characterize a specific pathogen and that can be recognized by the adaptive immune cells or antibodies [68]. The recognition of the antigens by specific antibodies is the key point of the adaptive immune response. In order to activate the adaptive immune response, antigens are processed and displayed by specialized cells (APCs).

Antigen presentation is divided into two different processes; one is specific for intracellular antigens such as viruses or tumorigenic cells, the other method is more specific for extracellular antigens (Figure 3).

- Intracellular antigenic peptides are bound to molecules known as class I Major Histocompatibility Complex (MHC I) and the new formed complex (MHC I + Ag) is exposed on the surface of an APC or any other nucleated cells [69]. There are two different ways to present the antigen: the direct or the cross-presentation. In the first process, the infected cells process and expose on their surface the complex (MHC I + Ag) and they activate the adaptive immune response [70]; the second way is the cross-presentation. In this case, Ag peptides, produced by infected or tumorigenic cells, are processed and exposed on the surface of APCs that bind and activate the immune response.
- Extracellular antigenic peptides are linked to MHC II and this complex is expressed in professional immune APCs that activate the adaptive response [68].

The main cellular actors of the adaptive immunity are lymphocytes that develop from the myeloid lineage in the bone marrow. Lymphocytes are divided in two major categories: T and B lymphocytes. The main difference between the two types is that T lymphocytes mediate the cellular immunity while the B lymphocytes act in the humoral immunity producing antibodies, soluble molecules that recognize antigens [68].

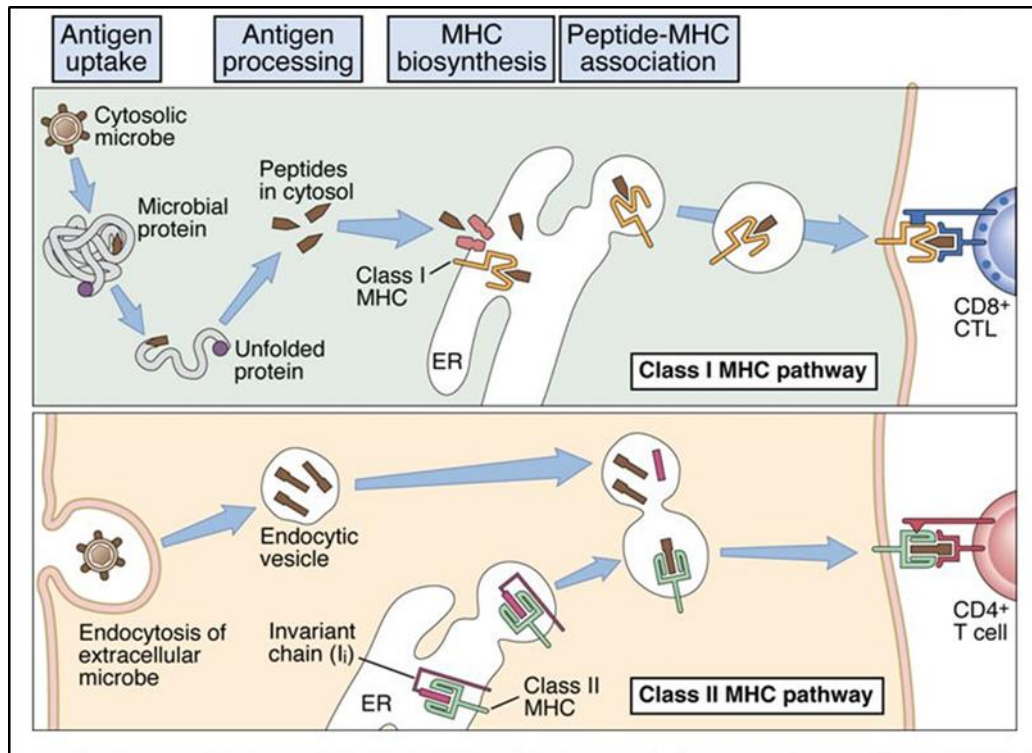


Figure 3 Antigen presentation
 Intracellular antigens are bound to MHC I and the complex (MHC I + Ag) is exposed on the surface of an APC or any other nucleated cells. Extracellular antigenic peptides are linked to MHC II and this complex is expressed in professional immune APCs that activate the adaptive response. Figure reproduced from [57].

1.3.4 T cell biology and activation process

T lymphocytes originate from hematopoietic stem cells (HSCs) maturing in lymphoid progenitors first and then in T lymphocytes precursors that migrate from the bone marrow to the thymus where they complete their maturation [69]. The maturation process consists of T cell proliferation, expression of the T cell receptor (TCR) and co-receptors, and two types of selection; the positive selection allows T cells with a TCR recognizing MHC class I to grow, the negative selection eliminates T cells with a strong bind to self-antigens through a phenomenon called “clonal deletion”. While the positive selection facilitates the development of potentially useful T cells, the negative selection ensures the mechanism of tolerance. During their maturation, T cells also undergo a rearrangement of their TCR encoding genes to generate a variety of cells that can bind different antigens [69]. In the

process of T cell maturation, CD4 and CD8 co-receptors are also expressed with a switch from double-negative (CD4⁻CD8⁻) to a double-positive (CD4⁺CD8⁺) T cells. Double positive T cells undergone the selection process, turn into single positive (CD4⁺ or CD8⁺) T cells in the thymus medulla [69]. After maturation, single positive T cells leave the thymus and reside in the periphery as naïve T cells.

There are many subtypes of T cells; the main categorization distinguishes CD8⁺ and CD4⁺ cells. CD8⁺ cells are cytotoxic T cells and they actively kill the infected cells; CD4⁺ cells are also designated as “helper” cells and they activate other types of cells such as phagocytes, B cells or other T cells. The main characteristic of the CD4⁺ helper lineage is the ability to produce cytokines. On the basis of the type of cytokines they produce, T helper cells are divided into Th₁ and Th₂. The cytokine profile of Th₁ includes IFN- γ , a pro-inflammatory and anti-tumour cytokine. Th₂ subset produces IL-4, IL-5 and IL-13; they are known to have anti-inflammatory functions. Another lineage known as TH₁₇ producing IL-17 is currently the centre of numerous studies because it has both pro-inflammatory and anti-inflammatory functions and its role is still unclear [71]. The last important subset of CD4⁺ cells is constituted by regulatory T cells. These cells express CD25 (α IL-2 receptor) and FoxP3 (a transcription factor). T_{reg} function is to suppress the immune response and regulate the self-tolerance. [69].

Effector CD4 ⁺ T cell	Cytokines	Function	Effect
Th1	IFN- γ	Macrophage activation	Cell-mediated immunity
Th2	IL-4, IL-5, IL-13	Alternative macrophages activation, eosinophil and mast cell activation	Anti-parasite immunity, allergic response
Th17	IL-17, IL-22	Neutrophil recruitment and activation	Anti-fungal and anti-bacterial immunity
T _{reg}	IL-10, TGF- β	Immunosuppression	Tolerance

Table 2 T helper cell subtypes

CD4⁺ helper T cells are divided into many subtypes. Th₁ cells produce IFN- γ , a pro-inflammatory and anti-tumour cytokine. Th₂ subset produces IL-4, IL-5 and IL-13; they are known to have anti-inflammatory functions. Another lineage known as TH₁₇ produces IL-17. Regulatory T cells (T_{reg}) express CD25 (α IL-2 receptor) and FoxP3 (a transcription factor). T_{reg} function is to suppress the immune response and regulate the self-tolerance.

T cells circulate in our body in a resting state (naïve T cells) and they need an activation process to execute their functions [67]. Antigen recognition is a necessary signal for T cell activation; naïve T cells require antigen recognition in order to have an antigen-specific response. Generally, antigens are presented to T cells by specific APCs, the dendritic cells (DCs) [69]. The interaction between naïve T cells and DCs is mediated by the recognition of

the “Ag+MHC” complex by the T cell receptor (TCR). This first step of recognition is sustained by co-stimulatory signals; one of the co-stimulatory pathways involves CD-28 receptor on the T cell surface binding the B7-1 and B7-2 molecules on APCs [67]. Without an appropriate CD-28 co-stimulation, T cell activation is not achieved. CD-28 signals promote survival, proliferation and differentiation of activated antigen-specific T cells. The activation process is the result of a balance between stimulatory and inhibitory signals. The inhibitory receptors include the Cytotoxic T Lymphocytes Antigen 4 (CTLA-4) and the Programmed Death Protein 1 (PD-1). Disposing of inhibitory signals is important to mediate processes like tolerance and control the length and magnitude of the immune response [69].

The activation process can be summarized in three important steps: the antigen recognition, the clonal expansion and the differentiation in effector T cells. After the antigen encounter, T cells are activated (or more accurately “antigen-primed”); they change some surface receptors and acquire the ability to produce certain cytokines. The most important cytokine produced is IL-2 that sustains T cell growth, proliferation and differentiation. IL-2 stimulates the massive proliferation of antigen-specific primed T cells known as “clonal expansion”. This pool of primed T cells undergoes changes in gene expression and start the differentiation process which produces effector T cells with different functions that can co-operate to eliminate the infection [69].

1.3.5 Immune response to cancer

In 1957, MacFarlane and Burnet proposed the “immune surveillance hypothesis” which stated that the immune system recognizes and destroys transformed cells before they form a tumour and it also kills the tumour after it is formed [72]. The role of the immune response in cancer development was demonstrated by numerous animal studies where immunodeficient mice were more susceptible to cancer than immunocompetent mice [73-75]. Burnet theory was based on the fact that transforming cells with malignant potential express new antigens [72]. The presence of specific cancer antigens was previously determined by Old and Boyse; their findings showed that mice immunized with specific tumour antigens were protected against the same type of cancer [76]. Cancer neo-antigens include mutational antigens (p53), overexpressed antigens (HER-2) or germ cells specific genes (MAGE, NY-ESO1) [77].

The evolution of the immune surveillance theory is the “cancer immunoediting” which is a dynamic process consisting in three phases: elimination, equilibrium and escape [78].

- The **elimination phase** represents a modern and revisited version of the immune surveillance; tumours are recognized and eliminated by the immune system before any

clinical sign. When a cancer cell is not eliminated it enters in the equilibrium phase and the tumour remains in a dormant state [78].

- The **equilibrium phase** prevents tumour progression and maintains tumour cells in a quiescent and latent state [78]. This stage is a critical point strictly controlled by the adaptive immune system. The role of the adaptive immune response was demonstrated by an experiment in which mice exposed to a chemical carcinogen (MCA) with no sign of tumour growth were treated with monoclonal antibodies (anti-CD4, anti-CD8 and anti-IFN- γ) in order to deplete the adaptive immune mediators. The immune suppressed mice were more prone to develop tumour compared to the immunocompetent control group [79].
- The **escape phase** occurs when cancer cells acquire the ability to bypass the immune response and start a progressive growth. This is probably a consequence to the immune selective pressure which can drive genomic changes in tumour cells to modify their immune susceptibility. Tumour cells are no longer recognized by the immune system for different reasons such as a modification in their antigens or induction of an immune suppressive tumour micro-environment [78].

The immune signature in tumours is represented by the infiltration of immune cells (T and B cells, NKs, macrophages etc.) and immune molecular mediators (cytokines, chemokines, growth factors etc). One of the cellular tumour immune components are tumour associated macrophages (TAMs) derived from peripheral blood and recruited, via chemokine attraction, in the tumour site [80]. TAMs can differentiate –in a process known as polarization- in two different populations: M1 and M2. M1 macrophages are mainly induced by IFN- γ and produce pro-inflammatory cytokines such as TNF, IL-1 β and IL-6. M2 subtype includes a heterogeneous class of macrophages stimulated by cytokines (IL-4, IL-12, TGF) and glucocorticoids; M2 have immuno-regulative functions and are associated with tumour promotion. Macrophages are important mediators of the immune response to cancer and are also affected by the stress signalling. In particular, ovarian cancer cells undergoing adrenergic stimulation (NA treatment) increased the production of C-C Motif Chemokine Ligand 2 (CCL2) also known as monocyte chemoattractant protein-1 (MCP-1), a chemokine that induces the recruitment of monocytes/macrophages [6]. It has been shown that CCL2 is produced by cancer cells and promotes cell migration, proliferation and metastasis [7-10]. In an *in vivo* restraint stress model of ovarian cancer, CCL2 up-regulation in primary tumours correlates with macrophage (F4/80+) infiltration and promotion of tumour growth [6]. Another *in vivo* study correlates the CCL2 network to M2 macrophage (Arg1+) infiltration in

metastatic lungs of breast tumour-bearing mice, suggesting the idea that stress and macrophages recruitment might also have a role in distant metastasis [11].

Another cellular immunological component of the tumour micro-environment is represented by the Tumour Infiltrating Lymphocytes (TILs). The tumour immune signature and in particular, the analysis of TILs can help to generate an immune profile of cancers. In a meta-analysis on human cancers, different experimental procedures were used to evaluate the relative leucocyte fraction in different solid tumours [81]. In addition, prognostic values were attributed to different cell subsets; high levels of CD8⁺ T and CD45RO⁺ memory T cells were generally correlated with a favourable outcome [82]. The prognostic utility of TILs was also remarked in several studies on cutaneous melanoma [83, 84]. Clark et al. defined the criteria to categorize TILs infiltration in melanoma: absent TILs, non-brisk (TILs in one or more foci) and brisk (TILs on the entire base of the tumour)[85]. Intra-tumoural CD8⁺ cells are also reported to be associated with a better ovarian cancer prognosis [86]. Immunohistochemical analysis for TILs was performed on epithelial ovarian cancers and it showed that a high CD8⁺/CD4⁺ T cells ratio improved patients' survival. In particular, the beneficial CD8⁺ effect was negatively influenced by the presence of regulatory (FoxP3) T cells [86].

1.3.6 The role of PD-(L)1 axis in physiology and cancer

Programmed cell Death Ligand 1 (PD-L1), also known as cluster of differentiation 274 (CD274) or B7 homolog 1 (B7-H1), is a trans-membrane protein usually expressed on antigen presenting cells (APCs) but also on the surface of various cell types [11]. The function of PD-L1 is closely related to Programmed cell Death protein 1 (PD-1), a member of the immunoglobulin superfamily expressed on B and T cells discovered in 1992 by Honjo et al [12, 13]. PD-1 and PD-L1 interaction results in the inhibition of the T cell activation and proliferation [14]. Honjo et al concluded that PD-(L)1 signalling is part of the CD28-B7 family of co-stimulatory molecules involved in the T cell activation. However, while co-stimulatory molecules promote T cell activation, PD-(L)1 signalling pathway promotes the downregulation of T cell activity. The same immunomodulation is exerted by the cytotoxic T lymphocytes antigen-4 (CTLA-4). The fine process of T cell regulation has been shown to play a role in the peripheral tolerance by blocking the expansion or inhibiting activated autoreactive T cells [14]. This role has been confirmed by studies on PD-1 deficient mice developing autoimmune diseases such as diabetes, dilated cardiomyopathy and lupus-like autoimmune diseases [15-18].

Although PD-1 expression on T cells is normal after the activation process [87], PD-1 overexpression is associated with T cell exhaustion phenotype [88]. PD-(L)1 axis has been

shown to play a pivotal role in cancer immunology [89]. As a matter of fact, PD-L1 is expressed in numerous cancers such as melanoma, lung and lymphoma [90-92]. PD-1 and PD-L1 interaction is therefore used as an escape mechanism by cancer cells to induce T cell dysfunctional exhaustion. Although the molecular mechanisms of T cell exhaustion are still not completely understood, PD-1 on T cells has the ability to bind PD-L1 on cancer cells and start a downstream pathway that culminates with immunosuppression [89, 93]. PD-L1 is also expressed in cancer cell lines and tumour tissues of ovarian cancer [89, 94, 95].

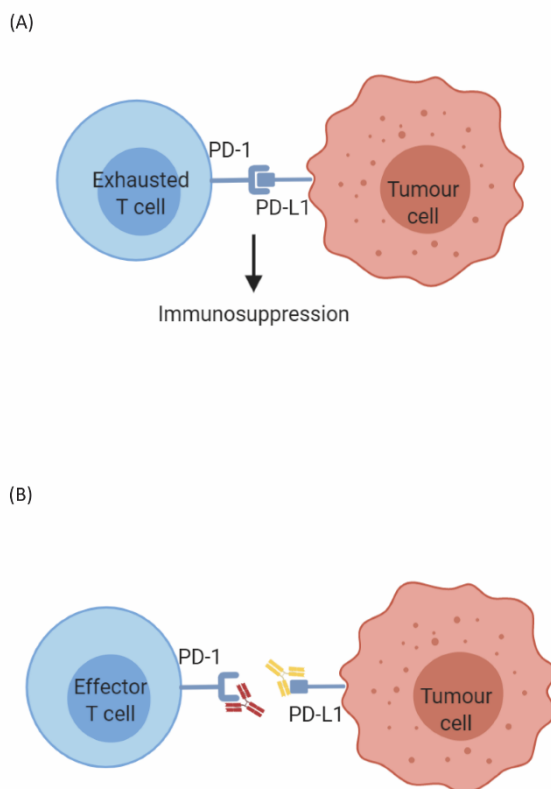


Figure 4 PD-1 and PD-L1 interaction and checkpoint inhibitors

(A) Mechanism of tumour immune evasion. The interaction of PD-1 on T cells with PD-L1 on tumour cells leads to immunosuppression and it is a (B) Immune checkpoint blockade. Monoclonal antibodies against PD-1 or PD-L1 are used as immunotherapy of cancer. By binding PD-1 or PD-(L)1, they prevent their interaction and immunosuppression.

1.3.7 Programmed cell Death Ligand 1 (PD-L1) expression in cancer

The PD-(L)1 axis has been shown to play a crucial role in cancer immunology [89]. PD-L1 is expressed in numerous cancers and PD-1 is overexpressed in T cells presenting an exhausted phenotype [95, 96]. The molecular mechanism through which cancer cells escape the immune response can be due – among other processes- to PD-1 and PD-L1 interaction which leads to immunosuppression (Figure 4A) [97, 98]. Also, PD-L1 expression on cancer cells can

be induced by IFN- γ [99], suggesting the idea that PD-L1 signalling is inducible and dependent to the immune microenvironment.

The role of PD-(L)1 axis on cancer immunology has promoted a new branch of immune-based cancer therapies. In this field, the blockade of PD-1 and PD-L1 interaction represents a strategy to prevent immunosuppression and improve the immune response against cancer (Figure 4B) [100]. PD-L1 expression in cancers has been considered a biomarker for immunotherapy in different cancer types including melanoma, lung and bladder [101]. However, knowledge of the molecular mechanisms at the basis of PD-L1 expression on cancers and the role of PD-1 and PD-L1 interaction in shaping the tumour immune microenvironment is still deficient.

Although PD-L1 expression has been shown to be a predictive biomarker for cancer immunotherapy efficacy [101], the idea of PD-L1 expression as unique and reliable parameter correlated to a beneficial response to the immune checkpoint therapy has been abandoned [102]. The expression profile of immune checkpoints has been demonstrated to be informative for some cancers [103-105]. However, PD-L1 expression as an exclusive parameter does not provide sufficient information on the immune response against cancer [102]. Other immune parameters such as the immune tumour infiltration (macrophages and TILs), and the production of cytokine (IFN- γ , IL-6, IL-17 etc.), chemokine (CXCL9 and CXCL10) and growth factors have been added to PD-L1 expression in the tumour for a more accurate prognostic evaluation [102, 104-106].

1.3.8 IFN- γ and PD-L1 expression

Among the parameters that characterize the cancer-immune microenvironment, IFN- γ has a major role in the cancer immunoediting and it has been associated with pro-inflammatory and anti-tumour functions [107]. Mutations in FN- γ signalling components often occur in cancer cells that become insensitive to the cytokine [108]. In addition to the anti-tumorigenic role, IFN- γ mRNA profile also predicts the response to PD-L1 blockade. In particular, the expression of IFN- γ -related genes such as CXCL10 and *granzyme B* correlates with response to PD-1 checkpoint blockade (Pembrolizumab) in melanoma patients [109]. The evidence of multiple genes involved in the regulation of IFN- γ in the tumour suggests a complex molecular mechanism. The production of IFN- γ by activated immune cells creates a pro-inflammatory tumour microenvironment with anti-tumorigenic properties. The induction of a pro-inflammatory response can also trigger the tumour escape processes. In this context, the interdependence of IFN- γ and PD-L1 expression has a crucial impact. PD-L1 positive tumours should be divided into two categories: (1) tumours that intrinsically express PD-L1

and (2) tumours expressing PD-L1 in response to IFN- γ [99]. In the first case, PD-L1 is merely reflecting the presence of the immune therapy target. In the latter case, PD-L1 expression is indicative of the tumour immune response. For instance, PD-L1 positive tumours can also be correlated with TILs and IFN- γ production [102].

1.3.9 Cancer immunotherapy: PD-1 and PD-L1 immune checkpoint inhibitors

Immuno-oncology is based on the concept that cancer cells tend to escape the immune response and cause an immune suppressive microenvironment that allows the tumour to grow. One of the reasons why immune therapies are thought to be a good approach to cancer is because of the immunoediting theory and the fact that the majority of tumour cells are immunogenic. Immune therapies against cancer include a wide range of approaches from vaccination with tumour antigens to the adoptive cellular therapy with anti-tumoural T cells. In this research, the main focus is the immunotherapy based on the blockade of PD-1 and PD-L1 interaction. The checkpoint inhibition is achieved with the development of monoclonal antibodies against PD-1 or PD-L1.

Several clinical trials on PD-1 and PD-L1 inhibitors have shown an anti-tumour efficacy of these agents. In particular, an anti-PD1 phase I clinical trial was started in 2010 in solid tumours including in melanoma, non-small cell lung cancer (NSCLC) and colorectal carcinoma [110]. The prospective of immune therapeutic agents was very promising for melanoma and a phase III trial with anti-PD1 antibody (Nivolumab) has led to the approval as anti-cancer agent by the Food and Drug Administration (FDA) in USA [111] [112]. Pembrolizumab, a mAb binding PD-1, is used in patients with advanced solid tumours and elicits better responses in patients with Merkel cell carcinoma and melanoma [113]. Nivolumab is another anti-PD-1 mAb used in a phase 3 trial for melanoma in addition to CD8⁺ T cell vaccination [111]. This therapeutic approach increases the number of antigen specific T cells including CD3⁺, CD4⁺ and CD8⁺ TILs and IFN- γ secreting cells with augmented tumour-cytolytic effector activity [111, 114]. Anti-PD-L1 mAbs also have been tested in a multicentre phase I trial to patients with advanced cancers including non-small-cell lung carcinoma (NSCLC), melanoma and renal-cell carcinoma [115]. PD-L1 blockade showed an induced tumour regression in 6%-17% of the cases and a stabilization of the disease [115]. In a phase I clinical trial in metastatic urothelial bladder cancer, Anti-PD-L1 mAb has been proven to shrink the tumour in 43% of the patients [116].

The evaluation of immunotherapy in the clinic has been weakened by the fact that a single agent with a specific target is unlikely to overcome complex dynamic mechanisms that drive the tumour immune microenvironment. In addition, tumours adapt to changes and they can

develop resistance to the targeted monotherapy. The combined therapy with other anti-cancer agents may therefore improve immunotherapy efficacy. Immune checkpoint inhibitors can be combined to different drugs such as immune regulators such as mAbs against cytotoxic T-lymphocyte associated protein-4 (CTLA-4), lymphocyte-activation gene 3 (LAG-3) and T-cell immunoglobulin and mucin protein (TIM-3) [117]. Other experimental therapies include the combination of immune checkpoint inhibitors with agents targeting metabolic enzymes such as indoleamine 2,3-dioxygenase (IDO). IDO is expressed in tumour and immune cells and inhibits the immune response via the catalysis of essential amino acids such as tryptophan, essential for immune functions. IDO inhibitors are being tested as immunotherapeutic agents alone or in combination with other immunotherapies [117]. Other combination strategies involve adjuvants that promote the antigen presentation process and enhance the pro-inflammatory Th1 and macrophages response. These adjuvants include Toll-like receptor (TLR) agonists and anti-CD47 mAbs [117]. Immunotherapy is often combined to classical anti-tumour approaches such as radiotherapy and chemotherapy. In particular, localized radiotherapy is useful in debulking the tumour and enhancing immunity by the release of immune molecules in response to the cellular damage. The association of immunotherapy with chemotherapy is based on the same principle: the ability of the chemotherapeutic agents to damage tumour cells enhances the immune response [117]. One of the limitations in the application of immunotherapy to solid tumours such as ovarian cancer is an efficient immune cell infiltration into the tumour mass. First, the baseline of TILs in the tumour has an important prognostic value. In addition, tumours with TILs are more responsive to immunotherapy [118]. The immune escape is regulated by several molecular processes involving soluble factors that can drive immune cell recruitment. In particular, the vascular endothelial growth factor (VEGF) has been proven to have an important role in the inhibition of TILs recruitment in the tumour microenvironment [119]. VEGF has also been shown to have immunosuppressive functions by inhibiting T cell development [120]. The suppression of T cell activity, especially the cytotoxic effector activity has been shown in peripheral immune cells and also in T cells derived from epithelial ovarian cancer ascites [121, 122]. This evidence has developed a new therapeutic strategy inhibiting the VEGF-mediated immunosuppression and enhancing the T cell tumour infiltration [123]. VEGF inhibitors (e.g. Bevacizumab) have shown a good clinical impact in NSCLC and metastatic colorectal cancer [124, 125]. Bevacizumab is also used in clinical trials in combination with PD-(L)1 inhibitors [126, 127].

1.3.10 PD-(L)1 blockade in ovarian cancer

In ovarian cancer, Hamanishi et al demonstrated the prognostic value of PD-L1 expression and CD8⁺ T cell-specific immune infiltration [82]. This has encouraged more studies to develop immune therapies to target PD-(L)1 molecular interaction. Although the PD-(L)1 blockade has shown potential in other cancers, its efficacy in ovarian cancer is still improving. The promotion of a combined therapy with PD-(L)1 blockade and other type of therapies is the current approach in ovarian cancer research [128, 129]. A multiple immune therapy was proposed with anti-PD-1/PD-L1 and anti-CTLA-4 antibodies or a combination of PD-(L)1 blockade with chemotherapy [130]. Combined PD-1 or PD-L1 blockade with chemotherapy (gemcitabine or paclitaxel) was tested in a mouse model of ovarian cancer showing that mice treated with combined therapy showed a TIL enriched tumour microenvironment and better survival compared to the monotherapy group [131]. Recent studies have proposed a combined therapy anti-PD-(L)1 and anti-VEGF monoclonal antibodies. A phase II clinical trial using nivolumab (anti-PD-1) and bevacizumab (anti-VEGF) in women with recurrent epithelial ovarian cancer (EOC) has shown a 21% increase in the clinical efficacy of checkpoint blockade and a progression-free survival of 9.4 months compared to platinum-based therapy [132].

Contrarily to expectations, PD-(L)1 blockade did not showed a major impact on the immune system functionality. Adverse immunological effects include fatigue, rash, pruritus, nausea and diarrhoea [112]. Serious adverse effects are rare (less than 10%) and include pneumonitis, sever skin reactions and colitis with gastrointestinal perforation [133].

PD-(L) 1 blockade presents some limitations. Patients treated with PD-(L)1 inhibitors experienced an initial response with a decrease of efficiency later on and resistance that occurs in most of the cases . The reason for the immune checkpoint blockade failure can be due to an evolution of cancer antigens or in a selection of resistance cancer clones [134]. The selective clonal pressure on cancer cells leads to neoantigen loss and non-immunogenic genomic aberrations [135].

1.3.11 Cancer immunogram

One of the improvements in cancer screening is the evaluation of the immune response and the prediction of the immunotherapy efficacy. Although the histopathological, molecular and genetic classification of a cancer is a fundamental diagnostic tool, this cannot be sufficient to predict the efficacy of immunotherapy. In this context, the cancer immunogram represents a framework based on a series of parameters indicating the likelihood of a tumour to response to immunotherapy and an assessment for a personalised therapy [136]. The

principal paradigms of the cancer immunogram and their correlation with PD-(L)1 blockade are listed below.

- Tumour mutational burden

The clinical efficacy of checkpoint blockade is measured by the evaluation of the objective response rate (ORR), a parameter based on the proportion of patients undergoing PD-(L)1 inhibitor therapy who achieved 30% decrease in target tumours [137]. PD-(L)1 inhibitors have been proven to be more effective in tumours carrying a high number of mutations in their genome [137, 138]. Genetic alterations work as neo-antigens increasing the immunogenicity of the tumour and triggering the immune response to cancer. Tumours with high mutational burden such as melanoma and non-small cell lung carcinoma (NSCLC) are highly immunogenic and respond better to checkpoint inhibitors [137]. An integrated genomic analysis of ovarian cancer specimens evaluating the genetic aberrations has shown that ovarian cancer mutations depend on the histological type of cancer. Generally, ovarian cancers present low prevalence of recurrent mutations and the ORR of patients treated with PD-(L)1 inhibitors is between 10% and 15% [139, 140].

- Immune cell infiltration

One of the most important requirements for checkpoint blockade efficacy is the tumour immune infiltration [102]. Monoclonal antibodies used as checkpoint inhibitors prevent the interaction between PD-1 on T cells and PD-L1 on cancer cells. In order to induce their effect, the presence of T cells in the tumour microenvironment is necessary. The presence of TILs is a prognostic parameter in several cancers including ovarian cancer [141]. Tumours are divided into “hot”, if they are immune infiltrated, or “cold”, if they have no TILs. Cold tumours are also divided into “immune desert” and “immune excluded”. Immune desert tumours are non-inflamed tumours with immunological ignorance as a main feature. This characteristic occurs when the immune system do not recognise the cancer neo-antigens and cannot produce an immune response [142]. Immune excluded tumours are immunogenic types of tumour that exhibit the immune privilege to be protected from immune infiltration [143]. This phenomenon is driven by a dysfunction of many processes regulating the immune cell infiltration. In order to invade the tumour, immune cells need to leave the blood stream. The extravasation process is led by adhesion molecules such as intracellular adhesion molecules (ICAM), vascular adhesion molecules (VCAM) and the endothelial leukocyte adhesion molecule (E-selectin) and the overexpression of these molecules has been associated with tumour immune infiltration in NSLC [144]. In a tumour, blood supply is provided by the formation of new vessels by a process called angiogenesis. This process is supported by the

production of the vascular endothelial growth factor (VEGF) in the tumour [145, 146]. Expression of VEGF has been associated with a reduced T cell infiltration in the tumour [147]. The immune infiltration is also guided by the chemokines (e.g. CXC chemokines and CCL2) production in the primary tumour [148].

- PD-(L)1 expression

It seems obvious that the expression of the immunotherapy target is important for the efficacy of the therapy itself. PD-L1 expression in cancers has been considered a biomarker for immunotherapy in different cancer types including melanoma, lung and bladder [101]. However, the expression of PD-L1 in tumour tissues as parameter to evaluate the immunotherapy response has been demonstrated to not be very effective. Other parameters such as the TMB and immune infiltration have shown a much more significant correlation with the tumour ORR [90, 137]. To further understand the value of PD-L1 expression as a prognostic marker for checkpoint blockade therapy, PD-L1 positive tumours should be divided into two categories: (1) tumours that intrinsically express PD-L1 and (2) tumours expressing PD-L1 in response to IFN- γ [99]. In the first case, PD-L1 is merely reflecting the presence of the immune therapy target. In the latter case, PD-L1 expression is induced by the anti-tumour immune response.

- Tumour cell metabolism

A particular metabolic feature of cancer cells is the aerobic glycolysis. Although glycolysis is a metabolic process activated by oxygen deprived cells, cancer cells convert glucose in lactate activating the glycolytic pathway even in non-hypoxic conditions [102]. This metabolic switch correlates with high levels of lactate dehydrogenase (LDH) to metabolise the lactate produced by the aerobic glycolysis. High LDH levels correlates with poorer outcome upon PD-(L)1 blockade [149]. Furthermore, the accumulation of lactate makes the tumour pH particularly acid which can impair immune functions [150].

1.4 3D tumour spheroid model

In vitro models consist of cells growing outside their normal biological context; the most used *in vitro* cell culture model used specific lab ware such as flasks or petri dishes in order to grow cells. A single cell suspension can grow in a flask forming a monolayer of cells on the bottom with cell medium on top providing nutrients. This experimental model is known as “2D cell culture” because cells are allowed to grow on a flat surface [151]. A new model for cell culture is the 3D spheroid model, in which cells grow in a 3D shape to recreate the *in vivo* growth. This model is considered more accurate and physiologically relevant compared to 2D cell cultures.

Cancer therapy is quickly evolving and the pre-clinical cancer research needs more accurate models to test new treatments. 3D tumour cultures are obtaining more attention as cancer models for their unique properties.

1.4.1 Advantages of 3D tumour spheroids

The advantage of the 3D model is that the aggregation of cells mimics the *in vivo* tumour structure. In spheroid, interconnections between cells and extracellular matrix form a compact 3D mass [152, 153]. Cells are distributed in different layers; the outside layer is directly exposed to the microenvironment while the inner core of the spheroid presents quiescent cells [152]. For the typical 3D structure and the spatial architecture, the penetration of drugs into the 3D structure follows a gradient of diffusion with external cells exposed to higher concentration compared to cells in the inside of the spheroid. Oxygen follows this gradient of diffusion as well creating a hypoxic center which resembles the hypoxic cores in tumour masses [154]. Another important feature of 3D models is the cell-cell and cell-matrix interaction and the potential to form spheroids co-culturing cancer cells with other types of cells [155, 156]. Spheroids are also useful to study tumour invasion and migration.

Although the 3D culture model represents an important improvement in cancer research, it presents some limitations. *In vivo*, tumours present a much more complex network of interaction, including other organs and the blood stream. The lack of blood vessels is an important limitation of this model because it drives important processes such as the immune cell extravasation and the metastasis spread. The model also presents experimental limitations. Some of the techniques to obtain spheroids have high cost of development and the reproducibility can be affected by the specific spheroid method. In addition, the numerous applications of the model together with experimental designs and analyses are still under optimization.

1.4.2 Techniques to generate spheroids

3D spheroids are generated with different experimental techniques. The most relevant are listed below.

- NASA rotating bioreactor

This technique was theorised at NASA's Johnson Space Center, where scientists thought to recreate the microgravity conditions to allow cells not to settle on the bottom of the culture container [157]. The bioreactor consists of a rotating wall vessel where cells are seeded on a porous substrate allowing gas exchange through a membrane [158, 159]. The continuous rotation of the vessel let the cells grow in 3D agglomerates. This model is excellent to study cell metabolism and for the creation of artificial tissues. By growing in the hollow of a fiber, the growth is constraint by the fiber wall, which is also a barrier between the spheroid and the culture medium [152].

- Scaffold-based culture

Bio-polymers such as collagen are used to form a gel matrix where cells can grow. In the matrix, cells form multi-layers and cells aggregates. This model recreates the tissue specific architecture and it is useful to study the cell-cell interactions, migration and invasion. Since the scaffold can limit the diffusion of soluble compounds, this method is inadequate to study drug response [152]. To improve the study of drug diffusion, the multicellular layer 3D model was introduced [160]. In this model, cells are grown on layers of collagen coated membranes. Although this model is useful for flux measurements, the cell multilayers do not recreate the *in vivo* tissue architecture [161].

- Hanging drop culture

In this technique, cells are growing in suspension in a small drop hanging on a cover slip. This method leads to the production of 3D spheroids rapidly and allows co-culture with different cell types. However, this method also presents some limitations due to the fact that the treatment is not possible [152].

- Non-adhesive coating

This technique uses ultra-low attachment plates to prevent cell attachment on the bottom surface. In this method cells grow in suspension in their culture media and form 3D spheroids [152]. This methodology presents multiple advantages such as the possibility of treating the spheroids directly in the culture media with the recreation of the *in vivo* gradient of diffusion. In addition, multicellular spheroids can be obtained by co-culturing different types of cells. The limitations of this technique are related to the difficulty of handling spheroids in suspension.

1.4.3 A 3D spheroid model of ovarian cancer and multicellular spheroids

One of the characteristics of solid tumours is their complex architecture which includes several cell types and extracellular matrix in a growing three-dimensional mass. Understanding the influence of the spatial structure of a tumour on the molecular mechanisms affecting cancer is crucial to investigate the progression of the tumour and the immune response [162]. Chapter 4 will illustrate the importance of the 3D spheroids in studying the immune infiltration, the response to hypoxia and the metabolic balance of ovarian cancer cells.

The main improvement of using a 3D spheroid model instead of a classic 2D cell culture is that it allows for the recreation of the architecture of the tumour mass. Furthermore, the establishment of multicellular spheroids with cancer and immune cells allows the evaluation of the interaction between the two cell types. Dealing with three-dimensional cell agglomerate improves the quality of the research by recreating some of the *in vivo* tumour features that cannot be easily reproduced *in vitro*.

1.4.4 Response to hypoxia in 3D spheroids

Hypoxia is a cellular response occurring when cells are deprived from the physiological levels of oxygen [163]. In mammals, the hypoxic stress is regulated by the hypoxic-inducible factors (HIFs) that modulate the expression of genes involved in several cellular processes such as metabolism, vascular remodelling, tumour progression and inflammation. In normal oxygen conditions, HIFs are hydroxylated at proline residues by specific enzymes (proline hydroxylases, PHDs) and form the Hippel-Lindau (VHL)-elongin B/C complex which is destroyed via ubiquitin-proteasome activity [164]. In an environment with low oxygen availability, PHDs are inhibited, HIFs are stabilized and mediate the expression of genes involved in pathways protecting cells from hypoxia [165]. Thus, the regulation of the proteasome components and the formation of (VHL)-elongin B/C complex depends on the availability of oxygen in the specific tissue microenvironment [165].

In the growing tumour mass, inner zones where the nutrients and oxygen struggle to penetrate create hypoxic cores. The lack of oxygen activates hypoxia-inducible factors (HIFs) that have an impact in the progression of the tumour and on the immune response [162]. In tumour spheroids, the spatial architecture of the tumour mass exposes cells to a concentration gradient of nutrients and treatments. Therefore, cells in the inner core of the spheroid are exposed to lower levels of oxygen and they can activate the hypoxia response [166].

1.4.5 Metabolic competition in the tumour microenvironment

The tumour microenvironment comprises non-tumour cells (e.g. fibroblasts and immune cells), the extracellular matrix (ECM) and soluble molecules (e.g. growth factors, cytokines and chemokines). The tumour relationship with the other cellular components of the microenvironment involves mechanisms that are critical in the progression of the tumour and can result in the elimination of the cancerous cells or the establishment of a pro-tumour milieu. The reason why the immunoediting process leads to the elimination of some cancers while in others the immune response fails supporting the tumour progression is still not clear. Among several mechanisms through which the tumour can escape the immune response, we evaluate a new interesting field of research based on metabolic competition. This hypothesis takes into consideration the variety of cells in the tumour microenvironment that competes for nutrients and oxygen to support their growth. Although angiogenesis aims to form new blood vessels to support tumour growth, the growing mass usually lacks in blood supply with formation of hypoxic inner cores. Therefore, the struggle of nutrients to penetrate the tumour mass makes the metabolic challenge more accentuated.

The upregulation of glycolysis in tumours produces higher levels of lactic acid which has a critical role in immunosuppression. Lactic acid suppresses CTLs proliferation of cytokine production resulting in a reduced cytotoxic activity [167]. After their activation, T cells induce glycolysis which is essential to support their effector functions. Since tumour and immune cells compete for glucose, malignant cells can strategically increment their glucose intake to suppress immune cell activity. A study using a mouse sarcoma model confirmed this hypothesis showing that glucose restriction in T cells in the tumour microenvironment alters the immune metabolism and effector functions [168]. This study has shown that immune cells co-cultured with cancer cells produced less IFN- γ , as confirmed also by our results in chapter 3. The decrease in IFN- γ is modulated, among other mechanisms, by the glucose restriction and mTOR activation. In line with this, addition of glucose to the co-culture media or the inhibition of mTOR activity increased the IFN- γ production [168]. This evidence shows that the modulation of metabolic pathways cooperates with other processes that lead to immunosuppression. In the tumour microenvironment, the metabolic alteration can be part of the escape program initiated by the tumour to induce immune dysfunction and allow tumour growth.

1.5 Hypothesis

The overarching hypothesis of this research is that adrenergic stress influences the immune response to ovarian cancer and cooperates to reduce the efficacy of PD-(L)1 checkpoint blockade. This research suggests a combined therapy with PRO and PD-(L)1 inhibitors to overcome the stress-induced immunosuppression and improve the PD-(L)1 inhibitor efficacy.

1.6 Aims of the thesis

The main goal of this thesis is to present a therapeutic approach with translational potential to improve PD-(L)1 checkpoint inhibitor efficacy in ovarian cancer.

On the basis of our hypothesis, this research focuses on the effects of adrenergic stress in the immune response to ovarian cancer. The adrenergic immune regulation in ovarian cancer will be explored in this thesis with the aim to:

- Examine the effects of NA and PRO on immune cells.
- Examine the effects of NA and PRO on ovarian cancer cells.
- Elucidate the molecular mechanism by which adrenergic stress affect PD-L1 expression on ovarian cancer cells.
- Develop a 3D spheroid model to study the immune and ovarian cancer cell interaction and how this is influenced by NA, PRO and stress.
- Test a combined therapy with PRO and PD-(L)1 inhibitor in a orthotopic syngeneic mouse model of ovarian cancer.
- Explore how PRO and/or PD-(L)1 inhibitor shape the immune signature of ovarian cancer.

1.7 Original contribution to knowledge

Although immunotherapy represents an approach to several cancers such as melanoma and renal cell carcinoma, the same efficacy has not been proven in ovarian cancer [81, 99]. With scientific evidence supporting that ovarian cancer is an immunogenic type of cancer, the current research focuses on the optimisation of immunotherapeutic strategies [100]. Inspired from the existing literature in the field of psychological stress affecting cancer progression, this research proposed a link between the ovarian cancer immunity and the adrenergic stress signalling [41, 101-104]. Exploring the biological effects of stress in ovarian cancer is important, as scientific evidence of psychological factors influencing the clinical outcome of the disease is currently supported [105-107]. Clinicians also agree that a major distress is experienced by cancer patients exhibiting symptoms of post-traumatic stress disorder, anxiety and depression [108]. In particular, the diagnosis of ovarian cancer is highly traumatic due to the devastating nature of existing therapies and the high mortality rate of

the disease [109]. The ambitious novel contribution of this research is to prove that the adrenergic signalling pathway regulates the immune response to ovarian cancer through a biological mechanism which influences the response of the tumour to PD-(L)1 blockade. This research also has the goal to provide fundamental knowledge for further investigation. In particular, several experimental models were optimized and represent a foundation for future studies.

2. Chapter 2 - Materials and methods

2.1 In vitro models

2.1.1 Ovarian cancer cell culture

The ID8 mouse cell line was kindly provided by Dr Premal Thaker, Washington University, St. Louis, USA (Material Transfer Agreement (MTA) in place). The cell line was grown in Dulbecco's Modified Eagle Medium (DMEM, Gibco) with 4% Foetal Bovine Serum (Gibco) and a supplement of Insulin-Transferrin-Sodium Selenite (Sigma-Aldrich).

Human ovarian cancer cell lines SKOV3ip1 and OVCAR8 were kindly provided by MD Anderson Cancer Center, Houston, USA (MTA in place). SKOV3ip1 were cultured in McCoy's 5a medium modified (Gibco) and 10% Foetal Bovine Serum (Gibco). OVCAR8 cells were cultured in RPMI 16490 medium with 10% Foetal Bovine Serum (Gibco).

All cells were cultured in T-75cm² filtered tissue flasks at 37°C, 5% CO₂. When cells reached 80-90% confluence they were passaged discarding the growth medium and detached using trypsin-Ethylene Diamine Tetra Acid (EDTA). Trypsin was inactivated after 2-3 minutes with fresh medium and the single cell suspension was centrifuged for 5 minutes at 500g. Supernatant was discarded and cells were re-suspended with growth medium, counted and seeded in the appropriate number (≈ 1 or 2×10^6 cells) in a T-75cm² flasks. Cell lines are routinely screened for mycoplasma contamination. Regulations to prevent issues such as cross-contamination, microbial contamination and phenotypic drift and validated as described in UKCCCR Guidelines for the Use of Cell Lines in Cancer Research (2000) [169]. This is enforced whereby only one cell line is handled at any one time and cells are passaged no longer than 3 months.

2.1.2 Hormones treatments

The concentration of the adrenergic hormone NA used to treat cells *in vitro* is generally 10^{-7} M because this is equivalent to physiological levels of the circulating hormone during stress conditions [170]. Since PD-L1 expression is the focus of the research, the ID8 murine ovarian cancer cell was exposed to different concentrations of NA and Real Time PCR was performed to evaluate the hormone concentration that stimulates cancer cells to express PD-L1. In consideration of the literature (Lutgendorf et al. 2003 [46]) and our protocol optimization, we used a concentration of NA (Norepinephrine Bitartrate salt, Sigma Aldrich) of 10^{-6} M for 24h.

The effect of NA in stimulating the adrenergic signalling pathway was pharmacologically blocked using Propranolol Hydrochloride (PRO) (Sigma Aldrich), a non-selective β -adrenergic

receptor (ADRB) blocker, at a concentration of 10^{-6} M [40, 46]. In order to efficiently inactivate the β -adrenergic receptors, PRO was added 30 minutes prior NA.

2.1.3 Cytokine treatments

Interferon-gamma (IFN- γ) is a pro-inflammatory cytokine produced by a large type of cells including T lymphocytes and cancer cells [69]. Cells were exposed to recombinant IFN- γ (Peprotech) at a concentration 20ng/ml for 24h as described by Abiko et al. [171]. To optimize the protocol, cell lines were also exposed to different concentrations (from 20ng/ml to 20pg/ml) of recombinant mouse IFN- γ alone or in combination with NA 10^{-6} M for 24h.

2.1.4 Splenocytes culture

Splenocytes were isolated from a fresh mouse spleen, mashed by placing them in a 40 μ m cell strainer and using a sterile syringe plunger. The strainer was positioned on a 50ml tube and growth media (RPMI and 10% FBS) was added. The single cell suspension containing splenocytes was centrifuged at 300g for 10 minutes and cultured RPMI 10% FBS. The whole single cell suspension was used in further experiments and cell viability was assessed by trypan blue exclusion (>95%) as per lab routine practice.

2.1.5 Splenocytes activation *ex vivo*

To optimise this procedure, splenocytes were activated *ex vivo* using different stimulants.

- CD-3 and CD28 stimulation with antibodies

A 6 well plate was coated with a mouse anti-CD3 monoclonal antibody (eBioscience) 5 μ g/ml O/N at 4°C or 2h at 37°C. Cells were seeded in the pre-coated wells in their relevant growth medium supplemented with a mouse anti-CD28 monoclonal antibody (eBioscience) 2 μ g/ml. Cells were incubated at 37°C, 5% CO₂ for 24h or 48h, harvested and screened for activation markers and IFN- γ production. Although this method allowed a T-cell specific activation, it was time consuming and problematic when assessing immune and cancer cells in co-culture. In particular, the level of activation was dependent on the cell number/anti-CD3 antibody ratio and there was a great loss of cells during the harvesting from the anti-CD3 coated plate.

- PMA/Ionomycin stimulation

A second protocol, based on culturing cells in medium supplemented with Phorbol 12-myristate 13-acetate (PMA) and Ionomycin, was used to activate immune cells *ex vivo*. PMA activates protein kinase C (PKC) which is enhanced by the Ionomycin, an ionophore that increase the intracellular level of Calcium (Ca⁺²). PMA and Ionomycin trigger the NF-AT and Ras signalling pathway mimicking the signalling of the T cell receptor (TCR) and its co-stimulus on CD28. These stimuli activate nuclear factors such as NF- AT, AP-1 and NF-KB

which bring to the expression of effector cytokine genes (IL-2 and IFN- γ) (Figure 5) [172]. Previous scientific evidence has shown that this method of *ex vivo* T cell activation is optimal to stimulate IFN- γ production[173].

The protocol was optimized for our specific purpose and cells were harvested and cultured in RPMI, 10% FBS supplemented with PMA 50ng/ml and Ionomycin 1 μ g/ml for 3h or 24h. This method was considered the most functional based different aspects: an efficient T-cell specific activation was achieved keeping the cells in a suspension culture; the cell yield was improved at the end of the process; it was possible to experiment shorter time points of activation; cells produced detectable IFN- γ after activation.

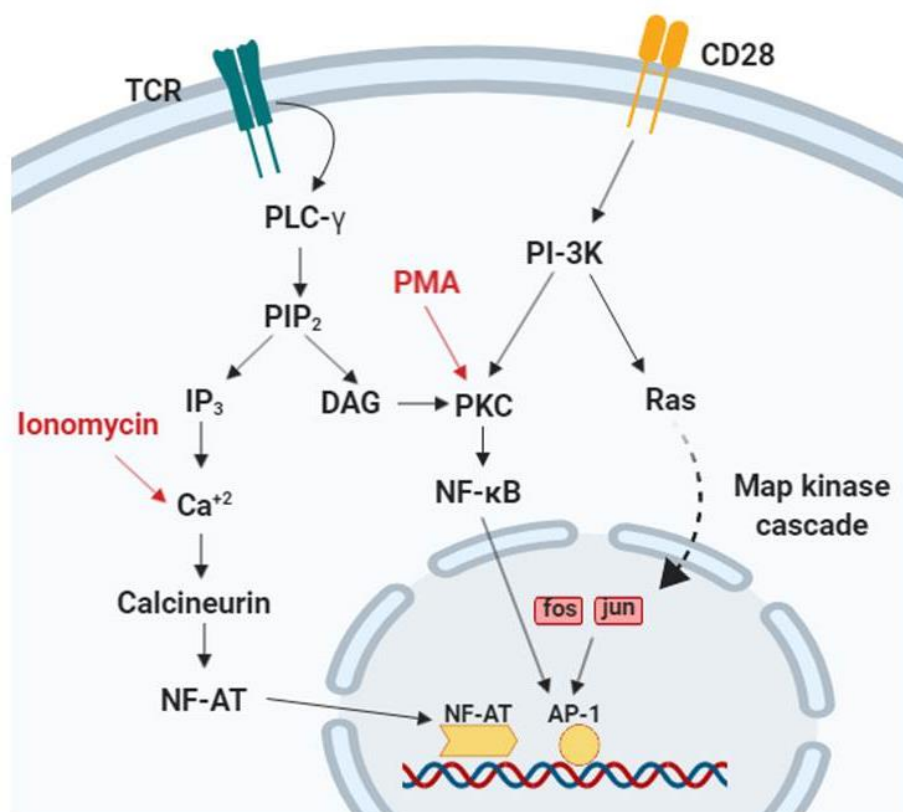


Figure 5 T-cell activation signalling pathway.

T-cell activation starts with the recognition of the antigen-MHC complex by the T-cell receptor (TCR) and a co-stimulatory stimulus on CD28. The TCR signalling involves the activation of the phospholipase C (PLC- γ) which cleaves the Phosphatidylinositol bisphosphate (PIP₂) into inositol trisphosphate (IP₃) and diacylglycerol (DAG). IP₃ stimulates the release of Ca²⁺ from the endoplasmic reticulum (ER) activating Calcineurin and allowing the translocation of the transcription factor NF-AT into the nucleus. DAG activates protein kinase C which activates the nuclear factor NF- κ B.

CD28 is associated with the phosphatidylinositol 3-kinase (PI-3K) which contributes to the activation of PKC and - at the same time - activates the Ras-dependent map kinase cascade which leads to the control of the transcription factor AP-1 through *fos* and *jun*. NF-AT and AP-1 transcription factors regulate the expression of genes sustaining cell proliferation and the production of effector cytokines such as IL-2 and IFN- γ .

Phorbol 12-myristate 13-acetate (PMA) is a phorbol ester used for the activation of the PKC. Ionomycin is an ionophore used to release Ca²⁺ from intracellular store such as ER. The combined stimulus from PMA and ionomycin activates NF-AT and AP-1 resulting in T-cell activation and effector cytokine production.

Trans-well co-culture: cancer cells and splenocytes

In order to avoid immune rejection, cancer cells and splenocytes were derived from the same species and strain of mouse (e.g C57BL/6 mice). To obtain a cancer antigen specific T cell activation, splenocytes derived from a C57BL/6 mouse were co-cultured with ID8 cancer cells. Splenocytes were pre-treated with a red blood cell lysis buffer (155mM NH₄Cl, 12mM NaHCO₃, 0.1 mM EDTA) and activated with PMA/ionomycin with or without the addition of NA or PRO and NA. After 24h cells were harvested and centrifuged at 300g for 10 minutes. The media was saved for further analysis and cells were re-suspended in fresh growth media and seeded in a 6 well plate with 2x10⁶ splenocytes per well. An insert with 0.8 µm pores (MERK Millicell Cell Culture Insert) was placed in each well and 50,000 ID8 cells were seeded with 1ml of ID8 complete growth media. Cells in co-culture were incubated at 37°C, 5% CO₂ for 24h.

2.1.7 3D spheroids model

Ovarian cancer spheroids were generated using a Coning Costar Ultra-low attachment 96 well plate (Sigma Aldrich) following the non-adhesive coating method illustrated in section 1.4.2. Cells were detached from a 2D cell culture using a cell scraper, re-suspended in the relevant growth medium and seeded at a density of 3,000 cells in 30µl of medium per well, then plate was centrifuged for 5 minutes at 300g. In order to form three-dimensional structure, cells were incubated at 37°C, 5% CO₂ for a week adding fresh media daily.

2.1.8 3D spheroid co-culture: cancer cells and splenocytes

ID8 cells in a single cell suspension were incubated with DiO (Excitation: 484nm; Emission: 501nm), a lipophilic tracer (Invitrogen) for at least 2h at 37°C, 5% CO₂. ID8 cells were seeded in an ultra-low attachment 96 well plate following the 3D spheroid protocol (3,000 cells in 30µl of medium per well). Cells were incubated at 37°C, 5% CO₂ for a week to let them aggregate into three dimensional spheroids.

Splenocytes activated *ex vivo* with PMA/Ionomycin with or without the addition of NA or PRO and NA were incubated with Dil (Excitation: 549nm; Emission: 565nm) lipophilic tracer (Invitrogen) for at least 2h at 37°C, 5% CO₂. 9,000 splenocytes were added to each spheroid in an ultra-low attachment 96 well plate and centrifuged for 5 minutes at 300g.

2.1.9 3D spheroid imaging

Each spheroid was imaged using confocal microscope (Leica). Microscope was set on 10x magnification, focused and a fluorescence excitation at 488nm was used to excite the

lipophilic dyes. Images were acquired using a sequential scan with two filters with different emission wavelengths ranges (DiO: 480-530nm, DiL: 550-630).

2.1.10 3D spheroid imaging: acquisition of data

Images were processed using CellProfiler 3.1.8 and a specific pipeline was used to acquire data for future analysis. Colour images were split into separate grayscale images to divide the acquisition with the two different wavelength ranges (green: spheroids; orange: splenocytes). A primary object was identified as “spheroid” using a diameter between 100 and 500 pixel units. This module was used to automatically identify the spheroid in the image and discard objects outside the provided range [174]. With this module small aggregates of cells were not recognized as “spheroids”. However, in some images more than one object was recognized as a “spheroid”. In these cases, only the object with the highest surface area was considered for the analysis. The splenocytes intensity (orange) was measured in the object recognized as “spheroid” to evaluate the level of splenocytes intensity inside the spheroid. Also, the splenocytes intensity (orange) in the whole image was measured to assess the intensity of the splenocytes outside the spheroid. The size and shape of object recognized as “spheroid” was measured taking into consideration the surface area, the eccentricity and solidity [175]. The surface area (2D) is an indication of the spheroid size counting the number of pixels in the region considered. The eccentricity (2D) (e) is the ratio of the distance between the ellipse foci and its major axis length. This range between 0 and 1, where $e=0$ is the degenerate case of a circle and $e=1$ is the degenerate case of a line segment [176]. The eccentricity value is taken as an indication of how circular the spheroid is. Solidity (2D only) is the proportion of the pixels in the convex hull that are also in the object recognized as “spheroid”. This value is an indication of how solid or fragmented the spheroid is.

2.1.11 3D spheroid imaging: analysis

To quantify the splenocytes “infiltration” into the spheroid the splenocytes intensity (orange) measured in the object recognized as “spheroid” was divided by the area of the object recognized as “spheroid” to obtain a relative intensity to the area.

$$\begin{aligned} \text{relative intensity}_{infiltration} \\ = \text{integrated intensity}_{splenocytes} \div \text{surface area}_{spheroid} \end{aligned}$$

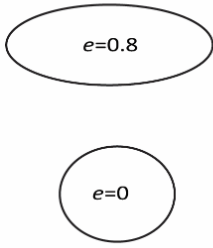
Pipeline step	Specifications	Description
Colour to grey	Convert red to grey. Convert green to grey.	A multichannel colour image is converted into multiple grayscale images. The channels of the colour image were split into separate grayscale images.
Identify primary object	Typical diameter of object: min 100 pixel units, max 500 pixel units	Automatic identification of the spheroid.
Measure object intensity	Object to measure: spheroid (primary object) Intensity to measure: splenocytes (red to grey conversion)	Measure of the splenocytes intensity into the spheroid area.
Measure image intensity	Object to measure: the entire image Intensity to measure: splenocytes (red to grey conversion)	Measure of the splenocytes intensity in the entire image
Measure object size and shape	Object to measure: spheroid (primary object) Surface area Eccentricity Solidity	Measure of the spheroid size and shape. Surface area: area of the spheroid surface. Eccentricity (e): indication of the spheroid roundness.  Solidity: indication of the spheroid fragmentation.

Table 3 CellProfiler pipeline for spheroid analysis

Spheroid images were processed using CellProfiler 3.1.8 and the specific pipeline was used to acquire data for future analysis.

2.2 Orthotopic *in vivo* model of ovarian cancer

2.2.1 Syngeneic mouse model of ovarian cancer

For this project, an immune competent syngeneic orthotopic mouse model was required to study the immune signature and the role of immune cells in ovarian cancer. *In vivo* experiments were conducted under a Project License and the procedures were carried out by myself (PiL/PpL holders: 70/8361; 197B25F01) with the help of expert personnel.

Mice were handled by an expert operator every day for two weeks before any experimental procedure; this allows the animals to adapt, recognize the operator and reduce their stress during any type of procedure. A schematic timeline of the *in vivo* procedures performed is shown in Figure 6.

Malignant mouse ovarian epithelial cells (ID8) were injected intraperitoneally (IP) in C57BL/6 female mice. Many scientific aspects and the animals' welfare were evaluated to decide the best experimental procedure. To optimize the protocol, we considered previous experiments with the same syngeneic model where 4×10^6 ID8 cells were injected IP. 9 weeks after cancer cells' injection, mice started to show signs of ascites and they presented a late stage ovarian cancer mostly spread into the peritoneal cavity. The new protocol was designed considering the necessity of an early stage tumour in order to assess the immune response into the primary tumour. In addition, the experiment length was strictly regulated by the osmotic pump (Alzet) release duration of 6 weeks. After these considerations, we calculate to inject 7×10^6 ID8 cells IP [177] and the end of the experiment was established at 4 weeks after cancer cell injection or at any signs of ascites.

Mice were randomised into 5 groups and all received cancer cells' injection. Within the groups, one was not exposed to restraint stress (Control) and the others underwent restraint stress (RS) and treatment with either a beta-blocker (PRO), PD-(L)1 inhibitor (PD-(L)1i) or both (Combo) as listed in Table 4.

Group name	Number of mice	Cancer	Stress	PRO	PD-L1 inhibitor
Control	8	7x10 ⁶ ID8 cells (IP)	no	No	No
RS	8	7x10 ⁶ ID8 cells (IP)	2h daily	No	No
RS+PRO	8	7x10 ⁶ ID8 cells (IP)	2h daily	2mg/Kg/d via osmotic pump	No
RS+PD-(L)1i	9	7x10 ⁶ ID8 cells (IP)	2h daily	No	200µg/mouse (IP)
RS+Combo	8	7x10 ⁶ ID8 cells (IP)	2h daily	2mg/Kg/d via osmotic pump	200µg/mouse (IP)

Table 4 Scheme of mice groups and treatments

Mice were randomised into 5 groups and all received cancer cells' injection. Within the groups, one was not exposed to restraint stress (Control) and the others underwent restraint stress (RS) and treatment with either a beta-blocker (PRO), PD-(L)1 inhibitor (PD-(L)1i) or both (Combo).

2.2.2 Osmotic pump implantation for Propranolol release

In order to block the adrenergic signalling, a constant administration of PRO was required. Daily IP injections of PRO were considered as an appropriate administration method. However, daily injections represent a chronic stress factor experienced by the mice that could impact the result of the experiment. Furthermore, this method did not provide a constant release of PRO since the drug levels fluctuate with a peak after the injection and a decrease over time. These considerations led to use osmotic pumps as a method of administration of PRO. Osmotic pumps (Alzet) are implantable pumps used for drug delivery that allow a constant release of PRO at a pre-determined rate for 6 weeks. Pumps were surgically inserted in the neck of the mice to ensure a continuous release and constant compound levels in plasma and tissues. The pumps were filled with sterile PBS for the groups not receiving the treatment or with Propranolol Hydrochloride (Sigma Aldrich) 2mg/Kg/d [40]. Mini pumps (2006, Alzet) were used with a maximum duration of 6 weeks and a flow rate of 0.15µl/h. The experiment ended exactly 6 weeks after the pump implantation to avoid emptying PRO reservoir in the pump.

The mini pumps were inserted subcutaneously on the back of the animals with a surgical technique which maintained the sterility of the pump. The surgery was performed by the personal license holder under supervision of the project licence holder and the named training and competence officer (NTCO). The personal license holder trained with the named veterinary surgeon (NVS) to assure a good surgical technique and gain expertise on how to

maintain aseptic conditions to avoid infections. Mice were anaesthetised with 1mg/Kg Metedomidine and 0.75mg/Kg Ketamine injected IP. When completely under general anaesthesia, Meloxicam 0.5mg/Kg was injected subcutaneously on the flank. A vertical incision – about 1cm long – on the neck allowed the Alzet mini pump subcutaneous insertion on the back of each animal. After the pump implantation, sutures were applied and 1mg/Kg Atipamezole was injected IP. The animals recovered from the general anaesthesia in few minutes, but they were monitored for few hours until they were alert and completely active. Animals that did not reach 20g in weight at the time of the surgery were excluded from the experiment. This decision was made in agreement with the NVS and the named animal care and welfare officer (NACWO) to assure that the animals were able to recover from anaesthesia and carry the pump with no movement constrictions.

Surgery and general anaesthesia were acute stress factors for the animals. For this reason, mice were left in their cages for a week to recover from the stress. At this point the levels of adrenergic stress hormones were assumed to be back to normal and the restraint stress procedure was started. Since the surgery was performed before cancer cells' injection we assume that the stress due to this procedure did not affect the results in terms of tumour growth or angiogenesis [43].

2.2.3 PD-(L)1 inhibitor treatment

PD1/PD-L1 inhibitor was bought from Cayman Chemical as a compound that blocks the interaction of PD-1 with its ligand, PD-L1. PD1/PDL-1 inhibitor treatment started 2 weeks after cancer cell injection. 200µg/mouse [178] of PD1/PDL1 inhibitor was administered with IP injections 3 times a week for 2 weeks [178]. PD1/PDL1 inhibitor was solubilized in DMSO and diluted in sterile PBS with DMSO concentration not exceeding 5mol/Kg or 10% of the injected volume [179].

2.2.4 Restraint stress procedure

To induce stress, a validated regimen of chronic repetitive restraint stress was used. This consisted in restraining mice in a 50ml conical tube for two hours per day, for a total of 5 weeks. The method allows the mice to move from supine to prone position but not from head-to-tail and ensures the mice to not feel any pain respecting the animal's health and well-being as expressed in the Code of Practice and required by The Animals Scientific Procedures Act [180, 181].

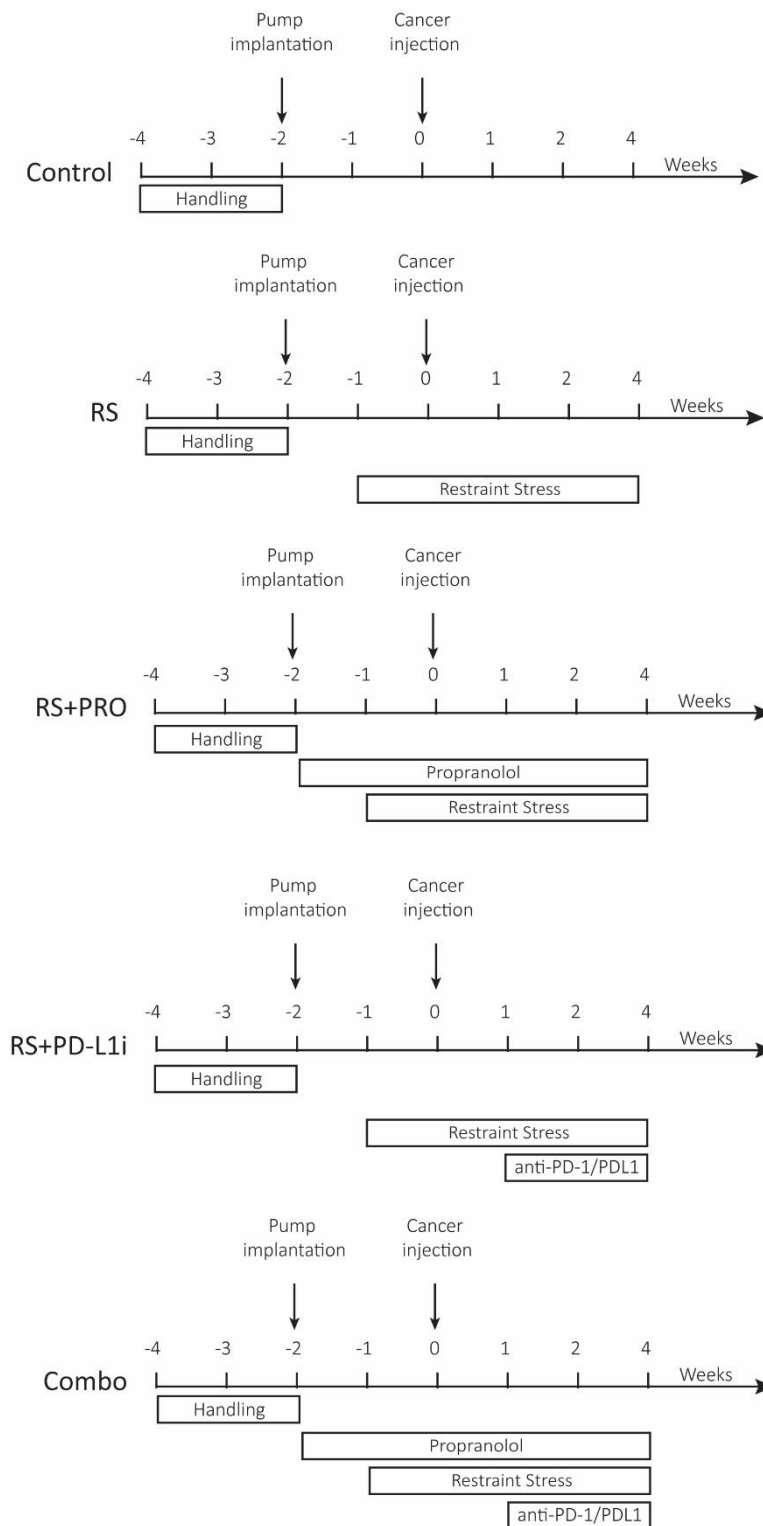


Figure 6 General schematic timeline for the in vivo procedures

Mice were handled by an expert operator every day for two week. Surgical implantation of the pumps (Alzet) allowed a constant release of Propranolol (2mg/Kg/d). Mice recovered from the surgery for 1 week before the restraint stress procedure started. Mice underwent restraint stress 2h/day for the entire duration of the experiment. The orthotopic cancer cells' injection (7×10^6 ID8 cells, IP) was performed 1 week after the start of the restraint stress procedure. Cancer injection was considered the start point of the experiment and after 2 weeks a PD-(L)1 inhibitor was injected (6 injection, 200 μ g/mouse, IP).

2.3 Human samples collection

Women with a diagnosis of ovarian cancer were recruited by Professor Premal Thaker at Washington University in St. Louis, USA. The project has been approved by the research ethic committee (HTA.PAF.0001) and the patients agree to participate with an informed consent. Patients completed a questionnaire prior surgery for the removal of ovarian cancer. The questionnaire is specific for patient with ovarian cancer (FACT-O, Functional Assessment of Cancer Therapy - Ovarian), it is part of the FACIT (Functional Assessment of Chronic Illness Therapy) Measurement System and measures the health-related Quality of Life (QoL) for people with chronic illnesses. Data were collected and analysed following the FACT-O scoring guidelines. The QoL is scored on the basis of the physical, social and emotional well-being . Ovarian cancer tissues were collected and processed by a clinical pathologist: the tissue was fixed and embedded in paraffin, then sectioned in about 5µm thick sections. Tissues were relaxed in a pre-heated 37°C water bath and picked up with positively charged slides. Slides were stored at room temperature for further analysis.

2.3.1 Immunohistochemistry

Ovarian cancer tissues were collected and processed into wax blocks and cut onto slides as 7µm sections by a clinical pathologist at the Washington University in St Louis. Slides were incubated at 56°C overnight, deparaffinised and rehydrated by using solutions of Xylene (2 washes, 5 minutes each), 100% ethanol (2 washes, 2 minutes each), 90% ethanol (2 washes, 2 minutes each), 70% ethanol (2 washes, 2 minutes each) and distilled water for 2 minutes. The area around the sample was blot dried and a PAP pen was used to create a hydrophobic barrier to contain the staining reagents. 3% hydrogen peroxide in methanol was added to cover the samples incubated in a humidified enclosed container for 20 minutes. The samples were submerged in Tris EDTA Tween 20, pH 9 for 20 minutes at 95° C and then cooled for 10 minutes. Samples were incubated for 1h with primary PD-L1 antibody (ThermoFisher) at a concentration of 2.5µg/ml. A Millipore IHC Kit containing blocking reagent, secondary antibody and streptavidin HRP was used following the manufacturer's instructions. A sufficient amount of freshly made chromogen reagent was added to the samples incubated for 30 minutes. Slides were washed with distilled water and dehydrated with serial dilutions of alcohols and xylene. Coverslips were mounted using mounting media and the samples are analysed with an optical microscope.

2.3.2 Analysis

The intensity and the localization of the stain were evaluated by two blinded observers considering 10 random spatial areas of each sample. For both PD-1 and PD-L1 a score between 0 (<1% stain), 1 (1-19% stain), 2 (20-49% stain) and 3 (>50% stain) was assigned for each area [182]. The mean of the scores was calculated and it represented the final sample score.

2.4 Gene expression analysis

2.4.1 Principles

Real-time quantitative PCR (qPCR) is a technique to quantify the differences in gene expression between samples [183]. This approach has been shown to support other observation data with a sensitive, quantitative, reproducible molecular method. For our purpose a RT-qPCR was used to quantify the levels of a specific mRNA sequence by comparing it to a specific housekeeping gene expression. The method consists of three steps: (i) total RNA extraction from cells or tissues, (ii) reverse transcription to convert RNA into cDNA and (iii) amplification of the cDNA [184]. A PCR reaction needs a cDNA as template, primers complementary to sequence of interest and a DNA polymerase. The products of the amplification are called “amplicons” and a fluorescent reporter is used to detect the amplification. In our experiments we used SYBR green as a reporter which emits fluorescence when it is bound to double strand DNA. During the reaction, the DNA amplicons increase and the SYBR green fluorescence increases proportionally giving an indirect indication of the final DNA products [185]. A computer software detects and collects the fluorescence emission data that are organized as a representative amplification plot [183].

2.4.2 RNA extraction from cells

RNA was extracted from cells using the RNeasy Mini kit (QIAGEN) following the manufacturer’s protocol and diluted in RNase-free water. Extracted RNA was quantified using NanoDrop spectrophotometer set to read absorbance at 260 nm and 280 nm. RNase-free water was used as a reference for zero absorbance and 1µl of RNA dilution was loaded. Purity was assessed with 260/280 ratio; RNA was considered pure with a ratio≈2.

2.4.3 RNA extraction from mouse tissues

Tissues were harvested, stored in a freezing vial containing RNA later and flash frozen by submersion in liquid nitrogen. Each tissue was homogenized using pipette tips and syringe needles. RNA was extracted from 30mg of tissue using the RNeasy Mini kit (QIAGEN) according to manufacturer’s instruction and diluted in RNase-free water.

2.4.4 cDNA synthesis

cDNA was synthesized with QuantiTect Reverse Transcription kit (Qiagen) following the manufacturer’s instructions and using ≤1µg of RNA for each reaction. Consistent quantity of RNA was used in all samples of each experiment.

2.4.5 Real Time PCR

For real-time PCR assay, the Rotor-Gene SYBR green PCR kit (Qiagen) was used with bioinformatically validated primers (QuantiTect Primer Assay, Qiagen). Each primer assay is specific for a gene and supplied as lyophilized mix of forward and reverse primer reconstituted with TE buffer pH 8 to obtain a 10x solution. Reactions were prepared following Qiagen's instructions maintaining consistent the amount of cDNA added in each sample. The cycling conditions also followed instructions; 40 cycles: 95°C for 5 minutes, 95°C for 5 seconds and 60°C for 10 seconds.

Data were expressed as relative gene expression normalizing for beta-actin as invariant endogenous control.

2.4.6 Data analysis

For data analysis, important terms are defined below [183]:

- Baseline: PCR cycles where the fluorescence is not detectable.
- Exponential phase: PCR cycles where the amplification occurs in an exponential manner, doubling the DNA at every other cycle.
- Threshold line: arbitrary line in the range of the exponential phase of amplification. The threshold line can be changed in every experiment to maintain all the C_T values in the exponential phase of amplification.
- Threshold cycle (C_T): cycle at which the fluorescence curve intercepts the threshold line.

The $\Delta\Delta C_T$ method was used to analyse the C_T values collected for the gene of interest and a housekeeping gene (Actin β) in each sample.

$$\Delta C_T = C_{T(\text{gene of interest})} - C_{T(\text{housekeeping gene})}$$

$$\Delta\Delta C_T = \Delta C_{T(\text{gene of interest})} - \Delta C_{T(\text{standard control})}$$

2.5 siRNA transfection

2.5.1 Principles

Transfection is a procedure to introduce foreign nucleic acids into cells, causing post-transcriptional modifications in the gene expression and produce genetically modified cells. The genetic modifications can be transient or stable depending on the nature of the nucleic acid introduced [186]. Our main purpose was to modify the ID8 cells in which the IFN- γ receptor1 (IFNGR1) was transiently knockdown (ID8/IFNGR1^{-/-}). In order to achieve a good transfection, the negatively charged nucleic acid needs to overcome the electrostatic repulsion of the double lipophilic cell membrane. Lipofectamine 2000 is a cationic liposome compound that forms complexes with the specific nucleic acid used (RNA in our case) allowing them to be taken up by the cells [187].

2.5.2 Protocol

ID8 were transfected using Lipofectamine 2000 (Invitrogen) and a solution (FlexiTube Gene Solution, Qiagen) of 4 siRNAs to knockdown IFNGR1. ID8 cells were seeded in a 6 well plate (1×10^5 cells/ well) and grew in complete media for 24h. Cell media was discarded and fresh opti-MEM media supplemented with Lipofectamine 2000 at a final concentration of 20ng/ml and the siRNA solution at a concentration of 10nM was added. As a negative control, a validated non-silencing siRNA with no homology to any known mammalian gene (AllStars Negative Control siRNA, Qiagen) labelled with a fluorophore emitting at 488nm was used as a transfection control.

2.5.3 Immunofluorescence (IF) on transfected cancer cells

Cell (35,000 cells per well) were seeded on sterile coverslips placed in the wells of a 6 well plate and incubated at 37° C, 5% CO₂ for 24h. Cells were exposed to hormones and cytokines for 24h as specified in section 2.1.2 and 2.1.3. After treatments, media was removed and cells were washed with PBS. A cold solution of 3% paraformaldehyde 2% sucrose was used for fixation at room temperature for 10 minutes. Cells were permeabilized with 0.2% TritonX-100 in PBS for 2 minutes. Cells were washed with PBS, coverslips were removed from the well and mounted on slides using DAPI-mounting media. A fluorescent microscope (Leica TCS SP5 LAS AF) was used for imaging. The images were scored using CellProfiler imaging software by calculating the intensity of the fluorescence in each area.

2.6 Flow cytometry

2.6.1 General principles

Flow cytometry is a cellular methodology used to detect size, granularity and fluorescent features of cells. Flow cytometry is based on the principle of light scattering and fluorescence emission after excitation from a laser beam striking single cells [188]. The light scattering gives morphological information about the cell (size and granularity) while the fluorescence is related to the type and quantity of the probe or antibody binding the cell. Flow cytometers are composed by three main elements: (i) the fluidics which are directing the single cell suspension to the light source, (ii) the excitation optics are the source of the light scattering or fluorescent light, (iii) the electronic detector which convert the light scatter and the fluorescent emission signal into digital data [189].

2.6.2 Fluorescence principles

In order to investigate the phenotypic profile of the cells, they are stained with specific antibodies conjugated with different fluorochromes. The main feature of a fluochrome is that it can absorb light a certain wavelength and emit fluorescence in a certain spectrum range. Detection of a positive signal is very sensitive and different fluorochromes are detected at different emission wavelengths allowing a multicolor detection and a multiparametric analysis. Moreover, certain antibodies are conjugated to tandem dye. The concept of this double fluorescent labelling is called fluorescence resonance energy transfer (FRET). When the first fluorochrome is excited, its energy is transferred to the one in the next proximity and the second fluochrome emits fluorescence[188]. Due to the tandem dye conjugation, the same excitation wavelength is used to excite fluochromes that will give different emission detection.

2.6.3 Cell staining

Flow cytometry was performed on a single cell suspension of splenocytes. 1×10^6 cells were re-suspended in PBS buffer 1% BSA and the fluorescent labelled specific antibody in the appropriate dilution. Our antibody panel include: a cell viability dye 7-AAD-(PE)-Cy5 (Miltenyi Biotech), anti-CD3-FITC (eBioscience, 0.25 μ g/test), anti-CD69-APC (BioLegend, 0.5 μ g/test) and Anti-PD1-PE (BioLegend, 0.5 μ g/test), anti-CD4-APC (Miltenyi Biotech) and anti-CD8-PE (Miltenyi Biotech). Cells were incubated with fluorescent antibodies at 4°C for 20 minutes, then washed and re-suspended in 1ml of buffer.

Data were acquired from a BD accuri C7 cytometer.

2.6.4 Compensation

Since each fluorochrome has a range of wavelength in the emission spectrum, some can overlap when multiple fluorochromes are used in the same experiment [188]. In order to overcome this problem and get false positive or false negative results, a process called colour compensation is used to correct the data acquired.

In our experiments colour compensation is determined by using no staining and single staining controls. These controls consist in running a test sample with one (or none) conjugated antibody and correct the gating process in order to minimize the false positive and false negative results.

2.6.5 Analysis with FlowJo

Data acquired with BD accuri C7 cytometer were analysed using FlowJo v.10 software. Cells were gated for singlets and live cells. Compensation correction was applied using no stained or single stained cells.

2.7 Enzyme-Linked Immunosorbent Assay (ELISA)

2.7.1 Principles

The basis of immunoassays is the antigen-antibody reversible binding which guarantee a sensitive and specific technique to detect and quantify biological substances [190]. Different assays are commercially available and for our purpose we used a direct sandwich ELISA. The principle of a sandwich ELISA consist in: (i) coating a solid phase with a capture antibody (Capt-Ab), (ii) add the sample containing the specific antigen (Ag), (iii) add an labelled antibody such as a biotin-conjugated detection antibody (B-Det-Ab) (iv) add an enzyme such as avidin-conjugated horseradish peroxidase (HRP) (v) add a substrate that reacts with the enzyme such as 2,2'-azino-bis(3-ethylbenzothiazoline-6-sulphonic acid (ABTS) [191]. The assay terminates with a spectrophotometric reading of the microplate which detects the colour development of each sample.

2.7.2 Protocol

ABTS ELISA kit (PeproTech) was purchased together with an ABTS ELISA buffer kit (PeproTech). ELISA for the detection of IFN- γ , IL-10 or PD-L1 was performed either on immune cell condition media or tumour protein homogenate. ELISA was performed following manufacturer's protocols.

96 well plates were coated with Capt-Ab overnight before adding samples and standards (2h incubation). A biotin-conjugated antibody (B-Det-Ab) was used as detection and an avidin-conjugated HRP enzyme was used to react with the ABTS substrate. The plate was washed 4 times and dry blotted between each step.

2.8 Mass Spectrometry

2.8.1 Principles

A mass spectrometer measures the mass-to-charge (m/z) ratio of ionized molecules [192]. This simple evaluation can be applied for large-scale proteomic analyses. Mass spectrometry (MS)-based proteomic aims to identify and quantify proteins in a mixture [193]. For this purpose, proteins are enzymatically digested to obtain peptides prior MS analysis. Peptides are then ionised, fragmented and detected in the mass spectrometer. The detection consists of MS/MS spectra of fragmented ions. This gives information about the composition of the parent ionised peptide, in particular about the amino acid sequence [193]. Processed MS/MS spectra are analysed with software applications (MASCOT) comparing the large amount of data obtained with a data base of characterized parental ions. Amino acid sequences are then matched with relative peptides and proteins.

2.8.2 Extraction of proteins

Proteins were extracted from spheroids (treated with NA or PRO) or from multicellular spheroids (co-culture of spheroids with splenocytes from stressed and non-stressed mice). Spheroids were collected from a 96 ultra-low attachment plate, disrupted adding a lysis buffer (RIPA, Table 5). Proteins were quantified in the lysate using DC protein assay (Bio-Rad) following manufacturer's instructions. Bovine serum albumin (BSA) was used as a protein standard and diluted from 1.5mg/ml to 0.2mg/ml. Absorbance was read at 750nm, the standard curve plotted to calculate the total protein concentration.

2.8.3 SDS-PAGE principles

Sodium dodecyl sulfate-polyacrylamide gel electrophoresis (SDS-PAGE) is a biochemistry analytical method to separate charged molecules on the basis of their molecular masses. This method, developed by Ulrich K. Laemmli in 1970 [194], is based on the principle of electrophoresis where charged molecules migrate in an applied electric field depending on their mass. SDS-PAGE is the most common method used to separate proteins using a protein denaturation detergent (SDS) which binds to the polypeptides and conferring them a uniform negative charge. Being all negatively charged, the proteins are separated in the electric field on the basis on their molecular mass.

2.8.4 SDS-PAGE Protocol

Stacking and resolving gels were prepared following the recipes shown in Table 5. 5µg of the protein samples were diluted with 2x Laemmli buffer and heated at 95° for 10 minutes. Gels

were placed into the Bio-Rad protean tank filled with running buffer (Table 5), loaded with protein samples and electrophoresed at 100V until the proteins reached the resolving gel.

2.8.5 Peptide preparation: destain, reduction-alkylation, digestion and extraction of peptides

The gel was extracted from the tank and the protein band was excised using a scalpel. Each gel band was placed in a micro-centrifuge tube containing 1ml of destain solution (Table 5), vortexed and left overnight at room temperature. The next day, the supernatant was discarded and 150µl of 100% acetonitrile was added to dehydrate the gel pieces. When the gels turned opaque, the acetonitrile was removed and the samples were incubated at 37°C for about 10 minutes with cap open to let them dry. 50µl of 10nM DTT solution (Table 5) was added to the samples which were vortexed and centrifuged briefly before incubating at 56°C in a thermomixer for 1h. The supernatant was removed before adding 50µl of 55nM IAA solution (Table 5) and incubate at room temperature for 45 minutes in the dark. The supernatant was discarded and the gel pieces were washed with 100µl of 25nM ammonium bicarbonate and dehydrated with 100µl of 100% acetonitrile. Before the digestion, samples were incubated at 37°C with cap open to let the acetonitrile evaporate. Samples were digested with 50µl of trypsin and 50µl of 25nM ammonium bicarbonate and incubated at 37°C overnight. The digested solution was saved in a new micro-centrifuge tube and the gel pieces treated with 150µl of extraction buffer (Table 5), vortexed, sonicated for 10 minutes and centrifuged briefly. The supernatant was added to the digested solution. The samples were dried with a speed-vac centrifuge and re-suspended in 12µl of 0.1% TFA.

2.8.6 Acquisition of data

Peptides were analysed by the Q Exactive Hybrid Quadrupole-Orbitrap mass spectrometer. Tandem mass spectra (MS/MS) were analysed by SEQUEST, a data analysis for protein identification. SEQUEST identifies collection of tandem mass spectra to peptide sequences that have been generated from databases of protein sequences.

2.8.7 Mass spectrometry data analysis

Protein-protein interaction (PPI) analysis was evaluated using STRING v11, an online free programme for protein analysis (30). STRING contains a biological database of known and predicted protein-protein interactions and it was used to obtain the statistical significance of the PPIs. Fold changes between the two treatment groups was calculated and p-values less than 0.05 were considered significant.

Buffer/ Reagent	Recipe
RIPA buffer	10 mM Tris-Cl (pH 8.0) 1 mM EDTA. 1% Triton X-100. 0.1% sodium deoxycholate. 0.1% SDS. 150 mM NaCl. 1 mM PMSF.
Running buffer	0.025M Tris 0.192M glycine 0.1% SDS Distilled water
Stacking gel (4.5%)	2.915ml distilled water 750µl 30% Bis-Acrylamide 1.25ml 0.5M Tris pH 6.8 50µl 10% SDS 100µl 10% APS 10µl TEMED
Resolving gel (10%)	3ml distilled water 2.5ml 30% Bis-Acrylamide 1.875ml 0.5M Tris pH 6.8 100µl 10% SDS 100µl 10% APS 10µl TEMED
Destain solution	25nM ammonium bicarbonate 50% acetonitrile
Dithiothreitol (DTT)	10µl 1M DTT stock (0.154g in 1ml 25nM ammonium bicarbonate) 990µl 25NM ammonium bicarbonate
Iodoacetamide (IAA)	122µl 450nM IAA stock (83mg in 1ml 25nM ammonium bicarbonate) 878µl 25NM ammonium bicarbonate
Extraction buffer	70% acetonitrile 5% formic acid

Table 5 Mass spectrometry buffers and reagent with correspondent recipe

2.9 Data Analysis

Graphs were generated using GraphPad Prism v.7 software. Data were shown as median \pm SEM. Biological replicates and details of the specific statistical analysis are shown in figure legends and results section. Tests were two-tailed and differences are considered statistically significant at $p < 0.05$.

**3. Chapter 3 - Adrenergic blockade
with Propranolol downregulates
IFN- γ production by immune cells
and PD-L1 expression on cancer
cells**

3.1 Introduction

3.1.1 Molecular effects of adrenergic stress on the immune response to cancer

The Sympathetic Nervous System (SNS) modulates cancer biology through different molecular mechanisms that involve DNA damage/repair processes, oncogenes activation and tumour progression [195, 196]. This chapter will focus on the effects of the adrenergic signalling pathway on cellular and molecular mechanisms that cooperate to regulate the immune response against cancer.

Many studies have supported a role of the adrenergic signalling pathway on tumour immunomodulation showing that NA and pro-inflammatory cytokines are strongly up-regulated in cancer patients [197, 198]. *In vitro* studies have shown that IL-6 mRNA expression and protein levels are enhanced in SKOV3ip1, Hey-A8 and EG ovarian cancer cells after exposure to non-selective beta-adrenergic receptor agonists such as NA, A or isoproterenol [198]. Similarly, IL-8 mRNA and protein levels increased in SKOV3ip1 and Hey-A8 cells after treatment with NA and decreased when cells were treated with Propranolol (PRO), a non-selective beta-blocker [199]. *In vivo* studies in orthotopic xenograft models of ovarian cancer showed that chronic stress increased NA levels together with tumour growth, angiogenesis, and metastasis. Interestingly, IL-8 silencing *in vivo* resulted in a significant reduction of tumour weight and number of metastatic nodules in stressed mice [199].

Adrenergic stress-mediated immune regulation can affect the bone marrow with up-regulation in the proliferation of hematopoietic stem cells, production of neutrophils and monocytes, and release of inflammatory leukocytes into the blood stream [200]. In *in vivo* models, stress induced the mobilization of hematopoietic progenitors to the circulation and secondary lymphoid organs. In particular, beta-adrenergic signalling has been shown to increase the recruitment of hematopoietic stem and progenitor cells (HSPCs) to the spleen and support a long-lasting splenic myelopoiesis [201]. The adrenergic signalling pathway influences the splenic NK cell population in a mouse model of stress due to sleep-deprivation. Spleen cells of sleep-deprived mice were analysed and showed a significant decrease in NK and NKT cell number with an increased beta-adrenergic receptor (ADRB) expression. This effect was reversed when mice were treated with Propranolol (PRO). Furthermore, NK cells of sleep-deprived mice showed a decreased cytotoxic activity when in co-culture with cancer cells [202]. This evidence supports the idea that adrenergic stress modulates the immune cell functions and the acquired stress-related phenotype in the immune cells persists when they are exposed to different stimuli. The hypothesis of an adrenergic stress imprint on immune cells is also supported by a finding that mouse bone marrow derived dendritic cells

(DCs) exposed to NA and activated with LPS were able to induce naïve T cell proliferation. However, beta-adrenergic stimulation induced down-regulation of IL-12p70, a cytokine promoting Th1 differentiation, with a shift in IL-12p70/IL-23 ratio in favour of IL-23 and a consequent deviation towards Th17 differentiation. In addition, co-culture of NA treated DCs with naïve T cells showed a significant lower production of IFN- γ , a Th1 specific cytokine and an increased production of IL-17A, produced by Th17 T cells [203]. This study demonstrates that the adrenergic immune control is a complex process which involves cytokine production and interactions between different cell types.

Stress can affect the adaptive T-cell mediated immune response by modulating T cells effector functions. Human and mouse CD8⁺ T cells were treated with NA during *ex vivo* activation with anti-CD3/anti-CD28. CD8⁺ cells decreased IFN- γ production when treated with NA during activation [204]. Interestingly, IFN- γ production was not affected by NA when CD8⁺ T cells were stimulated with IL-12, suggesting that the adrenergic signalling can suppress TCR-mediated T cell IFN- γ production, but this can be restored by the cytokine microenvironment (e.g IL-12). In conclusion, the adrenergic effects on immune cells can be described as dynamic and closely dependent on the immune stimuli established in the microenvironment.

3.2 Aims

This chapter aims to examine the effects of adrenergic stress stimulation via NA on PD-L1 expression on ovarian cancer cells, how this process is regulated and if it can be reversed by blocking the adrenergic signalling pathway with PRO. *In vitro* models of co-culture were used to mimic the immune-tumour interface in the tumour microenvironment. However, due the complexity of the mechanism proposed, extensive work on adrenergic immune regulation in ovarian cancer will be discussed in chapters 4 and 5 using a 3D *in vitro* and an orthotopic syngeneic mouse model of ovarian cancer.

The specific aims of this chapter can be summarized as follow:

- Examine the effects of NA, PRO and IFN- γ on PD-L1 expression on ovarian cancer cells.
- Assess the adrenergic regulation of immune functions with a focus on IFN- γ and interleukin-10 (IL-10) production.
- Propose a molecular mechanism of the adrenergic immune modulation in ovarian cancer.

3.3 Results

3.3.1 PD-L1 is expressed in tissues derived from ovarian cancer patients

First, PD-L1 expression in ovarian tumour tissues was assessed to evaluate the relevance of this immune checkpoint in our experimental model. Tumour tissues from patients undergoing ovarian tumour surgical excision were collected and processed at Washington University in St. Louis, USA. Immunohistochemistry (IHC) was performed following the protocol at section 2.3 and the samples were stained with an antibody for PD-L1 detection. In order to establish a relationship between stress and PD-L1 expression, the quality of life (QoL) of each patient was assessed by the completion of a questionnaire. The aim of the questionnaire was to evaluate the physical and psychological wellbeing of the patients in order to have an indication of their level of stress. Each questionnaire was scored following the FACT-O guidelines.

The cohort of 11 patients was ranked considering the QoL score (Table 6). PD-L1 expression and spread were evaluated for each patient as described in 2.3.1.

Data showed a non-significant correlation ($p=0.6242$; $r=0.1667$, $R\text{ squared}=0.02779$) between the QoL score and PD-L1 expression and between the histology of the tumour and PD-L1 expression (Figure 7A). Patient 2 was evaluated as negative for PD-L1 (PD-L1 intensity score ≤ 1), patient 4 was considered PD-L1 positive but with low PD-L1 expression and non-homogeneous spread (PD-L1 intensity and spread score between 1 and 2) and patient 10 was representative of high PD-L1 expression and homogenous spread (PD-L1 intensity and spread ≥ 2) (Figure 7B). Using the previous examples as guidelines for PD-L1 intensity, 3 patients out of 10 were considered PD-L1 high, 7 patients were considered PD-L1 positive and 1 was PD-L1 negative. PD-L1 was considered homogeneously spread in the tissue of 8 patients and non-homogenous for 2 patients.

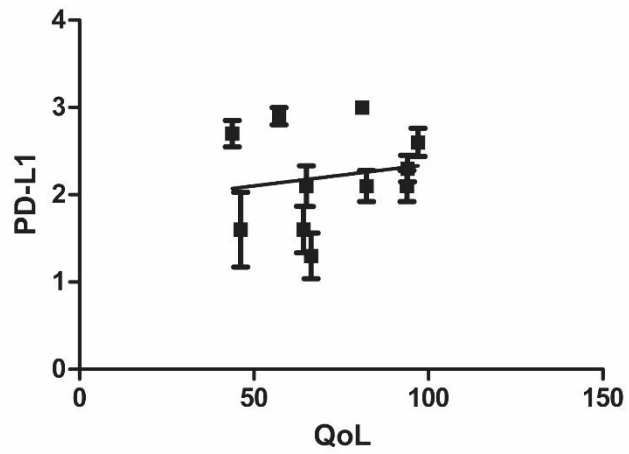
Although these data do not show any correlation between the QoL score and PD-L1 expression in human ovarian tumour tissues, PD-L1 is expressed at various levels in the tissues.

Patient	Histology	QoL (max 108)	PD-L1 intensity (0-3)	PD-L1 spread (0-3)
1	Mixed	43.8	1.4	2
2	Serous	46.2	0.9	n/a
3	Serous	57.2	2.8	2.9
4	Serous	64.2	1.6	1.6
5	Serous	65	1.9	2.1
6	Endometrioid	66.4	1.6	1.3
7	Serous	81	2	3
8	Endometrioid	82.3	1.6	2.1
9	Mixed	93.9	1.6	2.1
10	Mixed	94	2.5	2.3
11	Serous	97	1.6	2.6

Table 6 Patients' QoL and PD-L1 expression

Patients were ranked from the lowest to the highest QoL score. For each patient, tumour histology, QoL score and PD-L1 intensity and spread are shown.

(A)



(B)

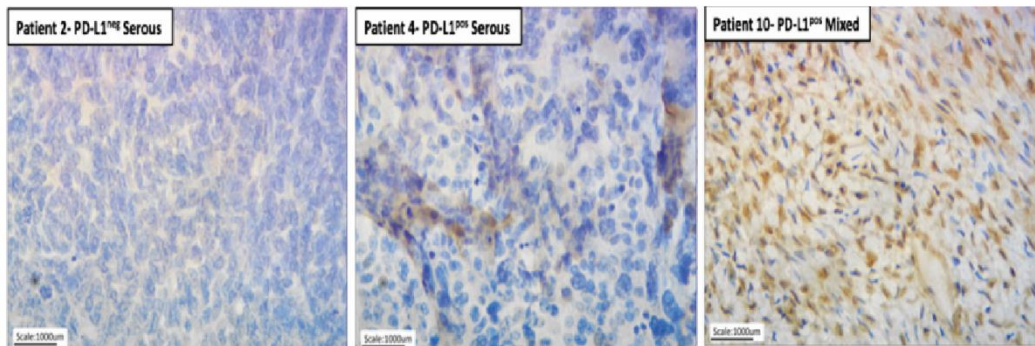


Figure 7 PD-L1 expression in tissues from patients with ovarian cancer

(A) The graph shows the QoL and PD-L1 spread scores. Mean \pm SEM is expressed and data were analysed with a Pearson correlation. ($p=0.6242$; $r=0.1667$, R squared= 0.02779). (B) Immunohistochemistry (IHC) detecting PD-L1 (brown) and cell nuclei (blue) was performed on tissues from ovarian cancer patients. Representative images from patient 2 (PD-L1 negative), 4 (PD-L1 positive with non-homogenous expression) and 10 (PD-L1 high and homogenous expressed) are shown.

3.3.2 PD-L1 was expressed in ovarian cancer cell lines treated with IFN- γ alone or in combination with NA or PRO plus NA

In order to explore the regulation of PD-L1 expression, PD-L1 mRNA was assessed in different ovarian cancer cell lines by qPCR. Cells were treated with NA (1 μ M), PRO (1 μ M) and recombinant IFN- γ (20ng/ml) or a combination for 24h using the protocols illustrated in 2.1.2 and 2.1.3. qPCR data was analysed using the $\Delta\Delta C_T$ method (discussed in 2.4.6) and PD-L1 expression was normalized to unstimulated cells.

In all cell lines, PD-L1 expression was significantly increased when cells were treated with IFN- γ compared to cells treated with NA or PRO alone. Neither NA nor PRO affected the observed IFN- γ increases in PD-L1 expression (Figure 8A, B and C). In the human ovarian cell line OVCAR8, PD-L1 expression was significantly increased in cells treated with IFN- γ in combination with NA compared to cells treated with PRO (Figure 8C).

These results have shown that PD-L1 expression in ovarian cancer cell lines is not affected by NA and PRO treatment. However, PD-L1 expression is significantly up-regulated when cells were treated with IFN- γ regardless of the addition of NA and PRO.

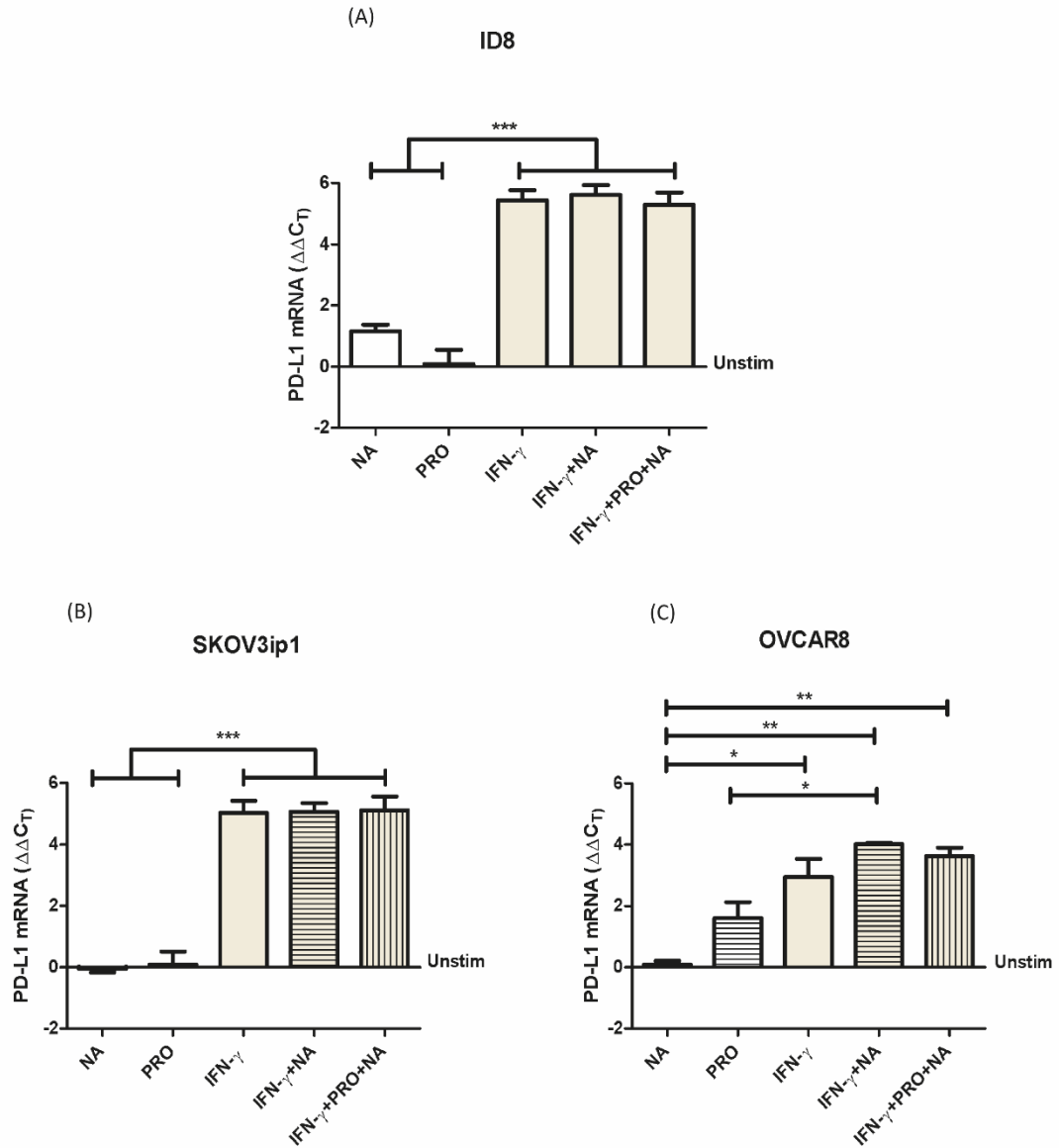


Figure 8 PD-L1 is expressed in ovarian cancer cells treated with IFN- γ

Ovarian cancer cell lines were treated with NA (1 μ M), PRO (1 μ M) and IFN- γ (20ng/ml) alone or in combination. Total RNA was extracted, reverse transcription and qPCR were performed to assess PD-L1 expression. Values are expressed in $\Delta\Delta C_T$ and normalized to unstimulated cells (Unstim). Mean \pm SEM is expressed and statistical significance was determined with one way ANOVA (Post-test: Bonferroni). * = $p < 0.05$, ** = $p < 0.01$, *** = $p < 0.001$. (A) PD-L1 mRNA expression in ID8 cells. (B) PD-L1 mRNA expression in SKOV3ip1 cells. Data are representative of three biological replicates. (C) PD-L1 mRNA expression in OVCAR8 cells. Data are representative of three biological replicates in (A) and (B) and two biological replicates in (C).

3.3.3 Immune cells activated *ex vivo* produced IFN- γ

The main sources of IFN- γ are immune cells that have been primed by a specific antigen and the aim of IFN- γ is to flag the presence of infected or tumorigenic cells [69]. Immune cells need a specific stimulus to be activated and stimulated to produce IFN- γ [67]. Immune cells were isolated from C56BL/6 mouse spleens and splenocytes were induced to produce IFN- γ with an *ex vivo* activation. Methods for immune cells activation are discussed in 2.1.5. Cells were activated with either anti-CD3/anti-CD28 or PMA/Ionomycin for 24h and IFN- γ in the culture media was evaluated by ELISA (method discussed in 2.7). Activated immune cells either with anti-CD3/anti-CD28 or PMA/ionomycin showed significant increased levels of IFN- γ in the media compared to the inactive immune cells that were left in growth media unstimulated (Figure 9). These results showed that activated immune cells produced IFN- γ at pg/ml levels.

These results confirmed the hypothesis that immune cells produced IFN- γ when appropriately activated *ex vivo*.

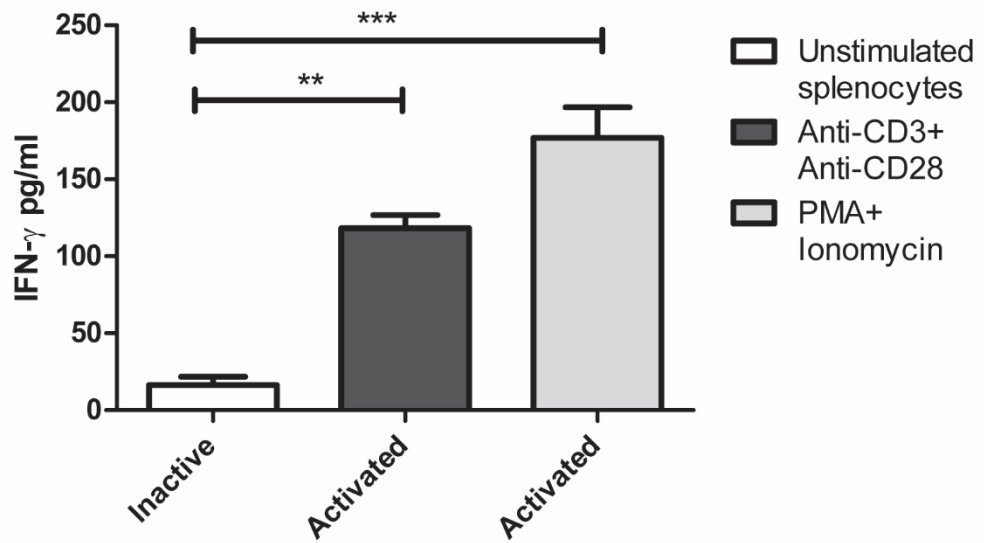


Figure 9 IFN- γ is produced by activated immune cells

Mouse (C57BL/6J) splenocytes were isolated from a spleen and activated *ex vivo* with two different methods: anti-CD3+anti-CD28 and PMA+ Ionomycin. ELISA to detect IFN- γ was performed on cell media after 24h activation. Mean \pm SEM is expressed and statistical significance was determined with one way ANOVA (Post-test: Bonferroni). * = $p < 0.05$, ** = $p < 0.01$, *** = $p < 0.001$. Data are representative of at least 3 biological replicates.

3.3.4 PD-L1 is expressed on ID8 cells after treatment with IFN- γ at different concentrations

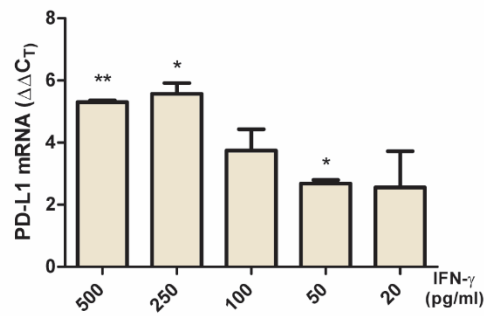
Because the IFN- γ levels produced from activated T cells were in pg/ml, IFN- γ regulation of PD-L1 expression in ovarian cancer cells was further evaluated.

ID8 cells were treated with 500pg/ml, 250pg/ml, 100pg/ml, 50pg/ml and 20 pg/ml of recombinant IFN- γ for 24h (protocols discussed in 2.1.2 and 2.1.3). Cells were harvested and PD-L1 expression was evaluated by qPCR (2.4).

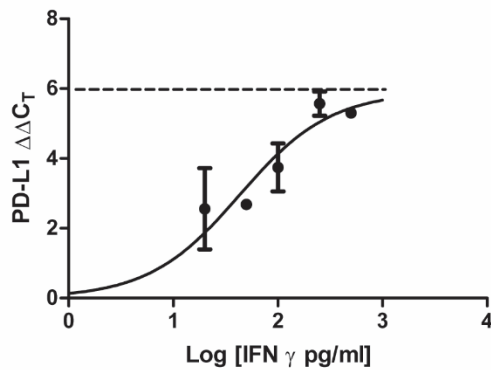
PD-L1 expression in treated cells was compared to the basal PD-L1 expression in unstimulated ID8 cells. PD-L1 was significantly upregulated in cells treated with IFN- γ even at lower concentrations of 500pg/ml, 250pg/ml and 50pg/ml ($p < 0.005$, $p < 0.05$, and $p < 0.05$) compared to the basal expression (Figure 10A). Data were transformed in $\log[\text{IFN-}\gamma]$ to obtain a dose-response curve. The concentration of IFN- γ inducing a response half way between the baseline and the maximum (EC50) was calculated (EC=43.12) (Figure 10B and C) [205].

Data presented here confirmed that levels of IFN- γ in the order of pg/ml can upregulate PD-L1 expression in ovarian cancer cells.

(A)



(B)



(C)

log(agonist) vs. response (three parameters)	
Best-fit values	
Bottom	= 0.0
Top	= 5.912
LogEC50	1.635
EC50	43.12
Span	= 5.912
Std. Error	
Top	0.6661
LogEC50	0.1836
95% Confidence Intervals	
Top	4.376 to 7.448
LogEC50	1.211 to 2.058
EC50	16.26 to 114.3

Figure 10 PD-L1 is expressed on ID8 cells treated with IFN- γ

ID8 cells were treated for 24h with different concentrations of IFN- γ (500pg/ml, 250pg/ml, 100pg/ml, 50pg/ml, and 20pg/ml). Total RNA was extracted, reverse transcription and qPCR were performed to assess PD-L1 expression. Values are expressed in $\Delta\Delta C_T$ and normalized to unstimulated cells. (A) Mean \pm SEM is presented and statistical significance was determined with one-sample t-test comparing each column to a hypothetical value ($\Delta\Delta C_T$ value for PD-L1 expression in unstimulated ID8 cells). Each column is representative of two biological replicates. * = $p < 0.05$, ** = $p < 0.01$. (B) Data transformed in Log[IFN- γ pg/ml] (C) Calculation of the EC50.

3.3.5 NA and PRO modulate IFN- γ production in immune cells

As shown in 3.3.2 and 3.3.4, IFN- γ can stimulate the up-regulation of PD-L1 expression in ovarian cancer cell lines. The ability of adrenergic stress to affect IFN- γ production in immune cells was assessed. Immune cells derived from a C57/BL6 mouse spleen were activated with PMA/ionomycin with or without NA or PRO plus NA for 3h and 24h and IFN- γ was evaluated in the cell culture media (protocols discussed in 2.1.5 and 2.7). At 3h activation, splenocytes activated *ex vivo* with PMA/ionomycin in combination with NA showed a significant increment in IFN- γ levels compared to inactive cells. In addition, activated immune cells with PMA/ionomycin alone or in combination with PRO plus NA showed no significant changes in IFN- γ levels (Figure 11A). After 24h activation, IFN- γ was significantly increased in immune cells activated *ex vivo* with PMA/ionomycin alone or in combination with NA compared to inactive immune cells (Figure 11B). IFN- γ levels decreased significantly when immune cells were activated *ex vivo* with PMA/ionomycin combined with PRO plus NA either after 3h and 24h after activation (Figure 11A and B).

These results have shown that NA can increase the production of IFN- γ after 3h activation. However, the level of IFN- γ increased after 24h activation regardless of NA addition. More importantly, IFN- γ levels significantly decreased in immune cells activated in the presence of NA plus PRO.

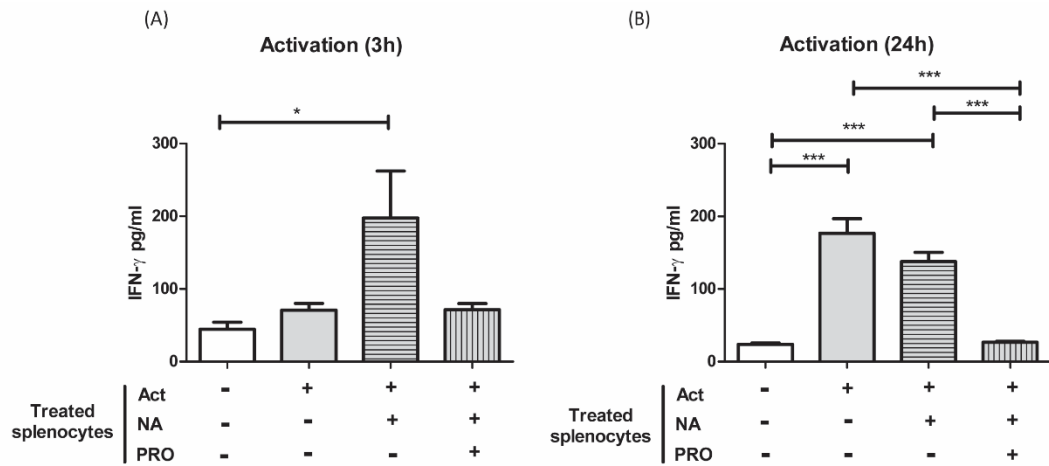


Figure 11 NA accelerates and PRO+NA inhibits IFN- γ production in activated immune cells

Splenocytes were activated *ex vivo* with PMA (50ng/ml) and Ionomycin (1 μ g/ml) for 3h or 24h. IFN- γ was detected in cell media by ELISA. IFN- γ is expressed in pg/ml. Mean \pm SEM is presented and statistical significance was determined with one way ANOVA (Post-test: Bonferroni). * = $p < 0.05$, ** = $p < 0.01$, *** = $p < 0.001$. Data are representative of at least 3 biological replicates. (A) IFN- γ levels after 3h activation. (B) IFN- γ levels after 24h activation.

3.3.6 PMA and Ionomycin affect PD-L1 expression: optimization of the co-culture experiment

The immune cell activation protocol is illustrated in 2.1.5. Briefly, immune cells were isolated from a mouse spleen, re-suspended in cell culture medium with the addition of PMA and ionomycin. After 24h, immune cells were co-cultured with ID8 cells following the trans-well co-culture protocol illustrated in 2.1.6. Before performing *in vitro* experiments with immune cells co-cultured with ID8, we assessed whether the addition of PMA/ionomycin to the culture cell media - essential for the immune cells activation – affected PD-L1 expression in ID8 cells and potentially impact my data. ID8 cells were cultured with PMA/ionomycin using the same concentrations used for the immune activation protocol (discussed in 2.1.5) and PD-L1 expression was assessed with qPCR (method illustrated in 2.4). PD-L1 expression in ID8 cells significantly increased when they were treated with PMA/ionomycin compared to the basal PD-L1 expression in unstimulated ID8 cells (Figure 12).

These results led to a further optimization of the protocol which was changed as described in 2.1.6.

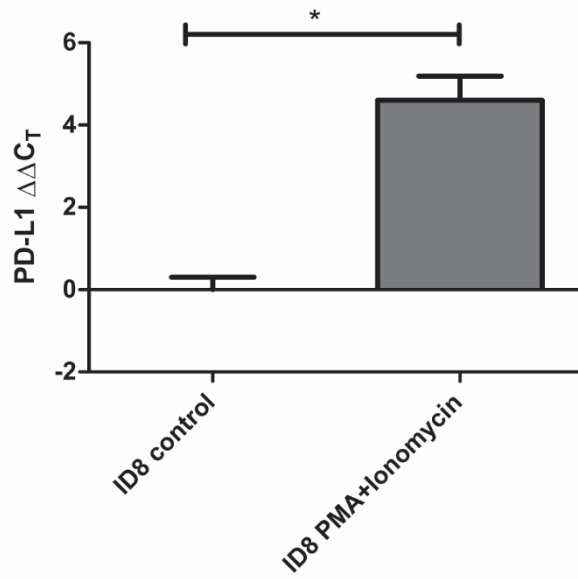


Figure 12 PMA and Ionomycin treatment up-regulate PD-L1 expression in ID8

ID8 cells were treated with PMA (20ng/ml) and Ionomycin (1 μ g/ml) for 24h. Total RNA was extracted; reverse transcription and qPCR were performed to assess PD-L1 expression. Values are expressed in $\Delta\Delta C_T$ and normalized to unstimulated cells. Mean \pm SEM is presented and statistical significance was determined with one-sample t-test comparing the two columns. Data are representative of two biological replicates. * = p<0.05.

3.3.7 PD-L1 expression in ovarian cancer cells is modulated by the presence of activated immune cells treated with NA and PRO plus NA

To assess if the IFN- γ adrenergic regulation influences PD-L1 expression, ID8 ovarian cancer cells were co-cultured for 24h with immune cells activated *ex vivo* with PMA/ionomycin alone or in combination with NA or PRO plus NA (protocol illustrated in 2.1.6). IFN- γ was detected in the co-culture media by ELISA and PD-L1 expression was assessed in ID8 cells by qPCR. In contrast with the results observed in splenocytes alone (Figure 11), IFN- γ levels in culture media of splenocytes co-cultured with ID8 cells remained below 50pg/ml (Figure 13A). PD-L1 expression was significantly ($p < 0.05$) increased in ID8 cells co-cultured with splenocytes that were activated with PMA/ionomycin alone or in combination with NA compared to the basal expression of PD-L1 on ID8 cells (Figure 13B). PD-L1 expression was not significantly different from the basal levels in ID8 cells co-cultured with inactive splenocytes or with activated splenocytes treated with PRO plus NA (Figure 13B).

Results have shown that immune cells failed to produce IFN- γ when in co-culture with ID8 ovarian cancer cells. In addition, PD-L1 expression was significantly upregulated when cancer cells were in co-culture with immune cells previously activated with or without the addition of NA.

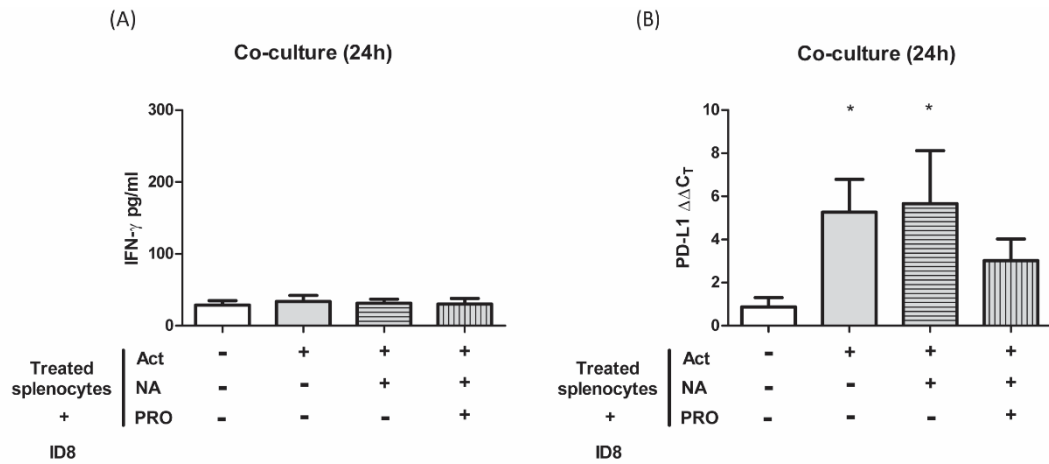


Figure 13 ID8 cells co-cultured with immune cells that failed to produce IFN- γ present different expression of PD-L1

ID8 cells were co-cultured for 24h with activated immune cells treated with NA or PRO plus NA. (A) IFN- γ was detected in cell media by ELISA. IFN- γ is expressed in pg/ml. (B) Total RNA was extracted from ID8, reverse transcription and qPCR were performed to assess PD-L1 expression. Values are expressed in $\Delta\Delta CT$ and normalized to unstimulated cells. Mean \pm SEM is presented and statistical significance was determined with one-sample t-test comparing each column to a hypothetical value ($\Delta\Delta CT$ value for PD-L1 expression in unstimulated ID8 cells). * = $p < 0.05$. Data are representative of at least 3 biological replicates.

3.3.8 Immune cells co-cultured with ovarian cancer cells increase IL-10 levels

The activated immune cells co-culture with ID8 cancer cells were next assessed for the production of the anti-inflammatory cytokine IL-10. Splenocytes were activated *ex vivo* for 24h or activated and then co-cultured with ID8 for 24h (protocols illustrated in 2.1.5 and 2.1.6). IL-10 levels were detected by ELISA in the culture media. At 24h, there were no significant changes in IL-10 levels among the different treatments (Figure 14A). IL-10 levels were significantly increased when ID8 cells were co-cultured for 24h with splenocytes activated *ex vivo* with PMA/ionomycin alone or in combination with NA compared to co-cultures with inactive splenocytes (Figure 14B). Furthermore, IL-10 levels decreased significantly when ID8 were co-cultured with splenocytes activated *ex vivo* with PMA/ionomycin combined with PRO plus NA (Figure 14B).

These data showed that activated immune cells in co-culture with cancer cells upregulated the production of the anti-inflammatory cytokine IL-10. More interestingly, the addition of NA plus PRO in the activation of immune cells inhibited the production of IL-10.

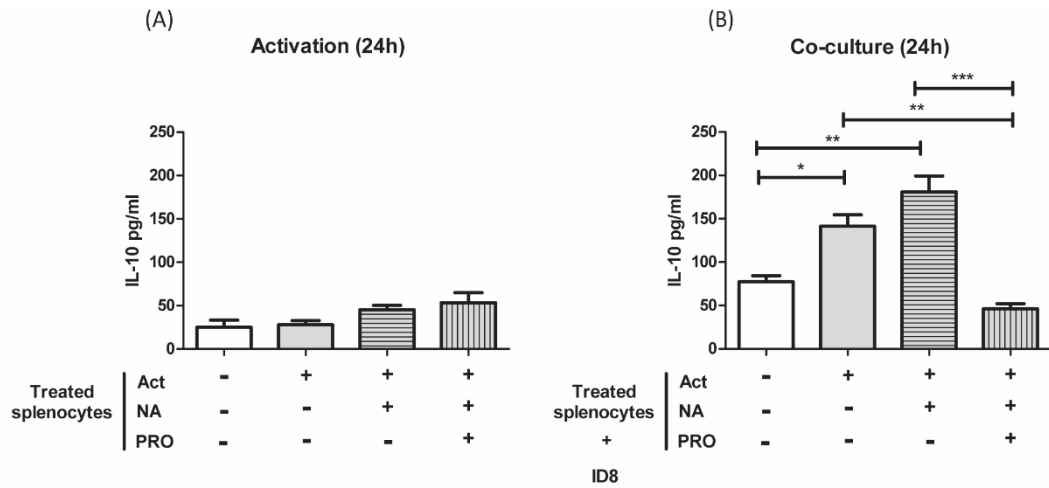


Figure 14 IL-10 levels increase in co-culture of ID8 and activated splenocytes (with or without NA treatment)
 ID8 cells were co-cultured for 24h with activated immune cells treated with NA or PRO plus NA. IL-10 was detected in cell media by ELISA. IL-10 is expressed in pg/ml. (A) IL-10 values in activated immune cells. (B) IL-10 values in activated immune cells co-cultured with ID8. Mean \pm SEM is presented and statistical significance was determined with one way ANOVA (Post-test: Bonferroni). * = p<0.05, ** = p<0.01, *** = p<0.001. Data are representative of at least 3 biological replicates.

3.3.9 IFNR1 was transiently silenced in ID8 cells but not in ID8 in co-cultured with immune cells activated *ex vivo*

To better understand the role of IFN- γ on PD-L1 expression, ID8 cells were transfected with siRNA to transiently silence the expression of the IFN- γ receptor-1 (IFNGR1). Co-culture experiments were used to investigate if PD-L1 expression on ID8 cells was mediated by the IFN- γ produced by the immune cells.

ID8 cells were transfected with Lipofectamine 2000 at 20ul/ml and a solution of 4 siRNAs. A validated non-silencing siRNA with no homology to any known mammalian gene labelled with a fluorophore emitting at 488nm was used as transfection control (protocol illustrated in 2.5). A fluorescent microscope (Leica TCS SP5 LAS AF) was used for imaging. Analysis of 10 random images for each treatment was performed using CellProfiler software by calculating the intensity of the fluorescence in each area recognized as a nucleus.

Cells transfected with the siRNA solution showed a significant ($p < 0.001$) decrease in the mean intensity compared to 488-cojugated siRNA (Figure 15B). IFNGR1 expression was assessed on control and knock down cells by qPCR. ID8 cells transfected with 1nM, 5nM, and 10nM of siRNA solution show a significant decrease in the expression of IFNGR1 ($p < 0.005$ and $p < 0.05$) (Figure 15C). Control and IFNGR1⁻ ID8 cells were co-cultured with splenocytes activated *ex vivo* with PMA/Ionomycin with or without NA or PRO. PD-L1 and IFNGR1 expressions were assessed on ID8 cells by qPCR. IFNGR1 expression was not significantly reduced in ID8 IFNGR1⁻ when in co-culture with immune cells (Figure 15D).

Although IFNGR1 was successfully silenced in ID8 cells, IFNGR1 was not significantly downregulated when cells transfected with siRNA targeting IFNGR1 were in co-culture with immune cells.

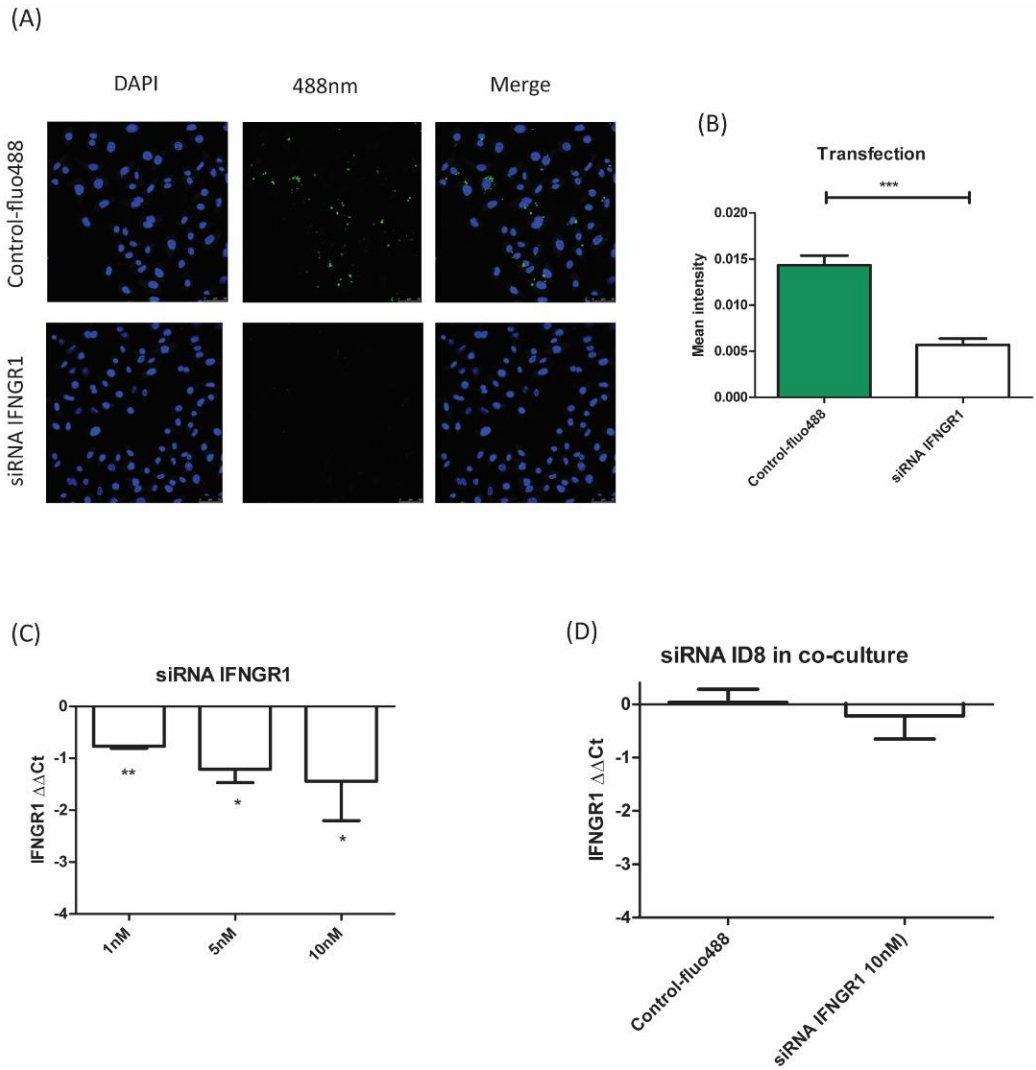


Figure 15 IFNGR1 was transiently knock down using siRNA

ID8 cells were transfected with Lipofectamine 2000 at 20ul/ml and a solution of 4 siRNAs. A non-silencing siRNA labelled with a fluorophore emitting at 488nm was used as transfection control. IFNGR1 expression was assessed on control and knock down cells by qPCR. (A) Representative images from transfected cells. Cell nuclei are labelled with DAPI (blue) and the control siRNA is conjugated with 488nm emitting fluorophore (green). (B) A relative intensity was calculated dividing the 488nm intensity for the number of nuclei detected in each image. Mean \pm SEM is presented and statistical significance was determined with one-sample t-test comparing the two columns. Data are representative of three biological replicates, *** = $p < 0.001$. (C) and (D) Total RNA was extracted from transfected ID8 cells alone or in co-culture with splenocytes. IFNGR1 expression was assessed by qPCR. Values are expressed in $\Delta\Delta Ct$ and normalized to each control. * = $p < 0.05$, ** = $p < 0.01$. Data are representative of 3 biological replicates. Mean \pm SEM is presented and statistical significance was determined with one-sample t-test comparing the columns to hypothetical value ($\Delta\Delta Ct$ value of the controls).

3.4 Discussion

The main goal of this chapter was to study the adrenergic regulation of PD-L1 expression in ovarian cancer. The data presented have shown that PD-L1 was expressed in the majority of tissues derived from patients diagnosed with ovarian cancer. In addition, PD-L1 expression intensity and spread was varied among tissues from different patients. Although there is no significant correlation between PD-L1 expression and the QoL of the patient, the cohort of patients was very small and more patients' data would be needed to confirm that PD-L1 expression may be not directly regulated by the levels of stress experienced by the patient.

Understanding how the adrenergic stimulus modulates PD-L1 expression in ovarian cancer is very challenging considering that the molecular mechanisms regulating PD-L1 expression in cancer are numerous and still not fully clear [206]. Previous scientific evidence has shown that PD-L1 expression is up-regulated by IFN- γ [99]. This hypothesis was confirmed in our experimental model with ovarian cancer cell lines up-regulating PD-L1 expression after stimulation with IFN- γ at different concentrations. This response was so robust that the addition of NA or PRO plus NA to IFN- γ did not make any significant changes. Ovarian cancer cells treated with NA or PRO alone did not show significant changes in PD-L1 expression, suggesting that NA does not directly regulate PD-L1 expression and that PD-L1 adrenergic modulation is much more complex.

It has been shown that immune cells express ADRB and respond to NA by increasing IFN- γ production [207, 208]. Results presented here suggest that NA can affect immune cell activation with a prompt IFN- γ production after 3h treatment. After 24h, activated immune cells significantly increased IFN- γ levels regardless of NA addition. The loss of the immune-regulatory effect of NA between 3h and 24h activation can be attributed to either; (1) the time of exposure to the hormone, which is crucial considering the very short half-life of NA [34]. (2) A prolonged exposure to NA, which can result in a down-regulation of ADRB and consequently in the loss of the downstream effect after 24h [209]. In conclusion, the data presented suggest that the addition of NA during the activation of immune cells hastens the early IFN- γ release. However, IFN- γ levels are not affected by NA after 24h activation.

Our data improved the understanding of adrenergic blockade in the immune modulation; while NA hastened the production of IFN- γ at 3h after activation, PRO significantly diminished IFN- γ levels in the culture media of activated immune cells at 3h and 24h. The anti-inflammatory role of PRO has been previously described in a mouse model of sepsis where splenocytes from mice treated with PRO decreased their ability of producing IFN- γ

[210]. Although the molecular mechanism of IFN- γ suppression after exposure to PRO remains unknown, these findings elucidate that the adrenergic signalling pathway and its blockade modulate IFN- γ production which can- in turn- regulate PD-L1 expression on cancer cells.

Our hypothesis is based on the adrenergic modulation of PD-L1 expression in ovarian cancer cells via the regulation of IFN- γ production in immune cells. Although in our *in vitro* model we found that NA had no direct effects on PD-L1 expression in cancer cells; it is important to consider that the tumour microenvironment is much more complex. For instance, NA can modulate processes such as cytokine production and infiltration of immune cells into the tumour. These events can also affect PD-L1 expression on cancer cells as described in section 3.1.1. However, we simplified the experimental model in order to investigate the role of adrenergic stimulus mediated by IFN- γ and immune cells. For this reason, immune cells were activated in the presence of NA or PRO plus NA for 24h, co-cultured with ID8 cells for 24h to examine the IFN- γ levels in the culture media and PD-L1 expression on cancer cells.

IFN- γ production was not upregulated by the activation of the immune cells or the addition of NA or PRO plus NA when in co-culture with ID8 ovarian cancer cells. These results showed that the presence of ovarian cancer cells is crucial in the modulation of the immune response regardless of the NA or PRO treatments. The molecular relevance of IFN- γ suppression in co-culture may be explained by several scenarios:

- Activated cells block the production of IFN- γ via PD-(L)1 mediated immunosuppression. This first hypothesis implies a physical contact between cancer and immune cells which is – in theory – excluded in our experimental model of co-culture (details in 2.1.6). However, it has been shown that PD-L1 can be released in extracellular vesicles that increase in number after IFN- γ stimulation [211].
- Activated cells suppress the production of IFN- γ with a transition from pro-inflammatory immune phenotype to an anti-inflammatory immune phenotype;
- Activated immune cells are induced to switch towards a less metabolic active resting immune cell phenotype with the suppression of IFN- γ production.

These findings can support a proposed mechanism which regulates PD-L1 expression on ovarian cancer. In particular, when immune cells encounter cancer cells they are stimulated to produce IFN- γ , which in turn can upregulate PD-L1 expression and led to a PD-L1-mediated immunosuppression. This microenvironment allows the tumour immune escape by blocking the production of the pro-inflammatory cytokines (e.g. IFN- γ) and inducing the production

of anti-inflammatory cytokines (e.g IL-10). NA supports IFN- γ production by the immune cells with no consequences for PD-L1 expression on cancer cells. However, the adrenergic blockade with PRO reduces the IFN- γ produced by the immune cells and – consequently - cancer cells are not triggered to express PD-L1.

This mechanism of regulation was evaluated by a transient knock down of IFNGR1 expression in ID8 ovarian cancer cells with siRNA. Although IFGR1 was successfully transiently silenced in ID8, these experiments showed that IFNGR1 can be re-expressed when ID8 cells are co-cultured with immune cells.

Findings from the cytokine analysis allow us to understand the regulation between immune and cancer cells. After 24h activation, immune cells did not show any significant changes in the levels of IL-10 regardless of their activation status or treatment. When in co-culture with ID8, activated immune cells with or without NA increased IL-10 levels, supporting the idea that the activated immune cells are undergoing a switch towards an anti-inflammatory phenotype. In the co-cultures with activated immune cells, higher levels of IL-10 were found in the media as well as the upregulation of PD-L1 expression in ID8 cancer cells, suggesting that PD-L1 and the production of anti-inflammatory cytokines might undergo an activation-dependent modulation. While the addition to NA did not significantly change the results, the treatment with PRO plus NA had an interesting outcome. In particular, PD-L1 expression was down-regulated in ID8 cancer cells co-cultured with immune cells activated with the addition of PRO plus NA and these cells also decreased the levels of IL-10 produced. This evidence confirms the hypothesis that PRO inhibits the immune cells IFN- γ production which might also down-regulate PD-L1 expression in cancer cells and prevent the anti-inflammatory (IL-10) immune response.

Taken together, these results reveal a critical role of adrenergic signalling in regulating the immune response and PD-L1 expression. Our findings support the idea that NA sustains the immune activation with the production of IFN- γ which can be the stimulus that upregulates PD-L1 expression on ovarian cancer cells. Experiments using PRO further support this theory. The addition of PRO inhibits IFN- γ production in activated immune cells and prevents PD-L1 expression on cancer cells. Our data have shown that IFN- γ suppression in co-culture of ID8 and activated immune cells (with or without NA) can be due to PD-L1-mediated immunosuppression and a switch to an anti-inflammatory pattern with production of IL-10. In the presence of PRO, the up-stream suppression of IFN- γ blocks the pro-inflammatory

response. However, the suppression of IFN- γ mediated by PRO also reduces PD-L1 expression in cancer cells and the anti-inflammatory switch with a decrease in IL-10 production. Although this research examined the adrenergic immunomodulation of PD-L1 expression in ovarian cancer, the complexity of the tumour microenvironment is not taken into consideration as long as the direct effect of NA on the tumour itself. In conclusion, this research enlightened the effects of adrenergic stimulation via NA and the blockade with PRO on the regulation of the immune response and PD-L1 expression in ovarian cancer cells proposing a molecular mechanism of a modulation via IFN- γ .

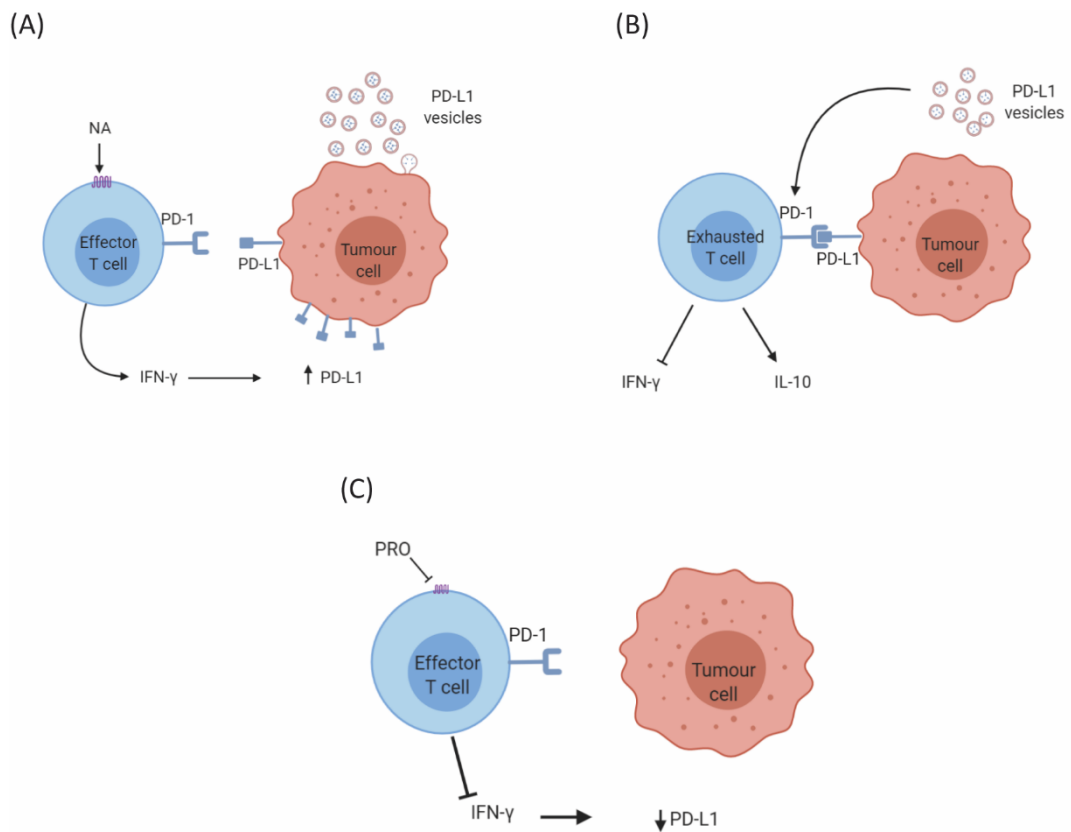


Figure 16 Proposed mechanism of PRO-mediated PD-L1 downregulation

(A) NA stimulation on effector immune cells accelerates IFN- γ production which leads to PD-L1 overexpression on cancer cells. PD-L1 can be expressed on the cancer cell surface and/or secreted in extracellular vesicles. (B) The interaction of PD-1 and PD-L1 leads to an exhausted T cell phenotype with blockade of IFN- γ and production of IL-10. (C) Propranolol (PRO) blocks the upstream production of IFN- γ and the IFN- γ -mediated PD-L1 expression on cancer cells.

4. Chapter 4 – Development of a 3D spheroid model of ovarian cancer to define NA, PRO, and stress-induced immune-tumour interactions

4.1 Introduction

4.1.1 Adrenergic stress and immune-tumour interaction

Tumour immune infiltration is an important parameter that correlates with a better prognosis in many cancer types and with the capacity of developing an anti-tumour immune response [84, 212-217]. The molecular mechanisms leading to an immune migration into solid tumours are still not fully understood. It is important to note that the immune cells able to penetrate the cancer mass can be pro or anti-tumour and the analysis of the immune cell trafficking can predict the cancer clinical outcome. For instance, a Th1 infiltration in the primary tumour is associated with a decreased metastatic invasion and an anti-tumour response led by cytotoxic T cells (CTLs). On the contrary, an anti-inflammatory tumour microenvironment with Th2 and T_{reg} infiltration leads to the progression of the tumour [218]. The immune control of the tumour also contributes to the inhibition of the tumour spread. Pre-metastatic niches establish a first attempt to evade immunity by reducing the cytotoxic effector functions [219]. This evidence supports the hypothesis that the metastatic power of a tumour and the immune infiltration are interdependent mechanisms.

The specific role of stress on the immune signature of ovarian cancer will be illustrated in chapter 5. Since tumour immune infiltration represents a prognostic parameter, this chapter will illustrate the effect of stress on this process by recreating the tumour three-dimensional structure *in vitro*. [220]. Furthermore, adrenergic stress can suppress the immune effector functions by modulating the metabolic pathway of immune cells (1.2.6). Since the metabolism of the cells is influenced by the 3D structure (1.4.4), this chapter will also assess the role of adrenergic stimulation on the metabolic program of the 3D tumour alone or in presence of immune cells.

Chronic stress can affect the immune response against tumour by initiating mechanism of immunosuppression [40]. Previous evidence has shown that adrenergic stress can regulate the immune system through the modulation of several processes such as T cell proliferation, differentiation and cytokine release [221, 222]. In chapter 3, we proposed a molecular mechanism through which the adrenergic modulation of the immune response to cancer involves the regulation of the PD-(L)1 axis. A scientific evidence of an effect of stress hormones on the ability of immune cells to migrate was been shown in a study on T cells. In this research, T cells exposed to NA or other stress hormones decreased their activation and migration ability by deregulating the actin cytoskeleton [170]. This evidence can bring to the hypothesis that the effect of stress on immune migration ability can have potential

consequences for the tumour immunity. However, the influence of stress on the ability of immune cells to infiltrate a 3D tumour mass has not been studied yet.

4.2 Aims

This research aims to:

- Develop a 3D tumour spheroid model for ovarian cancer in order to reproduce the tumour architecture;
- Develop a co-culture model to study the immune cells' interaction with an ovarian tumour 3D mass;
- Analyse the effect of stress and NA on the immune infiltration;
- Analyse the effect of stress and NA on the proteomic profile of 3D ovarian cancer spheroids.

4.3 Results

4.3.1 The immune cell infiltration in a 3D model of ovarian cancer is affected by immune cells activation, treatment and time in co-culture

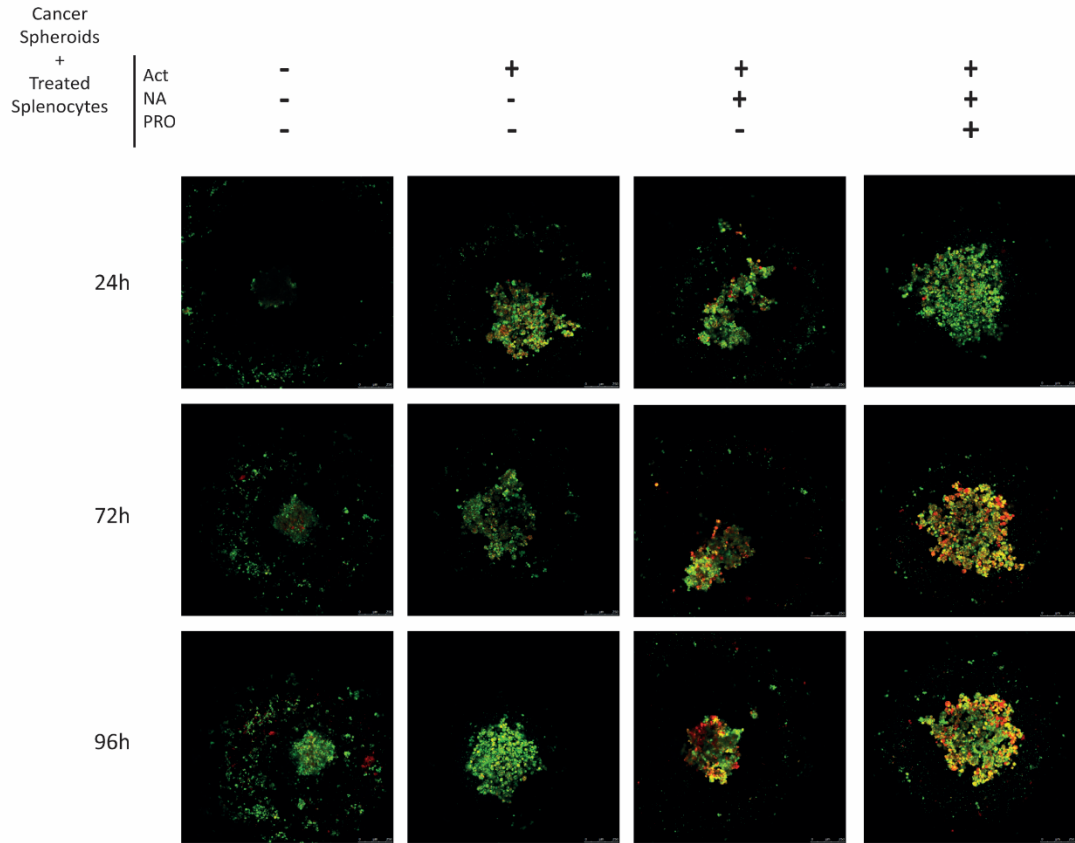
In order to study the immune cell infiltration into the tumour mass, we established a multicellular spheroid model. This was obtained co-culturing mouse ovarian cancer spheroids with spleen-derived cells. ID8 ovarian cancer cells were incubated with DiO lipophilic tracer and cultured in an ultra-low attachment plate for a week to let them aggregated into 3D spheroids. Splenocytes activated *ex vivo* with PMA/Ionomycin with or without the addition of NA or PRO and NA were incubated with Dil lipophilic tracer and added to the spheroids following the protocol illustrated in 2.1.8. The immune infiltration was evaluated by confocal imaging using an image analysis created for this purpose described in 2.1.10 and 2.1.11. Briefly, the relative intensity of immune cells (orange) was determined in the spheroid (green) surface area. Relative intensities among the different treatment groups were compared at 24h, 72h and 96h after co-culture.

Representative images of the multicellular spheroids are shown in Figure 17A. At 24h, immune infiltration was significantly higher in spheroids co-cultured with activated splenocytes regardless of the addition of NA or PRO plus NA compared to spheroids co-cultured with inactive splenocytes (Figure 17A).

After 72h and 96h of co-culture, immune infiltration relative intensity was significantly increased in spheroids co-cultured with activated splenocytes treated with PRO plus NA compared to the ones co-cultured with inactive immune cells (Figure 17B).

These data showed a higher immune cell infiltration at 24h in 3D spheroids co-cultured with activated cells. Infiltration is also modulated over time and increased in PRO treated activated immune cells.

(A)



(B)

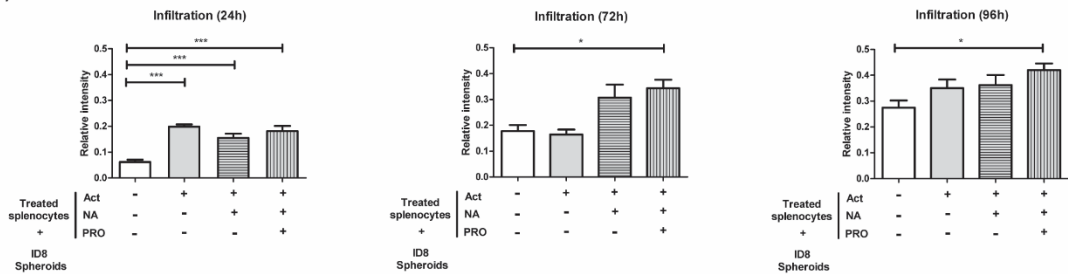


Figure 17 Immune cell infiltration in a 3D model of ovarian cancer is affected by immune cells activation, treatment and time in co-culture

ID8 ovarian cancer cells were incubated with DiO lipophilic tracer (green) and cultured in an ultra-low attachment plate for a week to let them form spheroids. Splenocytes activated *ex vivo* with PMA/Ionomycin with or without the addition of NA or PRO were incubated with Dil lipophilic tracer (orange) and added to the spheroids. (A) Representative images taken at 24h, 72h and 96h for each treatment group are shown. (B) Splenocytes relative intensity (orange) was calculated in the area of the spheroid (green). Graphs show relative intensities of each treatment group at 24h, 72h and 96h. Mean \pm SEM is presented and statistical significance was determined with one way ANOVA (Post-test: Bonferroni). * = $p < 0.05$, *** = $p < 0.001$. Data are representative of 3 biological replicates.

4.3.2 Adrenergic stress does not influence structural parameters of a 3D spheroids of ovarian cancer

In order to study the effect of NA and PRO on tumour spheroids, we evaluated other structural parameters of the tumour spheroids such as area, eccentricity and solidity. Detailed description of these parameters is shown in 2.1.10.

The surface area of the spheroid is an indication of the tumour mass growth. This can be related to a tumour increase or a consequence of the immune infiltration. The eccentricity is an indirect indication of the roundness of the spheroid. The solidity of the spheroid correlates with the disaggregation of the tumour spheroid.

Surface area, eccentricity and solidity did not show any significant difference among the different treatments or over time (Figure 18).

Results have shown that structural parameters of the spheroids were not affected by the different treatments.

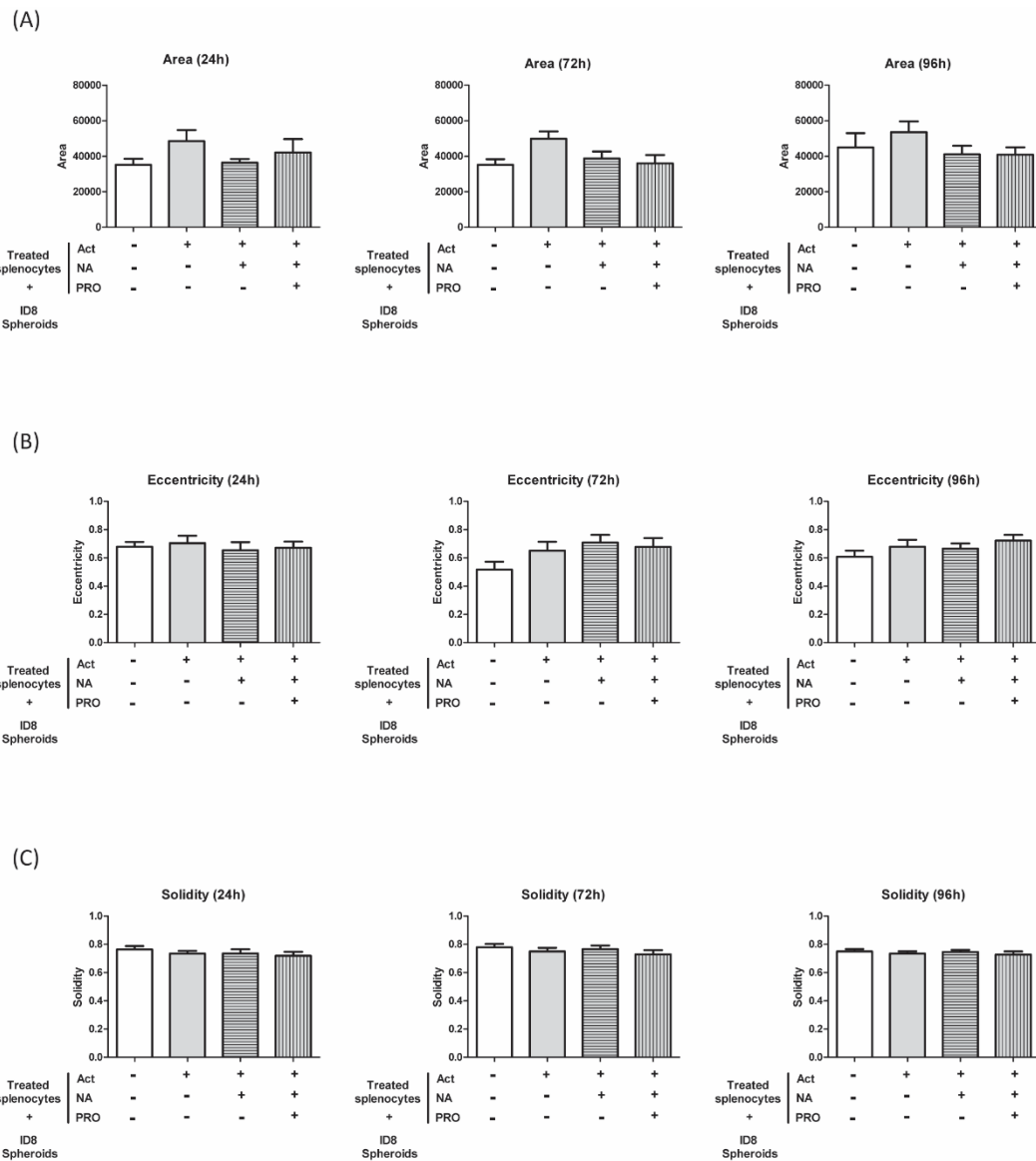


Figure 18 Adrenergic stress does not influence structural parameters of a 3D spheroids of ovarian cancer

ID8 ovarian cancer cells were incubated with DiO lipophilic tracer (green) and cultured in an ultra-low attachment plate for a week to let them form spheroids. Splenocytes activated *ex vivo* with PMA/Ionomycin with or without the addition of NA or PRO were incubated with Dil lipophilic tracer (orange) and added to the spheroids. (A) Surface area of each treatment group at 24h, 72h and 96h. (B) Eccentricity of each treatment group at 24h, 72h and 96h. (C) Solidity of each treatment group at 24h, 72h and 96h. Mean \pm SEM is expressed and statistical significance was determined with one way ANOVA (Post-test: Bonferroni). Data are representative of 3 biological replicates.

4.3.3 NA and PRO affect the proteomic profile of 3D spheroids of ovarian cancer

The proteomic analysis of the cancer spheroids showed the influence of NA or PRO on ovarian cancer. Ovarian cancer spheroids were incubated for a week in an ultra-low attachment 96 well plate following the protocol discussed in 2.1.7 and treated with NA or PRO for 24h. Proteins were extracted from spheroids, SDS-PAGE was performed, peptides were digested and analysed by the Q Exactive Hybrid Quadrupole-Orbitrap Mass Spectrometer as discussed in 2.8. Tandem mass spectra (MS/MS) were analysed by SEQUEST and the proteins obtained were analysed with STRING v11 online programme. Mass spectra counts were compared between the two treatment groups (NA and PRO). Proteins with significant changes in the two treatments groups (fold change>2) were analysed for protein-protein interactions (PPI). The analysis also allocates the protein networks to a specific signalling pathway. This matching protein-network has been performed using Gene Ontology or Reactome (free online software).

1183 total proteins were identified; proteins abundance in the PRO group vs the NA were a total of 40 with protein-protein interaction (PPI) p-value < 1.0e-16). In the NA group vs PRO, there was an abundance of 80 proteins with PPI p-value of 6.77e-10 (Table 7A). The PPI network map was obtained with a STRING analysis for PRO and NA samples (Figure 19 and Figure 20).

The protein identifications were analysed with Gene Ontology to identify the biological processes which they are involved in. In spheroids treated with PRO plus NA, there was an abundance of proteins involved in the oxidation-reduction process (FDR=1.22E-20) and in the metabolic process (FDR=3.47E-10) (Table 7B). Among the proteins involved in the metabolic pathway there were the alcohol dehydrogenase class 3 (Adh5), aldo-keto reductase members (Akr1a1, Akr1b7, Akr1b8, Akr1c13), aldehyde dehydrogenases (Aldh1a1, Aldh2), aldolase (Aldoa), enolase (Eno1).

In spheroids treated with NA the protein enrichment was involved in cellular (FDR=8.18E-10) and metabolic (FDR=2.61E-08) processes (Table 8A). In this case, the abundant proteins in the metabolic process included the pyruvate kinase (Pkm) and the glyceraldehyde-3-phosphate dehydrogenase (Gapdh).

The proteomic results were analysed also with the Kyoto Encyclopaedia of Genes and Genomes (KEGG) to evaluate their molecular interaction, reaction and relation networks. In spheroids treated with NA the proteasome subunits (E.g Psm2, Psm5, Psm1, and Psm14), increased (FDR=0.0039) compared to spheroids treated with PRO plus NA. Elongin

B (Tceb2) and elongin C proteins (Tceb1) also increased in spheroids treated with NA alone compared to spheroids treated with PRO plus NA (Table 8B).

These data evaluated the proteomic profile of cancer spheroid treated with NA alone versus spheroids treated with NA plus PRO. Results have shown an enrichment in protein involved in biological process such as metabolism.

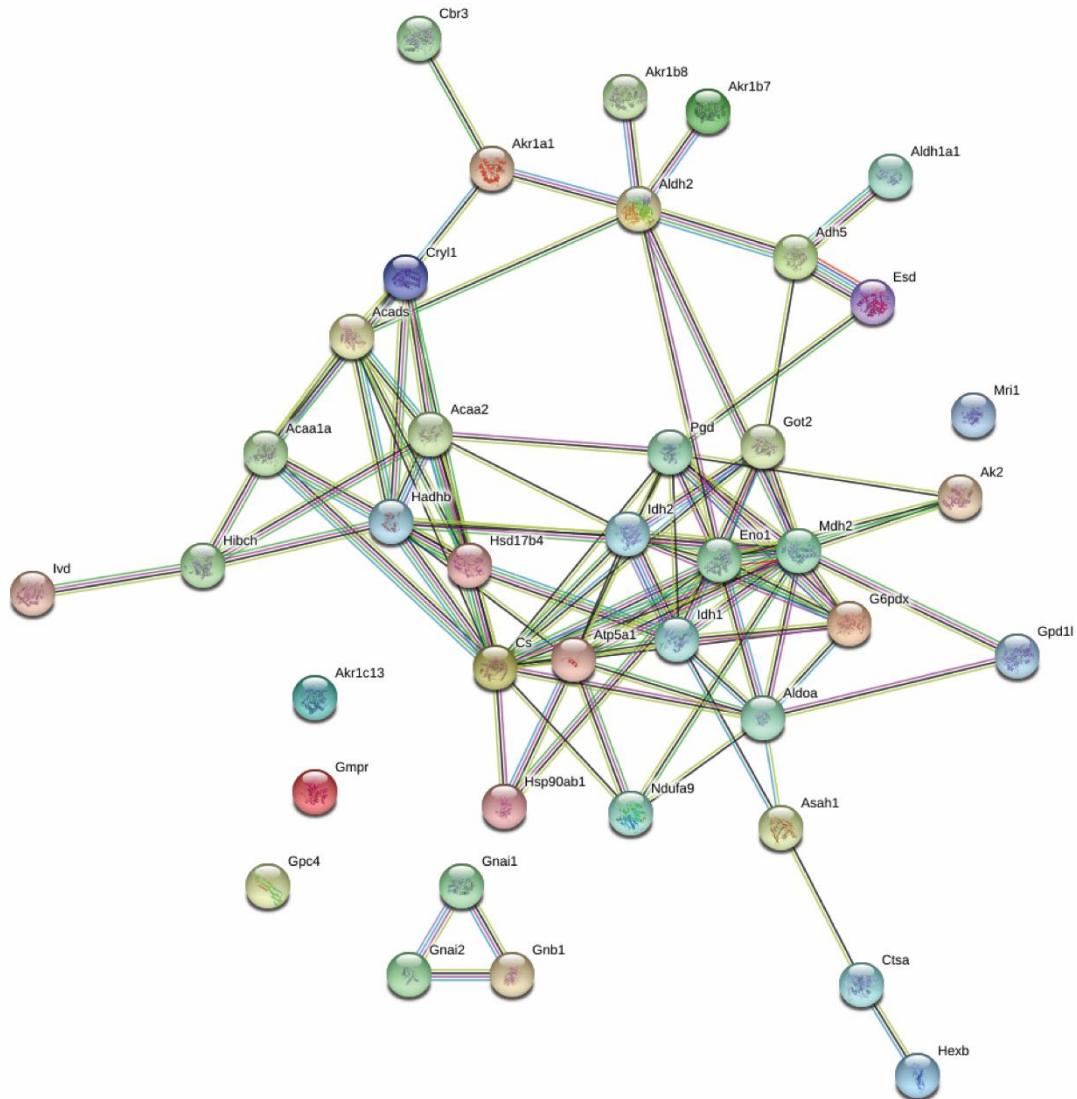


Figure 19 Spheroid (treated with PRO+NA) protein-protein interaction network map

Ovarian cancer spheroids were incubated for a week in an ultra-low attachment 96 well plate, treated with NA or PRO plus NA for 24h. Proteins were extracted, SDS-PAGE was performed, peptides were digested and analysed by the Q Exactive Hybrid Quadrupole-Orbitrap Mass Spectrometer. Tandem mass spectra (MS/MS) were analysed by SEQUEST and the proteins obtained were analysed with STRING v11 online programme. Mass spectra counts were compared between the two treatment groups (NA and PRO+NA). Proteins with significant enrichment in the two treatments groups (fold change>2) were analysed for protein-protein interactions (PPI) obtaining the map shown in the figure.

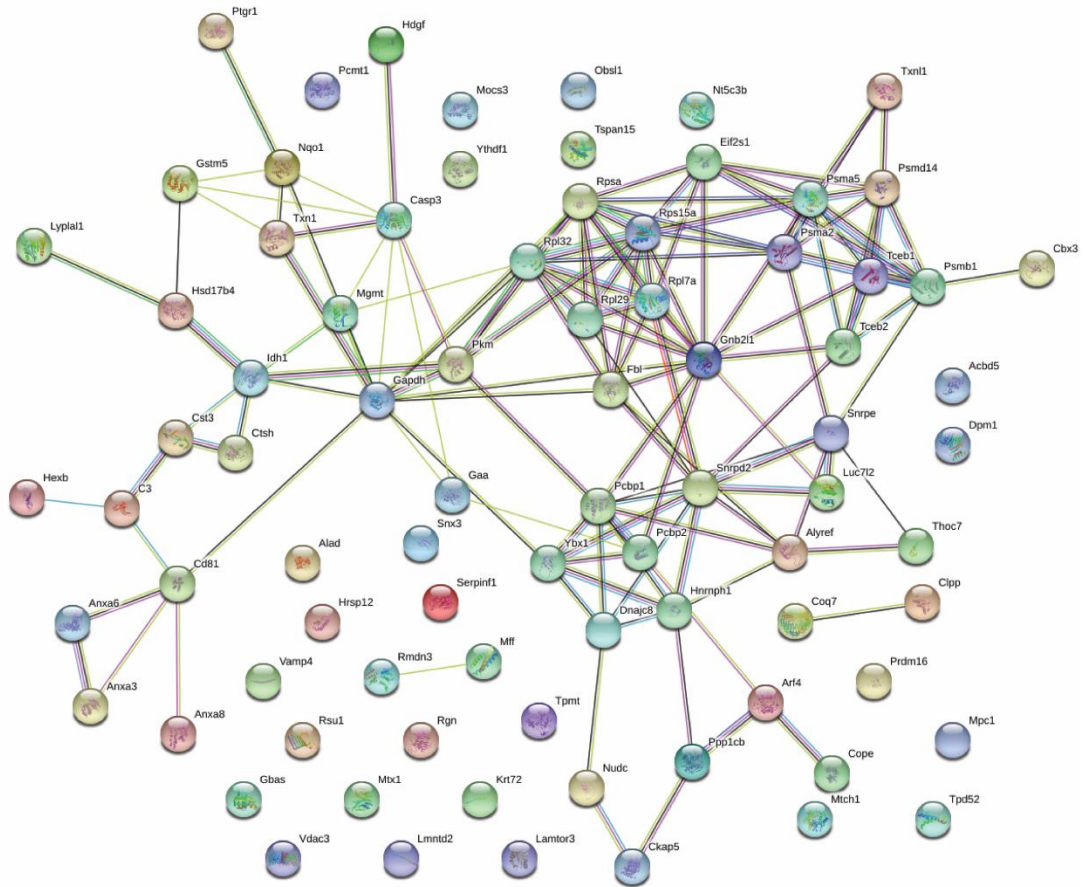


Figure 20 Spheroid (treated with NA) protein-protein interaction network map

Ovarian cancer spheroids were incubated for a week in an ultra-low attachment 96 well plate, treated with NA or PRO plus NA for 24h. Proteins were extracted, SDS-PAGE was performed, peptides were digested and analysed by the Q Exactive Hybrid Quadrupole-Orbitrap Mass Spectrometer. Tandem mass spectra (MS/MS) were analysed by SEQUEST and the proteins obtained were analysed with STRING v11 online programme. Mass spectra counts were compared between the two treatment groups (NA and PRO+NA). Proteins with significant enrichment in the two treatments groups (fold change>2) were analysed for protein-protein interactions (PPI) obtaining the map shown in the figure.

(A)

Sample	Total proteins (FC>2)	PPI enrichment p-value
Proteins enriched in PRO+NA	40	<1.0e-16
Proteins enriched in NA	82	6.77e-10

(B)

Process	Number of proteins enriched	Total proteins involved in the process	FDR	Proteins matching the process (labels)
Oxidation-reduction process	24	898	1.22E-20	Acaa1a,Acaa2,Acads,Adh5,Akr1a1,Akr1b7,Akr1b8,Akr1c13,Aldh1a1,Aldh2,Cbr3,Cryl1,Cs,G6pdx,Gmpr,Gpd1l,Hadhb,Hsd17b4,ldh1,ldh2,lvd,Mdh2,Ndufa9,Pgd
Metabolic process	36	8164	3.47E-10	Acaa1a,Acaa2,Acads,Adh5,Ak2,Akr1a1,Akr1b7,Akr1b8,Akr1c13,Aldh1a1,Aldh2,Aldoa,Asah1,Atp5a1,Cbr3,Cryl1,Cs,Ctsa,Eno1,Esd,G6pdx,Gmpr,Got2,Gpd1l,Hadhb,Hexb,Hibch,Hsd17b4,Hsp90ab1,ldh1,ldh2,lvd,Mdh2,Mri1,Ndufa9,Pgd

Table 7 Protein enriched in spheroids treated with PRO+NA (Gene Ontology analysis)

Ovarian cancer spheroids were incubated for a week in an ultra-low attachment 96 well plate, treated with PRO+NA for 24h. Proteins were extracted, SDS-PAGE was performed, peptides were digested and analysed by the Q Exactive Hybrid Quadrupole-Orbitrap Mass Spectrometer. Tandem mass spectra (MS/MS) were analysed by SEQUEST and the proteins obtained were analysed with STRING v11 online programme. Mass spectra counts were compared between the two treatment groups (NA and PRO plus NA). Proteins with significant enrichment in the two treatments groups (fold change>2) were analysed. (A) String analysis for protein-protein interactions (PPI). Total number proteins enriched are expressed comparing the two treatments group against each other. Enriched proteins showed a Fold Change (FC>2). (B) Gene Ontology analysis indicating the biological processes that the enriched proteins are involved in.

(A)

Process	Number of proteins enriched	Total proteins involved in the process	FDR	Proteins matching the process (labels)
cellular process	76	12459	8.18E-10	Acbd5,Alad,Alyref,Anxa3,Anxa6,Arf4,C3,Casp3,Cbx3,Cd81,Ckap5,Clpp,Coq7,Cst3,Ctsh,Dpm1,Eif2s1,Fbl,Gaa,Gapdh,Gbas,Gnb2l1,Gstm5,Hdgf,Hexb,Hnrnp11,Hrsp12,Hsd17b4,Idh1,Lamtor3,Luc7l2,Lyplal1,Mff,Mgmt,Mocs3,Mpc1,Mtch1,Mtx1,Nqo1,Nt5c3b,Nudc,Obsl1,Pcbp1,Pcbp2,Pcmt1,Pkm,Ppp1cb,Prdm16,Psm a2,Psm a5,Psm b1,Psm d14,Ptgr1,Rgn,Rmdn3,Rpl29,Rpl32,Rpl7a,Rps15a,Rpsa,Rsu1,Serpinf1,Snrpd2,Snrpe,Snx3,Tceb1,Tceb2,Thoc7,Tpd52,Tpmt,Tspan15,Txn1,Txn11,Vamp4,Vdac3,Ybx1
metabolic process	60	8164	2.61E-08	Acbd5,Alad,Alyref,Arf4,C3,Casp3,Cbx3,Cd81,Clpp,Coq7,Ctsh,Dpm1,Eif2s1,Fbl,Gaa,Gapdh,Gbas,Gnb2l1,Gstm5,Hdgf,Hexb,Hnrnp11,Hrsp12,Hsd17b4,Idh1,Luc7l2,Lyplal1,Mgmt,Mocs3,Mpc1,Nqo1,Nt5c3b,Pcbp1,Pcbp2,Pcmt1,Pkm,Ppp1cb,Prdm16,Psm a2,Psm a5,Psm b1,Psm d14,Ptgr1,Rgn,Rpl29,Rpl32,Rpl7a,Rps15a,Rpsa,Snrpd2,Snrpe,Snx3,Tceb1,Tceb2,Thoc7,Tpmt,Tspan15,Txn1,Txn11,Ybx1

(B)

KEGG description	Number of proteins enriched	Total proteins involved in the process	FDR	Proteins matching the process (labels)
Proteasome	4	45	0.0039	Psm a2,Psm a5,Psm b1,Psm d14
Ribosome	5	128	0.0081	Rpl29,Rpl32,Rpl7a,Rps15a,Rpsa
Carbon metabolism	4	118	0.0306	Gapdh,Idh1,Pkm,Rgn
Spliceosome	4	130	0.0306	Alyref,Pcbp1,Snrpd2,Snrpe
Biosynthesis of amino acids	3	75	0.0454	Gapdh,Idh1,Pkm

Table 8 Protein enriched in spheroids treated with NA (Gene Ontology and KEGG analysis)

Ovarian cancer spheroids were incubated for a week in an ultra-low attachment 96 well plate, treated with NA for 24h. Proteins were extracted, SDS-PAGE was performed, peptides were digested and analysed by the Q Exactive Hybrid Quadrupole-Orbitrap Mass Spectrometer. Tandem mass spectra (MS/MS) were analysed by SEQUEST and the proteins obtained were analysed with STRING v11 online programme. Mass spectra counts were compared between the two treatment groups (NA and PRO+NA). Proteins with significant enrichment in the two treatments groups (fold change>2) were analysed. (A) Gene Ontology analysis indicating the biological

processes that the enriched proteins are involved in. (B) KEGG analysis indicate the pathways that the enriched proteins are involved in.

4.3.4 Stress influences the metabolic program in multicellular ovarian cancer spheroids

To evaluate whether the effects of stress on immune cells influence the metabolic program of multicellular cancer spheroids, mice were exposed to restraint stress regimen for 5 weeks and their immune cells were isolated from the spleen, activated *ex vivo* and co-cultured with 3D ovarian cancer spheroids. Proteins were extracted from multicellular spheroids, SDS-PAGE was performed, peptides were digested and analysed by the Q Exactive Hybrid Quadrupole-Orbitrap Mass Spectrometer as discussed in 2.8.

Tandem mass spectra (MS/MS) were analysed by SEQUEST and the proteins obtained were analysed with STRING v11 online programme obtaining a PPI network map (Figure 21). The map shows three principal clusters of proteins involved in: metabolism (red), immune system (green) and RNA processing (purple).

Spheroids co-cultured with splenocytes derived from stressed mice showed abundance in proteins involved in metabolism (FDR=1.04E-19) such as aldolase (ALDOa), Glyceraldehyde-3-phosphate dehydrogenase (GAPDH), phosphoglycerate kinase (PGK1), enolase (ENO1) and pyruvate kinase (PKM). The proteins enriched in the stress group were also part of other biological processes involving the immune system (FDR=5.82E-08) and the RNA processing (FDR=5.97E-07) (Table 9).

Proteomic analysis of multicellular immune/cancer spheroids has shown an enrichment in proteins involved in metabolic processes, immune response and RNA processing.

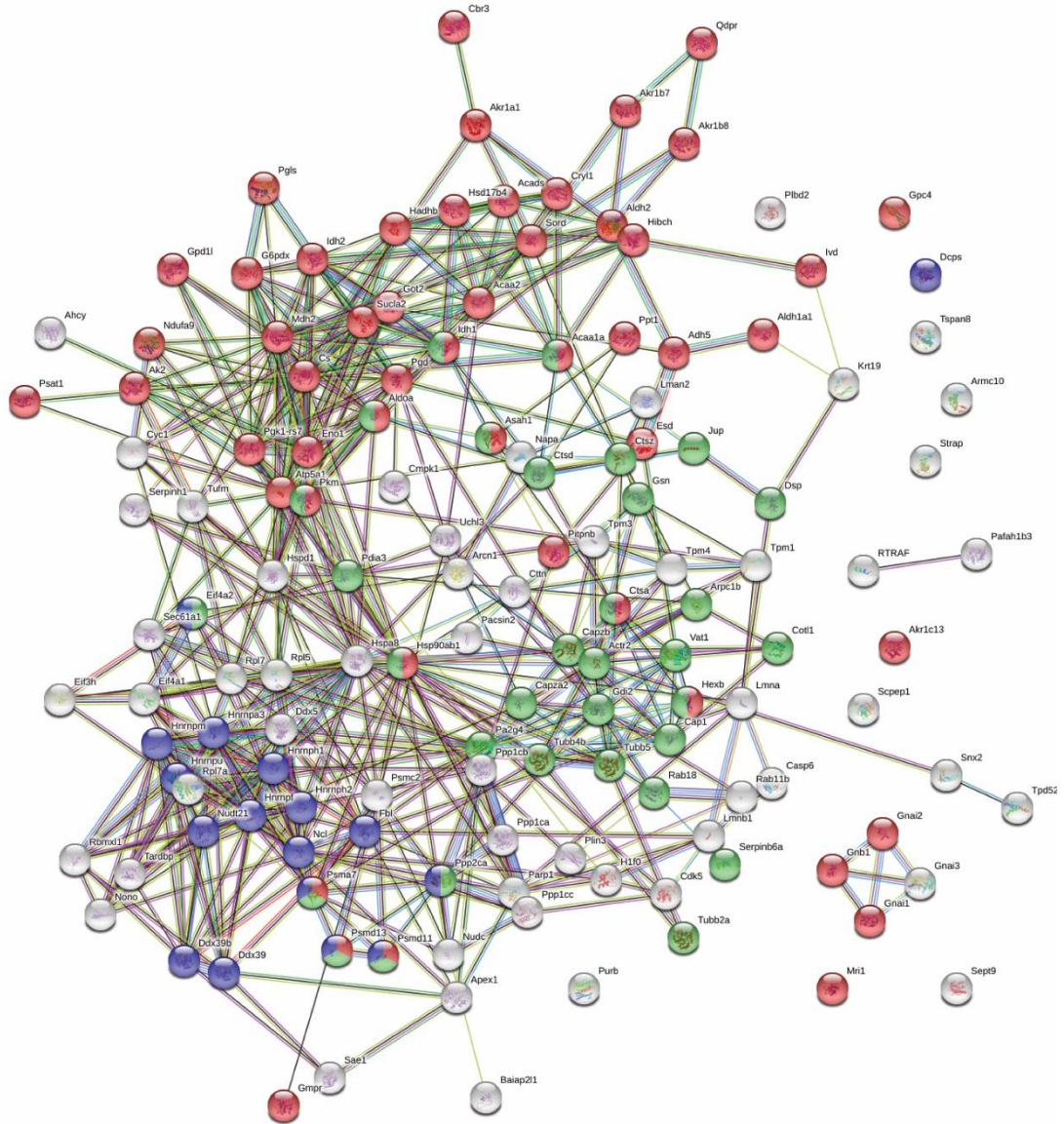


Figure 21 Multicellular spheroids protein-protein interaction (PPI) network map

Multicellular cancer spheroids were obtained co-culturing splenocytes with ovarian cancer spheroids. Splenocytes were isolated from mice undergone restraint stress for 5 weeks, activated ex vivo and co-cultured with 3D ovarian cancer spheroids for 24h. Proteins were extracted, SDS-PAGE was performed, peptides were digested and analysed by the Q Exactive Hybrid Quadrupole-Orbitrap Mass Spectrometer. PPI network map shows the proteins enriched (with a Fold Change>2) in the stress group compared to multicellular spheroids co-cultured with splenocytes from non-stressed mice. Three major pathways involve the proteins analysed: metabolism (red), immune system (green) and RNA processing (violet).

Process	Number of proteins enriched	Total proteins involved in the process	FDR	Proteins matching the process (labels)
Metabolism	52	1685	1.04E-19	Acaa1a,Acaa2,Acads,Adh5,Ak2,Akr1a1,Akr1b7,Akr1b8,Akr1c13,Aldh1a1,Aldh2,Aldoa,Asah1,Atp5a1,Cbr3,Cryl1,Cs,Ctsa,Eno1,Esd,G6pdx,Gmpr,Gnai1,Gnai2,Gnb1,Got2,Gpc4,Gpd1l,Hadhb,Hexb,Hibch,Hsd17b4,Hsp90ab1,ldh1,ldh2,lvd,Mdh2,Mri1,Ndufa9,Pgd,Pgk1-rs7,PglS,Pitpnb,Pkm,Ppt1,Psat1,Psma7,Psmd11,Psmd13,Qdpr,Sord,Sucla2
Immune System	33	1523	5.82E-08	Acaa1a,Actr2,Aldoa,Arpc1b,Asah1,Cap1,Capza2,Capzb,Cotl1,Ctsa,Ctsd,Ctsz,Disp,Eif4a2,Gdi2,Gsn,Hexb,Hsp90ab1,ldh1,Jup,Pa2g4,Pdia3,Pkm,Ppp2ca,Psma7,Psmd11,Psmd13,Rab18,Serpinb6a,Tubb2a,Tubb4b,Tubb5,Vat1
RNA processing	17	448	5.97E-07	Dcps,Ddx39,Ddx39b,Eif4a2,Fbl,Hnrnpa3,Hnrnpf,Hnrnph1,Hnrnph2,Hnrnpm,Hnrnpu,Ncl,Nudt21,Ppp2ca,Psma7,Psmd11,Psmd13

Table 9 Protein list of multicellular spheroids (Gene Ontology)

Multicellular cancer spheroids were obtained co-culturing splenocytes with ovarian cancer spheroids. Splenocytes were isolated from mice undergone restraint stress for 5 weeks, activated *ex vivo* and co-cultured with 3D ovarian cancer spheroids for 24h. Proteins were extracted, SDS-PAGE was performed, peptides were digested and analysed by the Q Exactive Hybrid Quadrupole-Orbitrap Mass Spectrometer. Enriched proteins (with a Fold Change>2) in the stress group were involved in three major biological processes: metabolism, immune response, and RNA processing.

4.3.5 The proteomic profile of multicellular immune/cancer spheroids converted into human homologous match pathways involved in metabolism

The analysis of the proteome of multicellular cancer spheroid can be indicative of which proteins are involved in different biological pathways. 3D cancer spheroids were co-cultured with activated splenocytes from stressed and non-stressed mice following the protocol discussed in 2.8. Proteins were extracted, SDS-PAGE was performed, peptides were digested and analysed by the Q Exactive Hybrid Quadrupole-Orbitrap Mass Spectrometer as discussed in 2.8. Tandem mass spectra (MS/MS) were analysed by SEQUEST and the proteins obtained were analysed with the online software Reactome. To better understand the translational value of our proteomic results, proteins identified in mouse spheroids were converted into the human homologous equivalent to match a human pathway. The pathways are representative of the analysed results. Each pathway shows several sub-pathways with the correspondent proteins representative of the query dataset. The number of proteins in the dataset that are part of the sub-pathway is indicated with the specific false discovery rate (FDR).

The analysis included proteins enriched in multicellular spheroids with ovarian cancer cells co-cultured with splenocytes isolated from stress mice using spheroids co-cultured with splenocytes from non-stressed mice as control. Among all orthologue human proteins obtained, 57 were part of metabolism pathway ($p=4.03E-09$; $FDR=1.14e-06$). In particular, metabolism of carbohydrate was the most representative sub-pathway with 14 proteins represented in the submitted data set ($p=2.96E-05$; $FDR=4.56E-3$). Among these, 3 (aldo-keto reductase 1 (AKR1a1), lambda-crystallin homolog (CRYL1) and sorbitol dehydrogenase (SORD)) out of 5 proteins were involved in the formation of xylulose-5-phosphate ($p=3.90E-05$; $FDR=0.004559$) (Table 10).

Proteomic data were analysed by converting them into human homologous. These results have shown proteins involved in metabolic processes.

Pathway name	Number of proteins enriched	Total proteins involved in the process	pValue	FDR	Number of reactions	Number of total reactions
Metabolism	57	2135	4.03E-09	1.14E-06	124	1982
Metabolism of carbohydrates	14	300	2.96E-05	0.004559	25	236
Formation of xylulose-5-phosphate	3	5	3.90E-05	0.004559	3	5
Metabolism of RNA	22	675	4.24E-05	0.004793	37	187
Metabolism of proteins	31	2012	0.13107	0.13107	102	873
Immune System	36	2373	0.126034	0.126034	48	1561
Innate Immune System	30	1186	1.59E-04	0.008881	26	661

Table 10 Reactome analysis of multicellular spheroids proteins converted into human homologues

Multicellular cancer spheroids were obtained co-culturing splenocytes with ovarian cancer spheroids. Splenocytes were isolated from mice that were restraint stressed for 5 weeks, activated *ex vivo* and co-cultured with 3D ovarian cancer spheroids for 24h. Proteins were extracted, SDS-PAGE was performed, peptides were digested and analysed by the Q Exactive Hybrid Quadrupole-Orbitrap Mass Spectrometer. Proteins identified in mouse spheroids were converted into the human homologous equivalent to match a human pathway with the online software Reactome. Each pathway specifies the number of proteins found in our experimental model, the total number of proteins involved in the pathway, the pvalue and the false discovery rate (FDR).

4.4 Discussion

3D tumour spheroids were successfully generated, and the model demonstrated the capability to reproduce *in vitro* the biological architecture of a tumour. An immune cell and cancer spheroid co-culture was used to assess the effect of NA, PRO and stress to the immune infiltration inside the tumour mass. In particular, the increase in the immune infiltration in spheroids treated with PRO plus NA gives an indication of the effects of beta-blockers on the immune cell trafficking. We have also shown a comprehensive proteomic analysis of spheroids. The analysis of the proteome in the cancer spheroids was indicative of the effects of NA, PRO and stress on the differential expression of regulators orchestrating biological pathways such as the cellular response to hypoxia and carbohydrate metabolism.

One of the findings of this research is the effect of NA and PRO on the ability of immune cells to infiltrate a 3D ovarian tumour mass. Tumour immune infiltration is a prognostic factor for the clinical outcome and for the prediction of responding to immune therapies [102, 212]. Previous evidence has shown that stress hormones such as NA deregulates the actin cytoskeleton of T cells and this can affect their ability to migrate [170]. Results showed that the cells' activation status is fundamental for immune infiltration. Furthermore, immune cells activated with the addition of NA plus PRO present a better infiltration compared to inactive immune cells and this was constant through time. However, this improvement might be activation-driven. Also, the image analysis is still not reflective of the biological sample and further analysis is still ongoing, including a mathematic study of the 3D tumour structure and informatics calculation of the infiltration rate. Further analysis on structural parameters that could have been affected by NA or PRO has shown that the size and the cell aggregation are not affected by the treatments. These results have shown that the model is appropriate for the study of cancer and immune cell interaction. However, an optimization of the downstream analysis could help to address other important questions. For instance, the expression of specific markers and an adequate imaging analysis could improve the understanding of the cell-cell interactions.

Further analysis was conducted to explore on a large-scale the proteome of the spheroids alone treated with NA or NA plus PRO to evaluate the effect of the adrenergic blockade. However, a further analysis comparing NA stimulation to unstimulated spheroids is the future prospective to assess the adrenergic proteomic regulation. Proteomic analysis was also performed in multicellular spheroids obtained co-culturing ovarian cancer spheroids

with activated immune cells isolated from a mouse spleen. The proteomic analysis was very informative in addressing the differential expression of proteins of 3D spheroids at different conditions. However, the results showed a broad range of proteins involved in different pathways that are connected to each other creating an extremely complex network. In addition, biological pathways are often very unstable with molecular regulators meticulously modulated to increase or decrease their function. For this reason, the results obtained by proteomic analysis are not entirely explicative, but they enlighten some aspects of this research and lead to interesting evaluations and further hypothesis.

Proteomic data will be discussed taking into consideration the specific biological pathway in which the proteins detected are involved, and the differential expression in the experimental treatments. One of the most represented pathways is the cellular response to hypoxia with a change in the proteasome components (E.g Psma2, Psma5, Psmb1, and Psmd14) and in elongin B (Tceb2) and elongin C proteins (Tceb1) in spheroids treated with NA alone compared to the ones treated with PRO plus NA. In the results shown above, NA treatment increased the expression of proteins involved in the normoxia pathway while in spheroids treated with PRO plus NA there is a reduction of the elongin B/C and proteasome components that suggests an enhanced response to the hypoxic stress. This evidence seems paradoxical considering that the oxygen culture conditions of spheroids in the two treatment groups are the same. An important consideration is that these results are interpreted comparing the two treatments without an indication on the basal activation of the hypoxic pathway in ovarian cancer spheroids left untreated. To understand the real impact of adrenergic stress on hypoxic ovarian tumour cells further analysis is needed. However, the regulation of hypoxic response is a crucial pathway in tumour biology and it stimulates cancer cells to adaptations related to tumour progression [154]. Furthermore, hypoxia enhances tumour angiogenesis, vasculogenesis, invasion and metastasis [223-225] and is considered a negative prognostic factor in solid tumours [226].

The upregulation of the hypoxic stress response network in spheroids treated with PRO plus NA is in contrast with previous evidence showing that NA (*in vitro*) and chronic stress (*in vivo*) can induce accumulation of HIF1 α and the expression of downstream genes in a pancreatic cancer model and this effect is inhibited by PRO [227, 228]. In addition, some of the downstream genes regulated by HIFs such as VEGF and MMPs have been shown to be downregulated by PRO [40, 49]. With the results shown by the proteomic analysis not fitting the previous scientific evidence, the effect of adrenergic stimulation on the cellular response

to hypoxia pathway remains ambiguous. However, two reasons can justify the results obtained:

- The previous results were obtained in a pancreatic model, while our results are obtained from an ovarian cancer model. In the context of the ovarian tissue, NA is naturally more abundant and influence the cellular response [229].
- PRO treatment had a different effect on this specific experimental model. Treatments hardly diffuse into the 3D spheroid mass creating a gradient of concentration with the inner hypoxic cells exposed to a lower concentration of drugs [153, 230]. However, the specific diffusion of NA and PRO in tumour spheroids was not evaluated. It is known that NA has a very short half-life and can be metabolized by cellular enzymes such as catechol-O-methyltransferase (COMT) and monoamine oxidase (MAO) [231]. On the opposite, PRO is a synthetic agent metabolized by enzymes expressed primarily in the liver [231]. Considering also that PRO is highly lipophilic, a more pronounced diffusion of this drug into spheroids cannot be excluded.
- Although the inner hypoxic core of spheroids is representative of the in vivo tumour, it cannot replicate the complexity of the tumour microenvironment which includes vascular remodelling, inflammation and interaction with different cell types [154].

In the context of a solid tumour, a dysregulation of the response to hypoxia is a classical feature and the HIF signalling can also be triggered by the oncogenic pathways of tumour cells. Evidence has shown that the activation of HIF system and the expression of downstream genes is activated in tumour cells independently from the oxygen levels [232]. In particular, the activation of the hypoxic pathway from a non-hypoxic stimulus is supported by the fact that mutations in the pVHL block the oxygen-dependent hydrolysis of HIFs resulting in a constitutive activation of the HIF responsive genes [232].

HIF target genes play a key role as regulators of the cellular metabolism. However, metabolic reprogramming with a shift from oxidative to glycolytic pathways is a common characteristic of cancer cells [233]. The activation of the hypoxic response and the metabolic dysregulation both concur to the creation of an aggressive cancer phenotype with a complex interplay among different pathways. The intricate network of interactions involves many different enzymes regulating important reactions leading to the formation of intermediates that can connect to other pathways [232]. Results have shown that in all experimental conditions the protein enrichment includes proteins involved in the metabolic pathway. This evidence can correlate with either the HIF system or with a metabolic switch due to the cancer phenotype.

A change in many enzymes involved in different metabolic pathways was observed in our experimental models. The most representative metabolic pathways are listed below:

- Glycolysis

Expression of glycolytic enzymes can be directly controlled by the HIF system. In particular, expression of glucose transporters (GLUT), essential for the intracellular internalization of glucose, is HIF-dependent [234]. This consideration is important since GLUT1 expression is also regulated by adrenergic stress in immune cells [64]. Although proteomic data cannot be informative on the expression or internalization of glucose receptors, 3D spheroids could represent an excellent method to further investigate the hypoxic or adrenergic regulation of glucose intake and metabolism in both ovarian cancer and immune cells.

Glycolytic enzymes regulated by HIF are usually overexpressed in cancer cells confirming the hypothesis that high glucose metabolism in tumours can be due to either the response to hypoxia or the activation/suppression of oncogenes/tumour suppressors. Although HIF system has been correlated with the upregulation of the glycolytic pathway, glycolysis can increase in solid tumours independently from the hypoxic context. Pyruvate kinase M (Pkm), involved in the glycolytic metabolism, plays a crucial role in cancer as well. Results have shown a great increase of Pkm in either spheroids treated with NA or spheroids co-cultured with splenocytes derived from stressed mice. These data indicate that the regulation of the glycolytic pathway can be influenced by the adrenergic hormone treatment and also by the infiltrating immune cells. However, our results present a limitation in the evaluation of Pkm expression: (1) Pkm is expressed in two different isoforms (M1 is expressed in the muscles, heart and brain, and M2 expressed in foetal tissues and cancers [235]) and the specific isoform in the spheroids cannot be identified by proteomic MS/MS analysis, (2) Pkm expression does not correlate with the enzymatic activity which can be modulated by small molecules and metabolites [236].

- Pentose phosphate pathway

Cancer cells entering the glycolysis also support the energetic request with other side pathways. The pentose phosphate pathway is crucial for cancer cells since it provides NADPH and generates pentose phosphates to supply the high nucleic acid synthesis. In spheroids treated with PRO plus NA and spheroids co-cultured with splenocytes derived from stressed mice, enzymes involved in the pentose phosphate pathway such as glucose-6-phosphate dehydrogenase (G6PDX), 6-phosphogluconolactonase (PGLs) and 6-phosphogluconate dehydrogenase (PGD) are enriched. In particular, G6PDX catalyses the entry step to the pathway and has been shown to be upregulated both in hypoxic and cancer cells [232, 237].

The pentose phosphate pathway, as one of the main sources of NADPH, represents a major actor in sustaining the cancer cell metabolic demand and supports cancer cell survival and metastasis [238]. This pathway plays also a pivotal role in removing reactive oxygen species (ROS) [239]. Since stress hormones (cortisol and NA) induce the production of ROS in cancer cells [240], the data shown represent a first attempt to explore stress effects on the pentose phosphate pathway in ovarian cancer taking into consideration the hypoxic effect in a 3D spheroid model.

- Formation of xylulose-5-phosphate

Xylulose-5-phosphate is an intermediate of the pentose phosphate pathway and it plays a crucial role in metabolic diseases. The major role of xylulose-5-phosphate is to activate the carbohydrate response element binding protein (ChREBP), a transcription factor regulating glycolytic and lipogenic genes [241]. The role of xylulose-5-phosphate in ovarian cancer spheroids is hard to interpret on the basis of our results. In general, the formation of this intermediate can be correlated to an excess in carbohydrate intake in the cells. Since glucose intake is one of the main processes to be effected by adrenergic stress [64], we hypothesise that spheroids treated with PRO plus NA and spheroids co-cultured with splenocytes derived from stressed mice show an increased the formation of xylulose-5-phosphate because of their altered carbohydrate metabolism.

The modulation of different metabolic pathways is particularly important in regards to spheroids co-cultured with immune cells. In this experimental model, multicellular cancer spheroids recreate the metabolic competition between cancer and immune cells. Also, stress effects on immune cells create an indirect modulation of the co-culture itself. The attempt to explore the very complex interplay between stress, cancer and immune system was further complicated by the involvement of tumour glucose metabolism. However, this helped in understanding how both stress and cancer evasion mechanisms can impair the immune response to ovarian cancer. Furthermore, the insight into cancer and immune cells metabolism offers a starting point to elucidate how checkpoint inhibitors targeting PD-L1 can alter the tumour metabolism. In chapter 3, expression of PD-L1 on cancer cells was linked to IFN- γ production by immune cells. Also, PD-L1 immunomodulation has been proven to lead to a suppression of the anti-tumour response. In light of our results showing an increased network in the glucose metabolic pathway, it is possible that the interface between cancer and immune cells and therefore PD-(L)1 axis can also modulate the metabolic pathway of both cell types. A study on progressive sarcoma elucidates the role of PD-L1 as modulator of

the glucose metabolism in cancer and immune cells [168]. PD-L1, by enhancing the glycolytic pathway in cancer cells, depletes glucose for immune cells. The study also shows that PD-L1 inhibitor therapy restores the nutrient restriction of the immune cells and enhances their effector functions by increasing IFN- γ production. Although the use of PD-L1 inhibitor as a therapy for ovarian cancer will be examined in details in chapter 5, the evidence that checkpoint inhibitor therapy can be beneficial for cancer and immune metabolism support the hypothesis of an advantage of using a combined therapy that can reduce the negative effects of adrenergic stress and enhance the immune response.

Results showing the enrichment of proteins in spheroids co-cultured with splenocytes give an indication of the effect immune cells in the cancer model as well as the stress-dependent modulation of cancer immunity. Proteins from spheroids co-cultured with immune cells isolated from stressed mice and projected to human equivalents are involved in many biological pathways. One of the over-represented pathways is the cellular response to stress. This pathway includes the response to hypoxia, also noticed in spheroids treated with NA, and the heat shock protein 90 (HSP90) chaperone cycle for steroid hormone receptors (SHR). HSP90 is an evolutionary conserved protein which stabilizes more than 200 proteins that are mostly involved in the cell response to stress [242]. In order to fulfil its function, HSP90 binds other proteins (co-chaperons) and ATP forming a dynamic complex which clamps substrate proteins and assists them in achieving the correct folding or prevent their aggregation [243]. Steroid hormone receptors are part of the HSP90 substrates forming HSP90-SHR complexes that regulate their transcription factor functions. Modulation of HSP90 complexes, especially the ones regulating the glucocorticoid receptors (GRs), has been recently studied since it can correlate with psychological disorders such as post-traumatic stress disorder (PTSD), major depressive disorder (MDD) and anxiety [244]. In order to understand the importance of HSP90 and the SHR cycle in our experimental model, the concept of how psychological stress affects the biological processes is briefly revised. Stress signals let the hypothalamus produce the corticotropin releasing hormone (CRH) which stimulates the pituitary gland to produce adrenocorticotrophic hormone (ACTH). ACTH activates cortisol synthesis in the adrenal gland cortex [24]. Stress stimuli also produce NA from the noradrenergic loci cerulei (LC-NA axis) or the adrenal gland medulla [24]. Stress has therefore two different biological modulators (cortisol and NA) that bind different receptors and activates two separate signalling pathways. The evidence of having activation of the HSP90-SHR pathway in spheroids co-cultured with immune cells isolated from stressed mice is indicative that a cellular stress

response is in action and it is possibly driven by cortisol. In accordance with this hypothesis, tumour spheroids treated with NA do not activate the HSP90-SHR pathway since NA binding to the beta-adrenergic receptors activates the PKA mediated pathway.

Another pathway enriched in spheroids co-cultured with splenocytes derived from stressed mice is the RNA processing. In particular, many heterogeneous nuclear ribonucleoproteins (hnRNPs) are overexpressed. hnRNPs are important for the RNA export from the cell nucleus to the cytoplasm and for the mRNA translation in the cytoplasm [245]. Interestingly, they play a crucial role in cancer and metastasis. For instance, hnRNP expression in breast cancer correlates with augmented tumour proliferation and metastasis [246]. The reason why hnRNPs are correlated with cancer is that they regulate the expression of several oncogenes such as KRAS, HER2 and BRCA [247, 248]. hnRNPs are also involved in the post-transcriptional regulation of GLUT1 and in the chemokine expression in response to inflammatory stimuli [249, 250]. An increased hnRNP-mediated modulation of chemokines in spheroids co-cultured with immune cells isolated from stressed mice can affect two different aspects: (1) the attraction of immune cells into the tumour mass, (2) the increased migration of cancer cells. Although hnRNPs are linked to chemokine expression, their role in multicellular cancer spheroids is still not clear. In addition, many families of hnRNPs include different isoforms that cannot be identified with a MS/MS peptide analysis. However, our results indicate that the hnRNPs can be involved in the cancer/immune interaction and open to further investigation.

In conclusion, our results have demonstrated that PRO treatment has potential in increasing the immune cell infiltration into the tumour mass. This evidence is important considering the recreation of the 3D tumour architecture and the interaction between immune and cancer cells. Furthermore, the proteomic analyses of tumour and multicellular spheroids have highlighted the response to hypoxia and the switch in metabolism as pathways that influence the adrenergic immune regulation to ovarian cancer. Data shown so far suggested that the adrenergic stress and immune system interactions are important in ovarian cancer. In the next chapter, the effects of the adrenergic blockade with PRO on immunotherapy will be evaluated.

5. Chapter 5 – Combined therapy with propranolol and PD-(L)1 inhibitor decreases tumour burden, metastasis, and promotes an anti-tumour immune signature in ovarian cancer

5.1 Introduction

5.1.1 Cancer immune signature

The immune system responds to cancer eliminating malignant cells and repressing cancer development. In order to have an immune response against cancer, the specific tumour needs an immunogenic pattern and show specific tumour associated antigens as discussed in chapter 1. However, cancer cells can initiate an escape process which inhibits the immune response and allows tumour growth. The “immune signature” of a tumour has been described as the presence of specific immune cell subsets which have the ability to penetrate the tumour mass and produce an anti-tumour response [220]. The tumour infiltration consists in cells from the innate immune system such as macrophages and neutrophils; and adaptive immune cells including T and B lymphocytes [220]. Although the immune signature in a tumour is represented by cell infiltration, it is important to consider that immune cells are able to orchestrate an inflammatory environment which can inhibit or support cancer growth [78]. For this reason, the evaluation of the immune response to cancer distinguishes the anti-tumorigenic microenvironment from a pro-tumorigenic one. Recent studies have focused the attention on the adaptive immune response as the preferential route to contrast tumour growth and establish an acute pro-inflammatory response [119, 212, 251, 252]. Cells involved in this process are T lymphocytes which, by secreting cytokines such as IFN- γ , generate a strong inflammatory response which can expand the cellular pool of cytotoxic T cells (CTLs) guiding the tumour cell destruction and – potentially - elimination.

5.1.2 Adrenergic stress and Beta-blockers effects on the immune response to cancer

In chapter 3 we focused the attention on the role of NA on immune regulation without considering the direct effects of the adrenergic stimulus on the cancer itself. Pre-clinical studies have shown that the adrenergic pathway stimulation supports tumour progression, angiogenesis and enhance the metastatic power of cancer [40, 41, 253]. The molecular mechanisms regulating these processes are still not fully understood and several studies have speculated many potential mechanisms of action including the modulation of the immune system [254]. In this chapter, we take into consideration the direct effects of stress on cancer and the ones that can modulate the immune response and the microenvironment of cancer. As discussed before, the adrenergic stimulus has bidirectional effects on the sympathetic nervous system and the immune compartment [255]. The investigation of the adrenergic stress effect on ovarian cancer immune response is also supported by the potential of beta-blockers as anti-cancer agent as presented in chapter 1. In this chapter, we

focus the attention on the properties of PRO, a non-selective beta-blocker, on the immune response to cancer.

One of the most important roles of beta blockers is the anti-metastatic effect. Although this effect alone is already remarkable, it also may be important for the modulation of the immune response. In tumours spreading in other organs, the pre-metastatic niche establishes a first attempt to evade immunity by reducing the cytotoxic effector functions [219]. With the decrease of the metastatic spread, beta-blockers are beneficial in the restoration of the immune response. In addition, beta-blockers are involved in the endothelial release of nitric oxide (NO) which has been shown to correct the suppressed activation and infiltration of TILs [256, 257].

Surgery has a critical impact in cancer patients causing pro-metastatic, pro-angiogenic and immune suppressive signals [258]. Although the surgical removal of a primary tumour is a life-saving procedure in most cases, the perioperative period can affect the long-term cancer outcome. It is known that surgical stress causes perioperative and post-operative catecholamines release which contributes to immunosuppression in animals and humans [259]. Perioperative catecholamines and prostaglandins modulate the secretion of factors regulating the inflammatory pattern (e.g., IL-10, IL-6, TNF- α). At the same time, the primary tumour excision eliminates the tumour secreted factors (e.g., VEGF, IL-8, IL-6) that contribute to tumour spread and immune suppression. In this scenario, there is a fine balance between the molecular signals that support tumour progression and the ones that prevent tumour growth. Pre-clinical studies have shown that the beta-adrenergic blockade can reduce stress-mediated immunosuppression and that beta-blockers perioperative use improves the cancer immune competence [260-262].

The immunologic effects of beta-blockers include the modulation of immune cell activities and the peripheral distribution as described in chapter 3. *In vitro*, the ADRB signal decreases CD4⁺ T cell proliferation and induces changes in cytokine release [221]. The cytokine modulation is fundamental to determine the fate and differentiation of T cells [74, 222]. However, the effects of NA and ADRB stimulus on immune cells *in vivo* are much more difficult to interpret due to the complexity of the molecular mechanisms and the immune profile of the model being used. Dated *in vivo* studies have explored the beta-adrenergic stimulation effects on immune cells trafficking suggesting that catecholamines increase the circulating lymphocytes and decreased the number of lymphocytes in the spleen [263, 264]. The mobilization of splenic immune cells is due to an adrenergic alteration in the expression of lymphocyte adhesion molecules and it is independent from the NA vasoconstriction action

[265]. In contrast to this evidence, other studies have shown that the adrenergic stimulus (isoproterenol) increases the lymphocytes homing to the spleen and other peripheral organs [266]. In the context of cancer, the production of chemokines and the expression of chemokine receptors also play a crucial role in lymphocyte trafficking. NA via ADRB stimulation attenuates the expression of several chemotactic genes (e.g. CXCR4, CXCL10, and CCL2) in breast cancer cells (MDA-MB-231) [267]. In particular, the chemokine interferon- γ inducible protein 10kDa (CXCL10) has a significant role in attracting monocytes, T cells and NK cells. Although CXCL10 expression in cancer is correlated to an antitumor immunogenic role, it has been shown to have also a tumour-promoting effect in some cancers such as breast cancer, basal cell carcinoma and glioma [268-270].

An important role in the tumour immunomodulation via adrenergic stimulation is the production of IFN- γ . As mentioned in chapter 3, IFN- γ production is important for the regulation of the anti-tumour response and for PD-L1 expression in cancer cells. However, investigating the role of IFN- γ *in vivo* can be challenging due to the different actions exerted and the general anti-inflammatory tumour microenvironment established.

The classical mechanisms used by cancer cells to escape the adaptive immune response are based on inducing T cell dysfunction and immunosuppression. Nutrients competition between cancer and T lymphocytes can concur to downregulate the effector function of the immune cells leading to a less responsive immunity. A metabolic interaction between tumour and immune cells is represented by the action of indoleamine 2,3-dioxygenase (IDO). This enzyme is involved in the catabolism of tryptophan, an essential amino acid crucial for T cell differentiation and functions. Deficiency of tryptophan leads to the repression of T cell division and the accumulation of tryptophan catabolites induces T cell apoptosis and differentiation in Treg. IDO1 is expressed in tumours and acts as a regulator of the tumour immunity by inhibiting the anti-tumour immune response [271].

5.2 Aims

This study aims to:

- Explore the negative effects of restraint stress on the immune signature of ovarian cancer in an orthotopic mouse model;
- Examine the effects of a combined therapy of PRO with PD-(L)1 inhibitors in reducing tumour progression and improving the anti-tumour immune signature in an orthotopic mouse model of ovarian cancer.

The immune signature of ovarian tumours will be examined taking into consideration relevant markers for immune infiltration and immune cytotoxic activity. Also, the pattern of expression of growth factors involved in immune infiltration such as VEGF will be analysed.

5.3 Results

5.3.1 Combined therapy with PRO and PD-(L)1 inhibitor reduces tumour burden and metastatic nodules

As a start point, we wanted to establish whether a therapy with PRO, PD-L1 inhibitor or a combination of the two would influence the tumour burden in a syngeneic orthotopic ovarian cancer model (2.2). In addition, we wanted to confirm the anti-metastatic properties of the therapy with PRO and examine if this action was preserved when PRO was in combination with the checkpoint inhibitor.

Mice weights were evaluated pre-surgery and every week. In all groups, there is a significant gain in weight after the surgical insertion of the mini pump ($p < 0.001$). At week 4, there is a significant ($p < 0.005$) decrease between the weights of control mice compared to the mice receiving PD-(L)1 inhibitor (Figure 22B).

C57BL/6 mice undergoing restraint stress procedure were injected intraperitoneally with ID8 ovarian cancer cells and treated with PRO, PD-(L)1 inhibitor or a combination of the two as discussed in 2.2. Mice were sacrificed 4 weeks after cancer injection and gross necropsy was performed blind by an expert operator. Tumour weight was reported for all the groups and data were analysed using one way ANOVA statistical test. The group receiving the combined therapy with PRO and PD-(L)1 inhibitor showed a significant decrease in tumour weight ($p \leq 0.05$) (Figure 22D).

We also examined the effect of stress and different therapies on the tumour metastatic power by reporting the organs affected by metastatic nodules. Mice undergoing restraint stress showed a significant increase ($p \leq 0.5$) in the number of organs affected by metastatic nodules (Figure 22C). The organs usually affected by metastatic nodules were fallopian tubes in both the cancer control and cancer stress group. In the latter group, other organs were affected by metastatic nodules including liver, kidneys, diaphragm and colon. Mice treated with PRO monotherapy or PRO in combination with PD-(L)1 inhibitor showed a significant decrease ($p \leq 0.001$) in the number of organs affected by metastatic nodules (Figure 22C). Mice receiving PD-(L)1 inhibitor as monotherapy did not show a significant change in the tumour spread presenting enlarged fallopian tubes with metastatic nodules also in the peritoneal cavity, kidneys, diaphragm and intestines.

These results showed a potential of the combined therapy of PRO plus PD-(L)1 inhibitor with a decrease in tumour burden and in the number of organs affected by metastatic nodules.

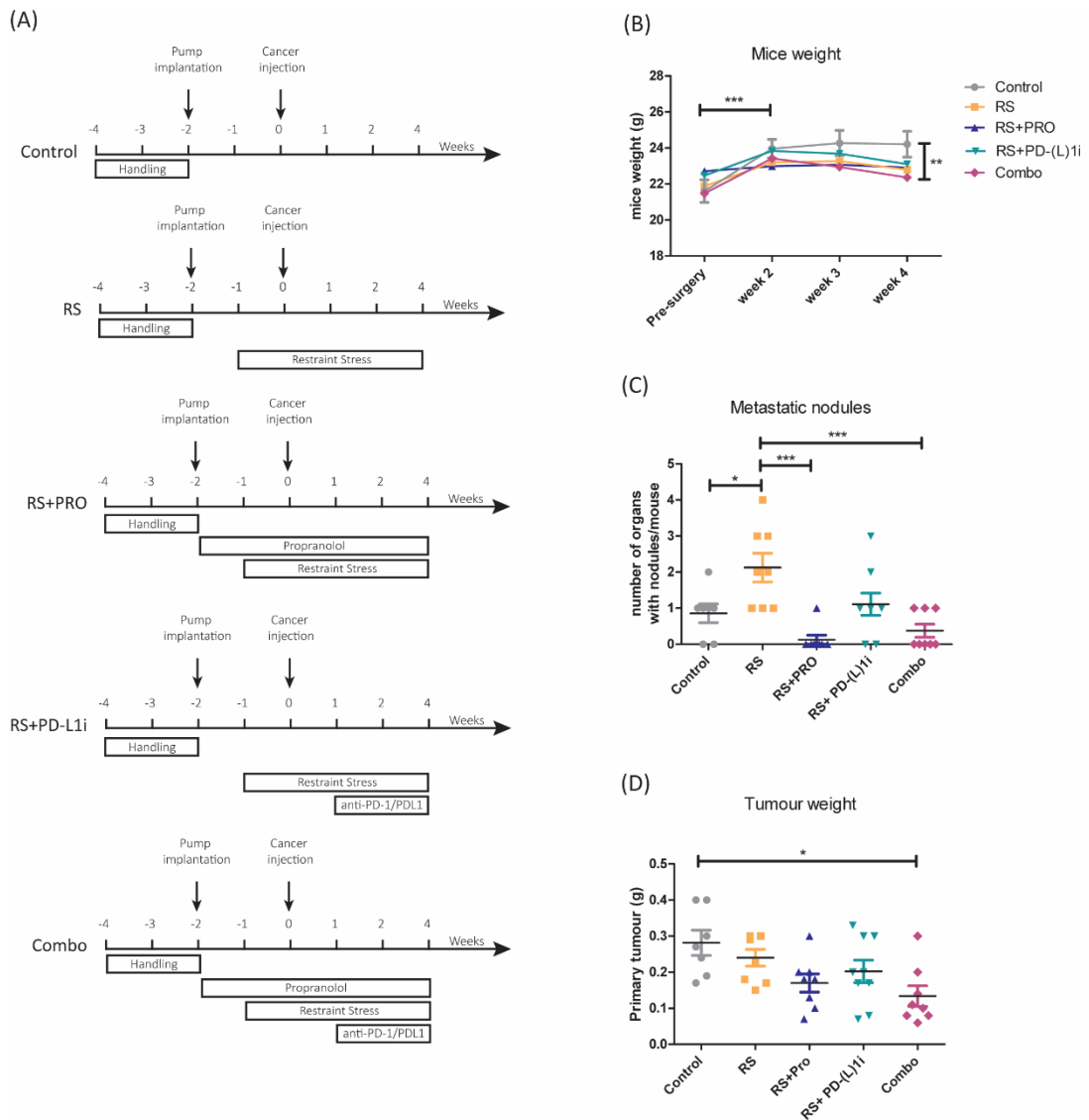


Figure 22 Combined therapy with PRO+PD-(L)1i decrease tumour burden and metastatic nodules.

Mice were randomized into 5 groups. (A) Schematic view of treatments for each group. (B) Mice weight was measured before surgery and every week after the cancer injection. (C) Tumours weights were reported in the graph. (D) Organs affected by metastatic nodules were reported by gross necropsy and the total number of organs affected for each mouse was plotted in the graph. Mean \pm SEM is expressed and statistical significance was determined with a one-way ANOVA test (Post test: Bonferroni). * = $p < 0.05$, ** = $p < 0.01$, *** = $p < 0.001$. Data are representative of 2 different *in vivo* experiments.

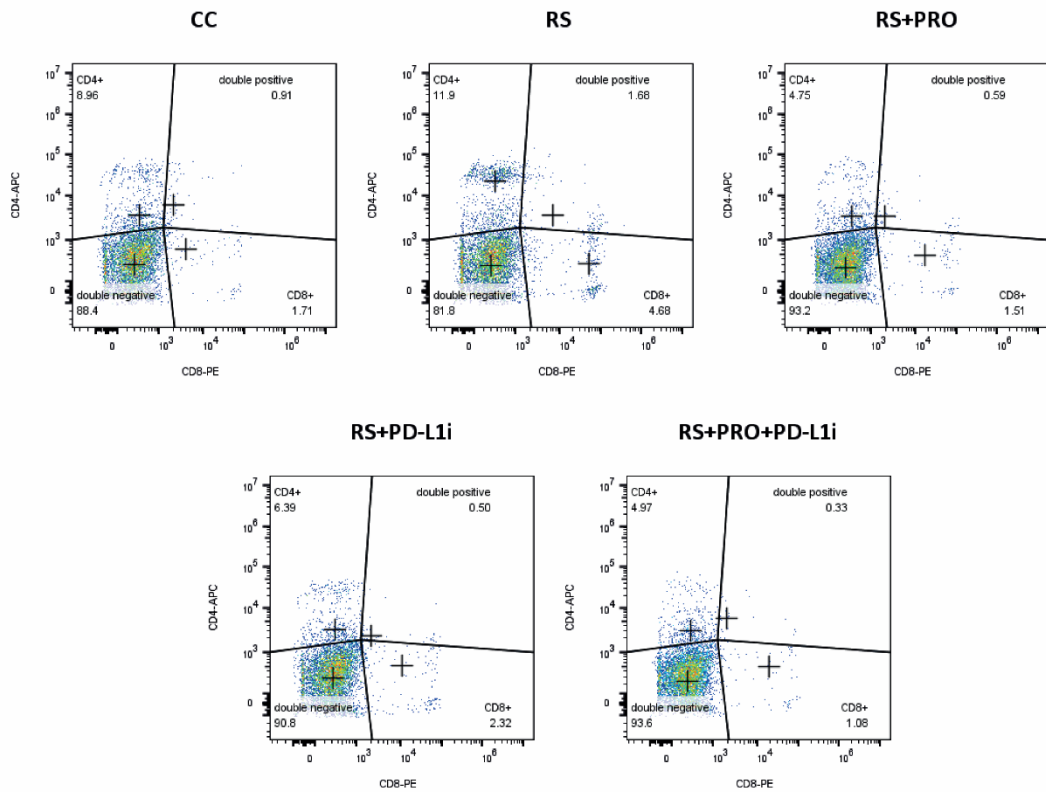
5.3.2 Combined therapy with PRO and PD-(L)1 inhibitor affects CD8+ cell population in the spleen of ovarian cancer bearing mice

To assess if stress or any of the treatment affected the splenic immune cell population, we evaluated T cell population in the spleen of tumour bearing mice. Spleens were collected and processed to obtain a single cell suspension as discussed in 2.1.4. The single cell suspension was incubated with fluorescent conjugated antibody and the ratio between CD4⁺ and CD8⁺ cells was analysed by flow cytometry. Data were analysed with FlowJo v.10, gating for live single cells and with an appropriate compensation correction (method discussed in 2.6).

CD4⁺ splenic population was not significantly affected by stress or by any of the treatments (data not shown). CD8⁺ cells significantly decreased ($p \leq 0.5$) in the spleen of mice receiving the combined therapy with PRO and PD-(L)1 inhibitor compared to mice undergoing restraint stress (Figure 23B).

In conclusion, the combined therapy (PRO + PD-(L)1 inhibitor) decreased the number of CD8⁺ splenic resident cells.

(A)



(B)

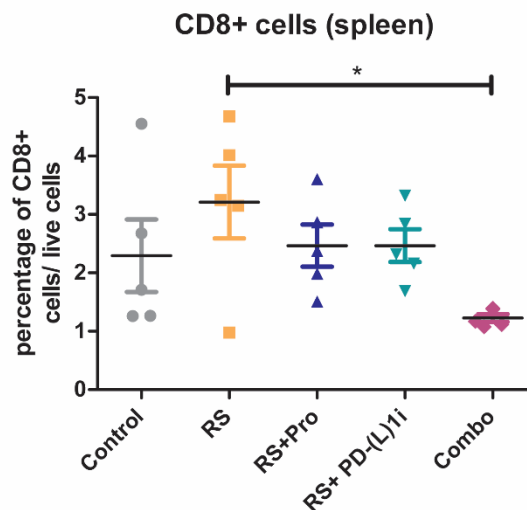


Figure 23 Combined therapy with PRO+PD-(L)1i decrease CD8⁺ cells resident in the spleen

Spleens were collected and processed to obtain a single cell suspension. (A) Representative gating flow cytometry plots showing CD4⁺ and CD8⁺ cell population on splenocytes from different experimental groups. (B) Percentage of CD8⁺ cells in the different groups. Mean \pm SEM is presented and statistical significance was determined with a one-way ANOVA test (Post test: Bonferroni). * = $p < 0.05$. Data are representative of 1 *in vivo* experiment; replicates are representative of different mice.

5.3.3 Restraint stress upregulates *CD3* and *CD4* expression, but not *CD8* in mouse tumour tissues

The role of stress on the tumour immune signature was examined by exposing mice injected with ovarian cancer cells to a restraint stress procedure (methodology illustrated in 2.2.4). Tumours were homogenized, total RNA was extracted, reverse transcription was used to obtain cDNA and qPCR was performed following the protocols discussed in 2.4. We assessed the expression of markers indicative of immune cell infiltration such as *CD3*, *CD4* and *CD8*. The mRNA values and the specific gene expression in tumours of stressed mice were compared to a hypothetical value of basal gene expression in the cancer control group.

CD3 and *CD4* mRNA expression increased significantly in tumours of mice undergoing restraint stress procedure compared to the tumours of control mice (Figure 24). *CD8* expression did not show any significant changes in tumours of mice undergoing restraint stress compared to the control group (Figure 24).

The evaluation of the T cell immune markers revealed a role of restraint stress with a significant increased expression of *CD3* and *CD4*. Interestingly, restraint stress did not significantly affect the expression of the CTL marker *CD8*.

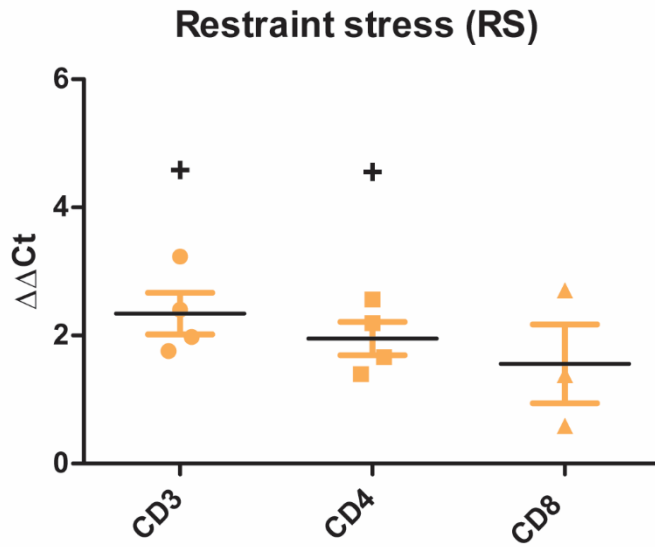


Figure 24 Restraint stress upregulates *CD3* and *CD4* expression, but not *CD8* in mouse primary tumour tissues

Tumours were homogenized and total RNA was extracted. Expression of different markers was assessed by qPCR. Values are expressed in $\Delta\Delta C_t$ and normalized to cancer control group. Mean \pm SEM is presented and statistical significance was determined with one-sample t-test comparing each column to a hypothetical value ($\Delta\Delta C_t$ value for expression of relative gene in the cancer control group). + = $p < 0.05$. Data are representative of 1 *in vivo* experiment; replicates are representative of different mice.

5.3.4 Combined therapy with PRO and PD-(L)1 inhibitor upregulates the expression of CD8 in mouse tumour tissues

Expression of T cell markers was examined in more detail in mice ovarian tumours by comparing all treatment groups (illustrated in Table 4). This was an evaluation of the tumour immune signature taking into consideration either stress or treatments as variables. For this reason, values of expression of each mRNA were normalized to the expression of the same mRNA in the cancer control group.

In the tumours of stressed mice treated with PD-(L)1 inhibitor, *CD3* mRNA expression increased significantly compared to mice undergoing restraint stress alone or mice receiving PRO ($p \leq 0.05$ and $p \leq 0.005$). Mice undergoing restraint stress and receiving the combined therapy with PRO and PD-(L)1 inhibitor, *CD3* expression significantly ($p < 0.05$) decreased compared to mice receiving PD-(L)1 inhibitor as monotherapy (Figure 25A). *CD4* mRNA increased significantly in tumours of stressed mice treated with PD-(L)1 inhibitor as monotherapy or combined with PRO ($p \leq 0.005$ and $p \leq 0.05$) (Figure 25B). *CD8* mRNA expression was significantly upregulated ($p \leq 0.05$) in the group of mice undergoing restraint stress and receiving the combination of PRO and PD-(L)1 inhibitor compared to the PD-(L)1 inhibitor monotherapy (Figure 25C).

In conclusion, these results have shown a regulation of the T cell markers in tumours of mice receiving different therapies. The combined therapy with PRO plus PD-(L)1 inhibitor has an interesting effect on the expression of the CTL marker CD8. In particular, CD8 expression is significantly upregulated in mice receiving the combined therapy combined to the PD-(L)1 inhibitor monotherapy.

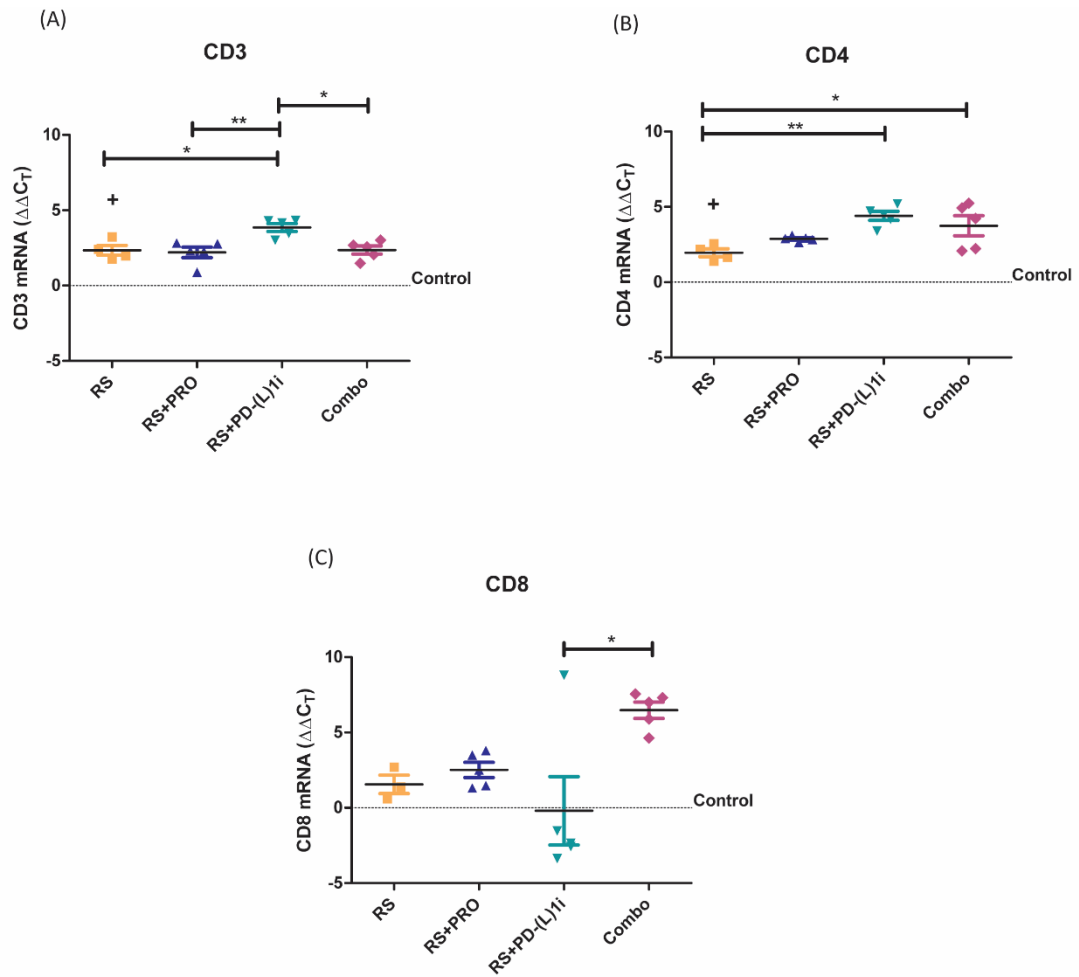


Figure 25 CD3, CD4 and CD8 expression in mouse primary tumour tissues

Tumours were homogenized and total RNA was extracted. Expressions (A) *CD3*, (B) *CD4* and (C) *CD8* were assessed by qPCR. Values are expressed in $\Delta\Delta C_T$ and normalized to cancer control group. Mean \pm SEM is presented and statistical significance was determined with one-way ANOVA (Post test: Bonferroni) and also with one-sample t-test comparing each column to a hypothetical value ($\Delta\Delta C_T$ value for expression of relative gene in the cancer control group). * = $p < 0.05$, ** = $p < 0.01$, *** = $p < 0.001$. + = significant vs Control ($p < 0.05$). Data are representative of 1 *in vivo* experiment; replicates are representative of different mice.

5.3.5 Therapy with PRO and/or PD-(L)1 inhibitor affects *VEGF* expression in mouse tumour tissues

To evaluate the role of angiogenesis, the expression of *VEGF* was evaluated in tumours of mice of all groups and normalized to the expression in tumours of the cancer control group. A significant upregulation ($p \leq 0.001$) in *VEGF* mRNA expression was evident in the tumours of mice undergoing restraint stress together with monotherapy of PRO or PD-(L)1 inhibitor compared to the restraint stress group. In addition, *VEGF* was significantly more expressed in tumours of mice treated with PD-(L)1 inhibitor compared to the ones treated with PRO. In the combined therapy with PRO and PD-(L)1 inhibitor, *VEGF* expression significantly decreased compared to either PRO or PD-(L)1 inhibitor monotherapy ($p \leq 0.001$) (Figure 26). It is important that the combined therapy does not affect *VEGF* expression which was upregulated by both monotherapies. This evidence sustains the hypothesis that, while the combined therapy with PRO and PD-(L)1 inhibitor can ameliorate the tumour immune signature, it does not influence the progression of the tumour.

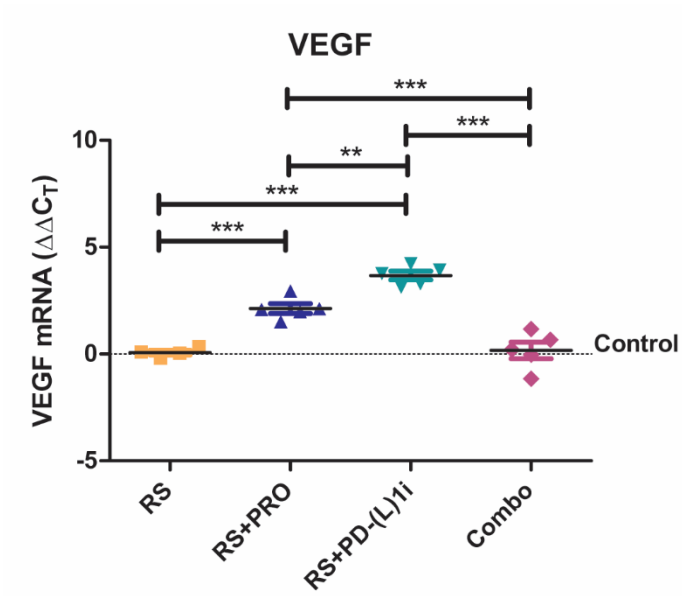


Figure 26 VEGF expression in mouse primary tumour tissues

Tumours were homogenized and total RNA was extracted. Expression of *VEGF* was assessed by qPCR. Values are in $\Delta\Delta C_T$ and normalized to cancer control group. Mean \pm SEM is presented and statistical significance was determined with one-way ANOVA (Post test: Bonferroni). ** = $p < 0.01$, *** = $p < 0.001$. Data are representative of 1 *in vivo* experiment; replicates are representative of different mice.

5.3.6 Combined therapy with PRO and PD-(L)1 inhibitor affects *Granzyme B* expression in mouse tumour tissues

Although *CD8* expression was an indication of the cytotoxic T cell tumour infiltration, we wanted to investigate the effector functions of the TILs. For this purpose, we evaluated the expression of *granzyme B* in mouse primary tumours. Expression of *granzyme B* mRNA in tumours of all treatment groups was normalized to the expression in the tumours of the cancer control group. In mice undergoing restraint stress and receiving PD-(L)1 inhibitor or the combination of PRO and PD-(L)1 inhibitor, Granzyme B mRNA expression was significantly upregulated compared to mice treated with PRO as monotherapy ($p \leq 0.05$ and $p \leq 0.005$) (Figure 27).

The results have shown that a monotherapy with PRO significantly reduced the expression of *granzyme B* in the tumour, which might affect the T cell functionality. On the contrary, combined therapy with PRO and PD-(L)1 inhibitor restored the *granzyme B* expression in the tumour.

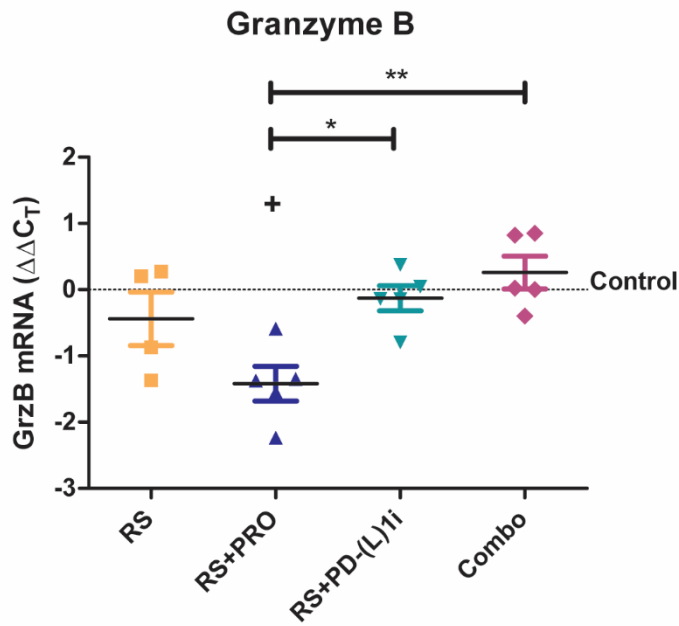


Figure 27 Expression of granzyme B in mouse primary tumour tissues

Tumours were homogenized and total RNA was extracted. Expression of *granzyme B* was assessed by qPCR. Values are expressed in $\Delta\Delta C_T$ and normalized to cancer control group. Mean \pm SEM is presented and statistical significance was determined with one-way ANOVA (Post test: Bonferroni). * = $p < 0.05$, ** = $p < 0.01$, + = significant vs Control ($p < 0.05$). Data are representative of 1 *in vivo* experiment; replicates are representative of different mice.

5.3.7 Therapy with PRO affects CXCL10 expression in mouse tumour tissues

The expression of the IFN- γ -induced gene *CXCL10* was evaluated to assess the response to IFN- γ in the tumour. Also, *CXCL10* gene encodes for a chemokine responsible for the attraction of numerous immune cells such as macrophages, NK cells, DCs and T cells. *CXCL10* mRNA expression was evaluated in the tumours and normalized to the expression of the gene in the cancer control group. *CXCL10* expression was downregulated in the group receiving PRO as monotherapy compared to the cancer control group (Figure 28).

CXCL10 expression was downregulated in tumour of mice treated with PRO. These results might exclude the hypothesis that a PRO monotherapy can increase the immune response to ovarian cancer.

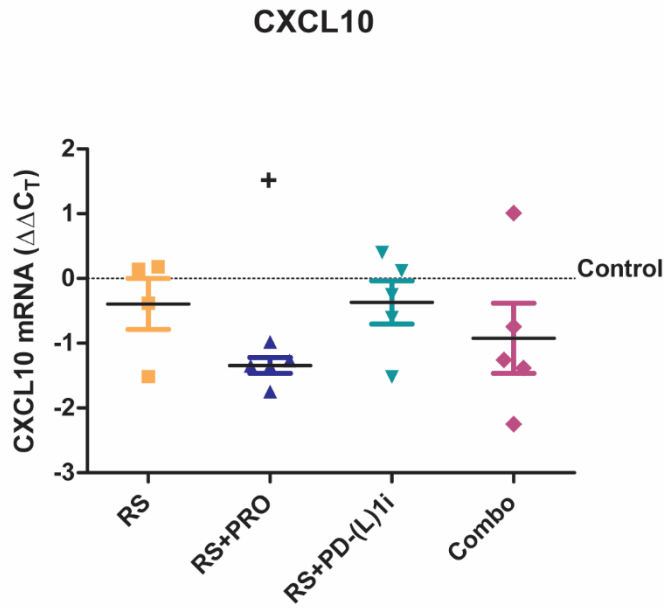


Figure 28 CXCL10 expression in primary tumour tissues

Tumours were homogenized and total RNA was extracted. Expression of *CXCL10* was assessed by qPCR. Values are expressed in $\Delta\Delta C_T$ and normalized to cancer control group. Mean \pm SEM is presented and statistical significance was determined with one-way ANOVA (Post test: Bonferroni). + = significant vs Control ($p < 0.05$). Data are representative of 1 *in vivo* experiment; replicates are representative of different mice.

5.3.8 Therapy with PRO affects *IDO1* expression in mouse tumour tissues

To further assess how the T cell function could be limited in ovarian tumours, the metabolic interaction between the tumour and the immune response was evaluated by assessing the expression of indoleamine2,3-dioxygenase 1 (*IDO1*) mRNA. *IDO1* mRNA expression was assessed by qPCR normalizing the values for the expression of the same gene in the cancer control group. *IDO1* was significantly upregulated in tumours of mice treated with combined PRO and PD-(L)1 inhibitor compared to monotherapy of PRO ($p < 0.05$) (Figure 29).

These results showed an unexpected upregulation of *IDO1* expression in tumours of mice receiving the combined therapy with PRO and PD-(L)1 inhibitor. Further analysis of these results will be discussed in 5.4.

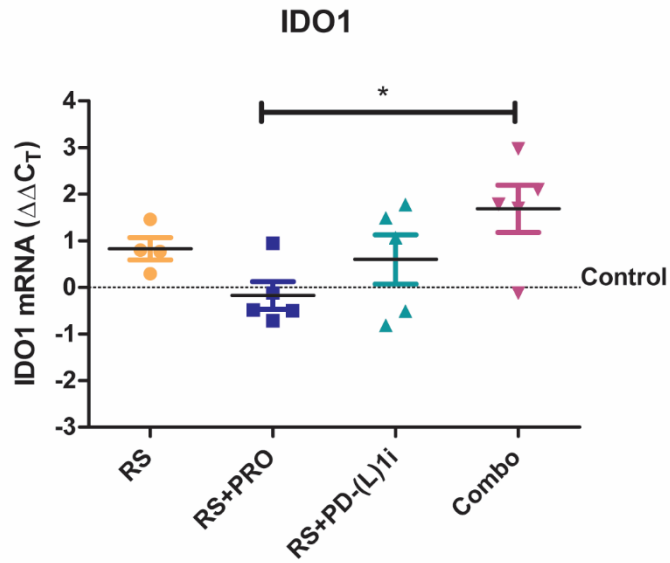


Figure 29 IDO1 expression in primary tumour tissues

Tumours were homogenized and total RNA was extracted. Expression of IDO1 was assessed by qPCR. Values are expressed in $\Delta\Delta C_T$ and normalized to cancer control group. Mean \pm SEM is presented and statistical significance was determined with one-way ANOVA (Post test: Bonferroni). * = $p < 0.05$. Data are representative of 1 *in vivo* experiment; replicates are representative of different mice.

5.3.9 Therapy with PRO and/or PD-(L)1 inhibitor affects *PD-L1* expression in mouse tumour tissues

The analysis of *PD-L1* expression in the tumour has been considered prognostic and predictive of the response to the therapy based on immune checkpoints blockade [101]. However - as extensively discussed in this thesis - *PD-L1* expression as immune tumour biomarker presents some limitations (1.3.11). *PD-L1* expression was assessed in order to have another indication of the immune signature of tumours of mice undergoing different treatments. *PD-L1* mRNA expression was evaluated normalizing the values for the expression of *PD-L1* in the cancer control group. *PD-L1* expression was upregulated in tumours of mice receiving PD-(L)1 inhibitor as monotherapy or in combination with PRO ($p < 0.005$ and $p < 0.05$) (Figure 30).

The upregulation of PD-L1 expression in all treatments compared to control confirms the hypothesis of a regulation of this gene either with PRO and/or PD-(L)1 inhibitor. Although restraint stress did not affect PD-L1 expression, mice receiving PD-(L)1 alone or in combination with PRO showed an upregulation of the gene expression.

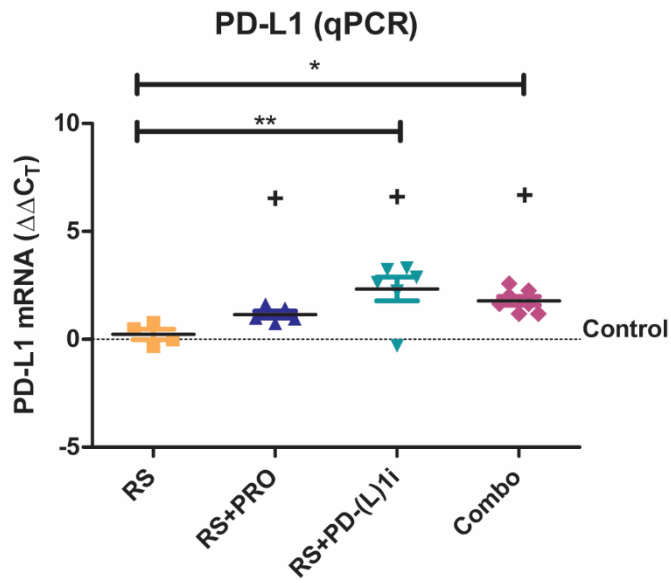


Figure 30 PD-L1 expression in primary tumour tissues

Tumours were homogenized and total RNA was extracted. Expression of PD-L1 was assessed by qPCR. Values are expressed in $\Delta\Delta C_T$ and normalized to cancer control group. Mean \pm SEM is presented and statistical significance was determined with one-way ANOVA (Post test: Bonferroni) * = $p < 0.05$, ** = $p < 0.01$, + = significant vs Control ($p < 0.05$). Data are representative of 1 *in vivo* experiment; replicates are representative of different mice.

5.3.10 PD-L1 and IFN- γ protein expression are not informative in the evaluation of the ovarian cancer immune signature

As discussed in 3.4, tumours can express PD-L1 intrinsically or in response to IFN- γ . To evaluate whether the expression of PD-L1 correlated with IFN- γ , we performed ELISA on tumour tissue homogenate. The results showed no significant changes in both PD-L1 and IFN- γ protein levels (Figure 31).

These experiments intended to assess the protein levels of PD-(L)1 and INF- γ . Although the statistical analysis showed no significant changes, both proteins' levels showed a similar trend in the tumours of mice receiving different therapies.

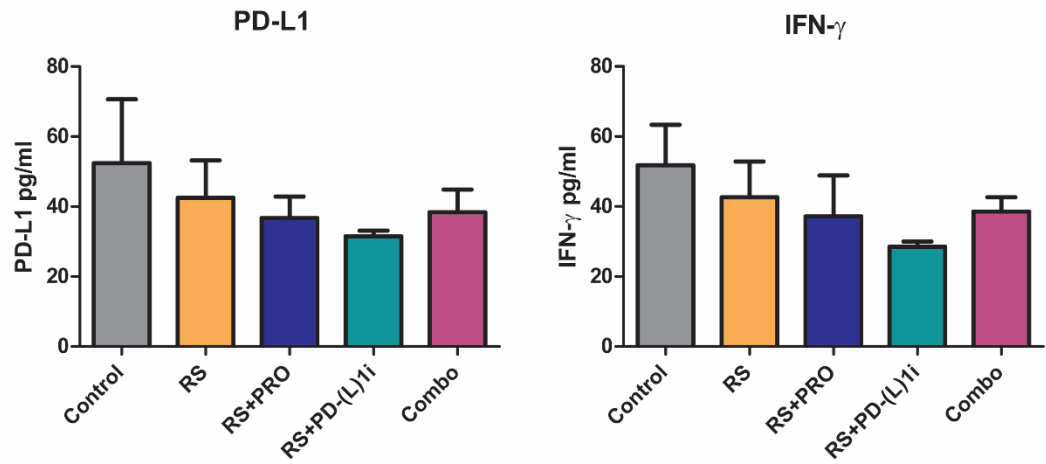


Figure 31 PD-L1 and IFN- γ protein levels in tumour tissues

Tumours were homogenized and total proteins were extracted. ELISA was performed to assess the levels of PD-L1 and IFN- γ . (A) PD-L1 (B) IFN- γ . Mean \pm SEM is presented and statistical significance was determined with one-way ANOVA comparing columns to each other. Data are representative of 1 *in vivo* experiment; replicates are representative of different mice

5.4 Discussion

In this study, the effects of chronic repetitive stress in a syngeneic orthotopic mouse model of ovarian cancer were investigated underlying the role of stress in the regulation of the tumour progression, metastatic power and the modulation of the immune signature of the tumour. Stress modulates the body responses to different stimuli, and it involves numerous biological processes regulated by both central nervous system (CNS) and the periphery [24]. As discussed in chapter 1, the biological effects are different depending on the duration of the stressor (e.g. acute or chronic stress). Scientific evidence on the impact of stress on the tumour immune regulation is evolving but not yet substantial and it involves a very complex bidirectional modulation between the sympathetic nervous system and the immune compartment [255]. The stress-mediated immune modulation brought to the hypothesis of using a combined therapy, which can mitigate the stress negative effects and - at the same time - and re-establish an improved immune response against cancer. To test this hypothesis, we evaluated the effect of a combined therapy using PRO and a PD-(L)1 inhibitor which resulted in a diminished tumour burden and metastatic spread. The combined therapy also affected the expression of specific immune markers in the tumour tissues supporting the idea of a modulation of the tumour signature with an improvement the anti-tumour immune response.

Previous studies have shown that restraint stress increases tumour burden and metastasis in *in vivo* cancer models [40, 272]. Our results support the hypothesis that stress promotes tumour progression and increases the number of organs with metastatic nodules. PRO showed a promising potential as anti-metastatic agent by reducing the number of metastatic organs observed. This evidence is relevant considering the assumption that the anti-metastatic power of beta-blockers can - in return - affect the immune response by regulating the immune infiltration. In this scenario, the immune regulation could be an indirect consequence of the reduced metastatic power which instead promotes a metastasis-mediated immune suppression.

The regulation of immune infiltration into the tumour is one of the most important and challenging aspects of this research. Previous evidence in *in vitro* models has shown an immune regulation mediated by NA [221, 222]. Thus, the hypothesis that chronic stress *in vivo* can also affect the immune activity has been tested. Chronic stress *in vivo* activates the sympathetic nervous system and upregulates the levels of circulating stress hormones including NA [273]. We discussed that the effects of the adrenergic stimulation are part of a

complex biological network involving other important immune regulatory stimuli. These include processes involved in immune cell development and differentiation, as well as the regulation of inflammatory cytokines which can have feedback effects and drive the immunity towards a specific fate [221, 222]. In addition, the adrenergic signalling pathway influences the peripheral distribution of immune cells. Studies on splenic lymphocytes have shown opposite results after adrenergic stimulation with an increased mobilization of the immune compartment in some cases or an increased homing of immune cells into the spleen [265, 266]. The analysis of the splenic immune compartment showed a decrease in the CD8⁺ resident T cells in mice treated with the combination therapy with PRO and PD-(L)1 inhibitor. This evidence supports the hypothesis of a mobilization of the CD8⁺ T cells from the spleen. The increased immune mobilization might be a consequence of an altered expression in the chemokine pattern. Hence, the decrease of CD8⁺ cell compartment in the spleen might reflect a chemo-attraction of these cells in other tissues such as the tumour.

For the complexity of multifactorial effects, the role of restraint stress *in vivo* regulating the tumour immunity cannot be easily interpreted. However, the analysis of the tumour immune milieu is the basis of diagnostic strategies used to determine the prognosis and predict the response to immunotherapy [274]. These strategies involve the evaluation of immune biomarkers in the tumour microenvironment that can provide prognostic and predictive information. A good cancer biomarker can predict the course of the disease and the response to specific treatments. Recent scientific research has demonstrated the importance of the immune markers as prognostic factors [102]. The evaluation of the immune context of a tumour takes into consideration different parameters that are clinically relevant and can help in shaping a patient-specific cancer therapy. Our results are based on the evaluation of the immune markers expression, using a method which can have a translational potential. One of the most important parameters used to assess the cancer immune signature is the analysis of the TILs populations. T cells infiltrating the tumour mass can be distinguished in CD4⁺ (T helper cells) or CD8⁺ (CTLs). The ratio in CD4⁺/CD8⁺ cell in the tumour has a crucial prognostic value, especially in ovarian cancer [212]. In our results, *CD8* expression was upregulated when mice were treated with a combined therapy with PRO and PD-(L)1 inhibitor suggesting an increase in the CD8⁺ T cell infiltration in tumours of mice receiving the combined therapy. This evidence supports the hypothesis of an increased T cell infiltration and a shift towards a CD8⁺ cytotoxic phenotype (CTLs). These results correlate with the expression pattern of the gene encoding for granzyme B, a serine protease produced specifically by CTLs. In tumours of mice receiving the PRO monotherapy, the expression of *granzyme B* is significantly lower

compared to the ones receiving the combined therapy indicating that PRO is not sufficient to restore the effector functions of the immune cells; hence, the immune checkpoint blockade is essential in order to restore the T cell cytotoxic functions.

Additional immune markers include the expression of IFN- γ and IFN- γ -related genes as an indication of the pro-inflammatory microenvironment as an effective immune response to cancer. We also evaluated the expression of *CXCL10*, a gene induced by IFN- γ and encoding for a chemokine. Although the results did not show a significant difference among the different treatments, *CXCL10* expression in the PRO monotherapy group was significantly lower than the cancer control group. These results might suggest that the IFN- γ responding elements are less effective when PRO is administered as monotherapy and support the idea that a combined therapy is more effective in the stimulation of a pro-inflammatory tumour microenvironment. Furthermore, *CXCL10* expression and secretion is essential for the chemo attraction of several immune cells such as macrophages, NK cells, dendritic cells and T cells. The lower expression of *CXCL10* in the PRO monotherapy group can also cause a decreased tumour immune infiltration indicating a feedback mechanism in which efficient effector functions of the immune cells are crucial to support the tumour immune infiltration.

Another immune marker is *IDO1*, which plays a role in the immune modulation by suppressing T cells function [271]. Since *IDO1* decreases the T cell functions, the increase in *IDO1* in the combined therapy with PRO and PD-(L)1 might seem controversial. However, recent evidence has shown that increased expression of *IDO1* is correlated with a positive response to PD-(L)1 blockade immunotherapy [275].

In the regulation of cancer immunity a crucial role is exerted by *VEGF* which has been shown to have a negative effect on T cell development and effector activities [121, 122]. Since *VEGF* tumour expression is also affected by chronic stress, we proposed the hypothesis that this growth factor can be one of the mediators of the stress-immune regulation. *VEGF*, as regulator of the vasculature, can affect the tumour immune infiltration. Although the augmented permeability of the blood vessels in response to *VEGF* is crucial for the extravasation of cancerous cells, it does not induce the mobilization of the immune cells. *VEGF*, by downregulating the expression of intercellular adhesion molecules (ICAMs) and the vascular cell adhesion molecules (VCAMs), regulates the leucocyte interaction with the endothelium and impairs the immune cells extravasation [123]. To confirm this hypothesis, recent studies have shown that higher *VEGF* expression in ovarian cancer tissues correlates with less immune infiltration and vice versa [119]. The pattern of *VEGF* expression in our tumour samples was very interesting. First, *VEGF* expression was not affected by restraint

stress as reported in literature; this could simply be due to the fact that we used immune competent mouse models compared to xenograft models (reported by others) [40]. *VEGF* expression also increased in mice treated with monotherapy of PRO. These results can be discussed by revising the expression of the ADRB in the ovary and in ovarian tumour tissues. Beta-2 adrenergic receptors are expressed in the ovary while alpha-1 adrenergic receptors are expressed in the blood vessels (Table 1). By blocking the beta-adrenergic signalling and not the alpha, PRO can lead to vasoconstriction [276]. The lack of blood supply activates the hypoxia response and – consequently - *VEGF* expression. Although *VEGF* expression increased in the PRO or PD-(L)1 inhibitor monotherapies, it decreased in the combined therapy. In addition, the expression of *VEGF* in the combined therapy group did not substantially differ from the control group demonstrating that *VEGF* expression, which can modulate the T cell trafficking and the tumour metastatic power, was not affected by the combined therapy of PRO and PD-(L)1 inhibitor.

Taken together, these results indicate that the therapy with PRO alone or in combination with PD-(L)1 inhibitor diminished the metastatic spread of ovarian cancer. Also, combined therapy with PRO and PD-(L)1 inhibitor can improve the overall outcome of the tumour by diminishing the tumour weight. Combined therapy can also improve the CD8⁺ cell mobilization from the spleen and -potentially- the infiltration of effector CD8⁺ T cells into the tumour establishing a pro-inflammatory microenvironment. The combined therapy did not affect *VEGF* expression, essential for the increase of metastatic nodules and the decrease of T cell trafficking into the tumour.

6. Chapter 6 - General Discussion and conclusions

6.1 Conclusions

The overarching hypothesis of this research is that adrenergic stress influences the immune response to ovarian cancer and cooperates to reduce the efficacy of PD-(L)1 checkpoint blockade. This research suggests a combined therapy with PRO and PD-(L)1 inhibitors to overcome the stress-induced immunosuppression and improve the PD-(L)1 inhibitor efficacy.

In this thesis, adrenergic stress has been shown to have an effect on the immune response to ovarian cancer by acting on different levels. Furthermore, the immune modulatory effects of adrenergic stimulation and the blockade with PRO have been proven to have consequences on PD-(L)1 inhibitor therapy. One of the findings of this research is that NA and PRO affect IFN- γ production by immune cells and consequently PD-L1 expression on ovarian cancer cells. Understanding the molecular mechanism of this process is extremely important to clarify the reason why blocking the adrenergic stimulus with PRO can improve PD-(L)1 blockade treatment. As demonstrated in chapter 3, PD-L1 expression in ovarian cancer cells can be triggered by exposure to IFN- γ . However, it is important to recall that PD-L1 can also be expressed in ovarian cancers independently from IFN- γ stimulation. Thus, by reducing IFN- γ -mediated PD-L1 expression, PRO drives the blockade towards the PD-L1 intrinsically expressed in the tumour (Figure 32).

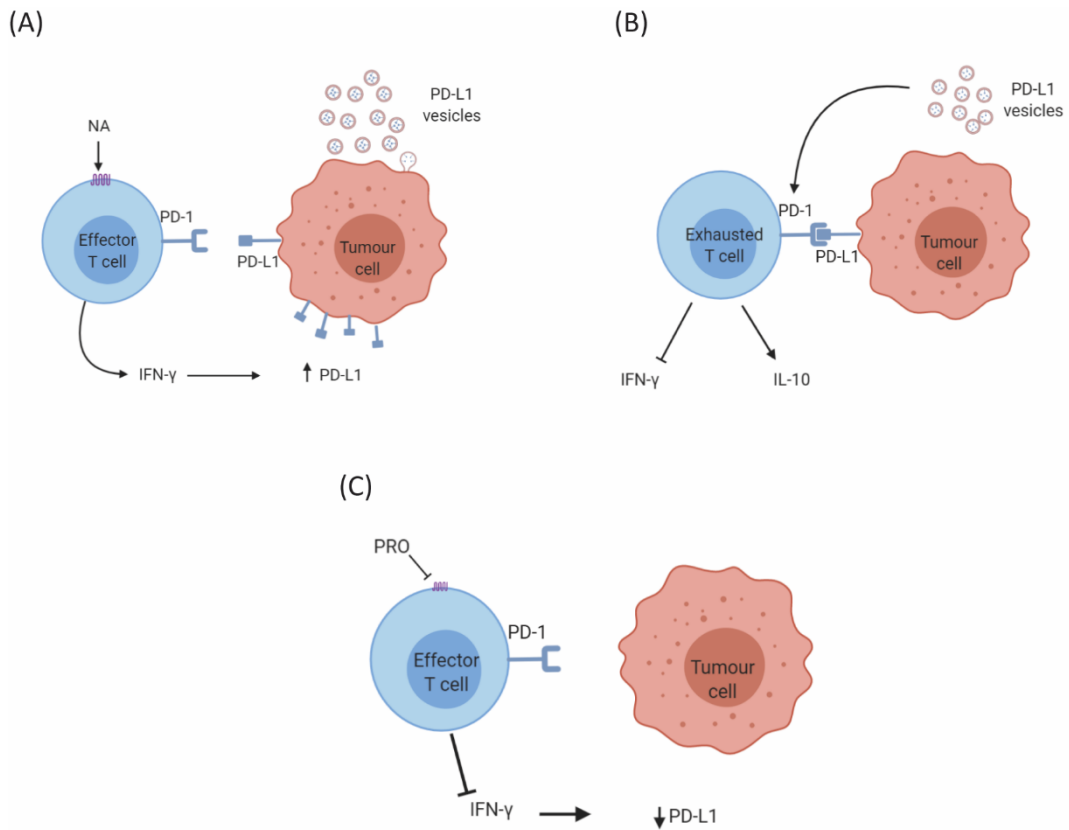


Figure 32 Proposed mechanism of PRO-mediated PD-L1 downregulation

(A) NA stimulation on effector immune cells accelerates IFN- γ production which leads to PD-L1 overexpression on cancer cells. PD-L1 can be expressed on the cancer cell surface and/or secreted in extracellular vesicles. (B) The interaction of PD-1 and PD-L1 leads to an exhausted T cell phenotype with blockade of IFN- γ and production of IL-10. (C) Propranolol (PRO) blocks the upstream production of IFN- γ and the IFN- γ -mediated PD-L1 expression on cancer cells.

Immune cell infiltration represents one of the most important parameters to improve PD-(L)1 blockade [102]. It is known that the response to checkpoint inhibitors targeting PD-(L)1 axis correlates with the expression of markers for immune cell infiltration [102]. Tumour immune infiltration is regulated by different mechanisms such as the production of chemokines in the tumour microenvironment [277]. Also the vasculature changes and the interaction with endothelial adhesion molecules drive the immune cells extravasation and tumour infiltration [123, 278]. The interaction between the immune cells and tumour microenvironment can support or block the immune infiltration [143]. This last feature makes the difference between inflamed and immune excluded tumours as discussed in 1.3.11. In inflamed tumours, the immunogenicity of the tumour is sufficient to guide the immune cells invasion into the tumour tissue. In the case of immune exclusion, tumour-reactive immune cells reside on the stroma and cannot penetrate into the tumour mass. Many events can prevent tumour infiltration of immune cells and promote the creation of an immune hostile microenvironment. These events can be driven by the tumour

extracellular matrix components or some of the metabolites produced by the cancer cells metabolic processes [279, 280]. This research demonstrated that PRO treatment might enhance the immune cell infiltration into ovarian cancer 3D spheroids, with an increase in the ability of PRO to overcome the molecular barrier of the tumour microenvironment. Although our findings are promising, the potential of PRO as a putative drug able to convert cold tumours in hot tumours is still unknown and further investigation is needed. However, the evidence of a correlation between PRO treatment and an enhanced tumour immune infiltration remains an important novel finding.

Evidence of an immunomodulatory effect of PRO inspired the last and most significant experimental model of the research in which a combined therapy with PRO and PD-(L)1 inhibitors was tested in an immunocompetent mouse model of ovarian cancer. This experimental model successfully demonstrated the advantages of the combined therapy with a reduced tumour burden and metastatic spread. Furthermore, the evaluation of immune markers in ovarian tumours of mice treated with the combined therapy suggests an increased immune infiltration and an anti-tumour immune response.

6.2 Limitations of the study

6.2.1 Limitations of the cell culture model

Cell culture lines are well established and widely used *in vitro* models in biomedical research to study cancer. There are many advantages to using cell culture models. They are easy to handle, they have the ability of producing large amount of cells in a very short time and numerous studies help to identify their properties. However, the use of cell lines in tumour biology has some limitations. One of the problems is the misidentification of the cell lines [281]. An examination of cell lines in use in laboratories between 1968 and 2007 estimated that between 18% and 36% of the cells lines were cross-contaminated [282]. Ovarian cancer cell lines are included in the list with 15 misidentified cell lines out of 51 still currently in use. A study on DNA analysis profiles of ovarian cancer cell lines, identified that the cross-contamination is usually with MCF-7 breast cancer cell lines [283]. To overcome this problem, our laboratory policy is that cell lines are handled one at the time.

Using cancer cell lines as *in vitro* models of tumours also raises the question of how well they represent the primary tumours. In particular, the tumour-derived cell lines can develop some genetic modification when grown *in vitro*. If this happens, the genetic drift causes a change in the cancer cells features that can modulate their response to treatments. The mouse cancer cell line ID8 derives from epithelial ovarian cells isolated from C57BL/6 mice and grew *in vitro* for at least 20 passages. These cells showed a transformed phenotype with loss of contact inhibition and cluster growth in agar. Since ID8 cells injected in the mouse peritoneal cavity developed tumours, they are a good representation of ovarian malignant cells [284]. For the human cancer cells, a study on multiple –omics and genome sequencing generated data compared cancer cell lines features to patient samples [285]. To overcome the problem of having a non-representative *in vitro* models of ovarian cancer, the choice of the human cell lines to use should be driven by an evaluation of the research to carry out [286]. For the purpose of our experiment, the specific histological subtype was not an important requirement. Therefore, we select two human cell lines with non-specific histological annotation: SKOV3 is largely used in publication with wild type p53; OVCAR8 are less used as experimental models, but more likely to represent high-grade serous carcinoma and they are mutated in p53 [286].

Although 2D cell monolayers are still the most popular *in vitro* models, they lack in the structural architecture typical of solid tumour tissues [287]. Cell aggregation is important to recreate the spatial organization of cancer cells and exhibits features of the tumour microenvironment [287]. One of the aims of this research was to recreate the tumour

microenvironment in which ovarian cancer cells were exposed to cytokines produced by the immune cells. This goal was partially achieved with the co-culture experiments where ovarian cancer cells were co-cultured with immune cells isolated from a mouse spleen. This model allows cells to be exposed to cytokine concentrations that are naturally produced by immune cells. However, the lack of a three-dimensional structure may affect cytokine diffusion. In a 3D solid tumour, the soluble molecules penetrate the tumour mass creating a gradient of concentration [288]. As a consequence, the out layer of cells is exposed to higher concentrations than the cells in the inner core. Furthermore, the inner core of the tumour tissue is also hypoxic. The cellular response to hypoxia activates the expression of genes involved in many signalling pathways that regulate processes such as metabolism, angiogenesis, tumour invasion and metastasis [226]. Hypoxia regulates tumour expression of VEGF which is involved in the tumour response to adrenergic stress and in the immune cell tumour infiltration [47, 123]. To overcome these problems, we established a 3D ovarian cancer spheroid model.

6.2.2 Limitation of the 3D spheroid model

Although 3D spheroids represented an excellent improvement in cellular *in vitro* models, there are still some limitations occurring. The diffusion of nutrients, oxygen and metabolites reflects - in part – the tumour tissue mechanisms. However, *in vitro* spheroids lack blood vessels that can support the molecular trafficking into the tumour mass. As discussed above, one of the consequences of poor oxygen diffusion inside the tumour core is the activation of signalling pathways that lead to angiogenesis. To solve this problem, spheroids need to be limited to certain sizes. The evaluation of the critical size of spheroids is dependent from the cells used [289]. In our experiments, spheroids were cultured for a maximum of 7 days and fresh media was added every day.

Creating a spheroid model for ovarian cancer represents an extremely difficult challenge. Ovarian cancer cells such as ID8 are derived from mouse ovarian surface epithelial cells (MOSEC) losing their morphology and growth inhibition after repeatedly passaging them *in vitro* [284]. The nature of these cells and their high invasiveness are responsible for their poor ability of forming spheroids. Aggregates formed by ovarian cancer cells are small and loose conglomeration of cells with a follicle-like structure [290]. The methodology used to create ovarian cancer spheroids allowed to partially overcome this problem and obtain compact 3D structures. However, ovarian cancer spheroids were extremely fragile creating difficulty in handling them for culture or experimental purposes. In addition, the spheroids floating in their culture medium influenced the performance of the downstream

experiments. RNA extraction from tumour spheroids resulted in very poor yield. This can be due to the fact that the number of cells in tumour spheroids is much lower than what is usually used to extract RNA. The difficulty of RNA isolation from spheroids could also be caused by a switch of cancer cells towards less metabolic active cells with lower production of RNA [288]. Although these limitations were faced, immunofluorescence imaging was successfully performed using lipophilic dyes that were added to the cells before the spheroid formation. Proteins were also isolated from tumour spheroids and used for large-scale proteomic analysis.

6.2.3 Limitations of the *in vivo* model

Translating *in vitro* findings into an *in vivo* model is crucial to predict the anti-tumour response in pre-clinical models. The experimental conditions are important to determine the adequate mouse model and obtain reliable results [291]. In orthotopic tumour models, cancer cells are injected in the original site of the tumour tissue development. Injecting cancer cells in orthotopic tissues improves cancer development due to the influence of the natural tissue microenvironment [292]. In an ovarian cancer model, ovarian cancer cells are injected intraperitoneally leading to the formation of a peritoneal, fallopian or ovarian tumours [177]. In order to study the immune response to cancer, an immune competent mouse model was used. Injecting cancer cells in an immune competent mouse can cause immune rejection. To overcome this problem allotransplantation of cancer cells were performed by injecting cancer cells derived from the same mouse strain. In our case, malignant mouse ovarian epithelial cells (ID8) were injected intraperitoneally (IP) in C57BL/6 female mice. In previous experiments with the same model, mice show signs of ascites and presented ovarian cancer mostly spread into the peritoneal cavity.

Although this model met the expectation of a reliable immune-competent mouse model, it presented some limitations. One of the problems was related to the constant delivery of PRO achieved by a surgical mini pump implantation on the back of the mice. Although this technique avoided daily injection to administrate PRO, it limited the study in many aspects. First, the surgery to insert the mini pump represented a stressor for the animals which could contribute to the promotion of tumour growth [43]. To solve this problem, surgery was performed before cancer injection or the restraint stress procedure. Another complication faced by the use of mini pumps for PRO delivery was that the maximum duration of the pump reservoir was 6 weeks. Changes in the experimental protocol were made in order to have an experimental model developing cancer in a brief period of time. Considering the recovery from the surgery and the start of the restraint stress procedure, the final timeframe between

the cancer cell injection and the end point of the experiment was 4 weeks. This specific protocol resulted in the production of relatively small ovarian tumours that were used to isolate RNA and proteins. However, the small size of the tumours was an important limitation of the model. Tumours were too small to be paraffin imbedded and the downstream analysis was confined to gene and protein expression. Also, due to the short timeframe for tumour development we were not able to collect ascites. However, previous work in our laboratory using this model has shown that stress can increase the amount of ascites (Dr Flint personal communication). Tumour-related processes such as angiogenesis and metastatic spread were still observed in the model.

Chronic behavioural stress can increase the catecholamines and cortisol plasmatic levels and promote tumour progression *in vivo* [40, 293]. Animal models of stress include different protocols such as physical stress model and cold housing. In our experimental model, restraint stress was used to produce stress-related response in mice. This model has been used to study post-traumatic stress disorders and the effects of the immune system [294]. Although the restraint stress model has been used to produce a stress-related response, the level of hormones produced in response to stress has not been evaluated in the specific model. Previous evidence has shown that chronic stress increase NA, A and cortisol levels in animal models [40]. However, the disadvantage of using this model is that animals can adapt to the chronic stress exposure and decrease their stress hormone levels over time [294]. Stress-hormone levels were assumed to be increased in the stress group compared to a non-stress group used as control. Indirect evidence of stress effects were obtained such as the increased tumour burden or metastatic nodules in stressed mice compared to non-stressed mice. Since stress includes the activation of the adrenergic and glucocorticoid pathways *in vivo* [24], the model used was not specific for adrenergic stress and the responses produced can also be related to cortisol.

6.3 Future perspectives

This research represents an insight in the adrenergic stress immune regulation in ovarian cancer. Cancer treatments are progressing and aim to personalised therapies that take into consideration every aspect of the disease. The psychological stress experienced by ovarian cancer patients can influence the response to anti-tumour treatment [293, 295, 296]. In this thesis, the role of stress in the immune response to ovarian cancer has been demonstrated to affect the response to PD-(L)1 checkpoint blockade. Although the work presented in this thesis proposed a mechanism of adrenergic immune regulation that can affect immunotherapy, it also raises several questions.

The complexity of the molecular mechanisms orchestrating the effect of stress on the immune response to cancer is described in this thesis. Many experimental improvements can be adopted to study the immune-cancer cell interaction. The most important limitations occur *in vitro*, where the complex network of regulation cannot be exemplified. For these reasons, our *in vivo* mouse ovarian cancer model can be used to study mechanisms of adrenergic stress.

The immune component affected by the adrenergic stress is still vast. PD-(L)1 blockade is based on the assumption that T cells can react against tumour cells. However, many types of immune cells are involved in the immune response against cancer. These include the innate immune system and the adaptive immune system [67]. Studying the immune response to cancer presented some limitations. For instance, the activation of the cell-mediated immunity is supported by other cell types such as dendritic cells. Also, T cells subtypes can act differently and create a pro or anti-tumour immune response. Adapting the *in vitro* experimental models to study one specific cell subtype reaction to adrenergic stress stimulation can represent an improvement. However, the adrenergic effect can be modulated by the presence and function of other immune cell types. These considerations raise the dilemma of studying the effects of adrenergic stress on a specific T cell subtype or on the total immune cell compartment to not interfere with their complex network of interactions. The answer to this question is maybe an integration of both single cell and multicellular experimental data analysis.

The analysis of tumour and multicellular spheroids led to meaningful results opening the way to a new approach to cancer immunology research. Spheroids imaging analysis has been demonstrated to be an excellent experimental model to screen the response to treatments and the interaction between different cell types. The optimisation of the imaging assay parameters will contribute to a better understanding of the tumour architecture and the

influence of the microenvironment in the response to treatments. The proteomic analysis of cancer and multicellular spheroids enlightened upon the importance of cellular metabolism in shaping the immune response to cancer. In particular, the role of glucose metabolism in cancer has been the focus of recent research and the regulation of the metabolic pattern can be a potential strategy to enhance the immune response to cancer and improve immunotherapy efficacy [55, 168]. Our results have shown that stress can influence the immune and cancer metabolism. However, the molecular mechanisms involved in the process and the consequences to cancer immunity still warrant further investigation. This knowledge can potentially lead to a new field of this research which elucidates the role of NA and adrenergic stress in cancer/immune metabolism.

Although psychological stress is correlated with adrenergic stimulation, it also involves the glucocorticoid response [24]. However, this thesis focused solely on the role of adrenergic pathway and the influence of glucocorticoids will need to be investigated with regards to the cancer immunology. This consideration leads to a future evaluation of glucocorticoids effects on the tumour immunity and the impact on immunotherapies targeting immune checkpoints.

6.4 Novel contribution to knowledge

Data presented in this thesis contribute with compelling evidence to the elucidation of the effects of stress on PD-(L)1 immunotherapy in ovarian cancer. The study focused on the molecular mechanisms involving the adrenergic stress signalling pathway impact on the immune response to ovarian cancer providing a therapeutic approach with translational potential. The research produced results sufficient to conclude the following novel contributions:

- The activation of the adrenergic signalling pathway via NA and the inhibition of ADRBs with PRO induce changes in the immune functions that reflect in a regulation of PD-L1 expression on ovarian cancer cells. A molecular mechanism elucidating the adrenergic regulation of PD-L1 expression in ovarian cancer is proposed.
- A novel 3D tumour spheroid model for ovarian cancer has been successfully developed and proven to reproduce the structural tumour architecture. This model improved the study of immune cell infiltration into the tumour mass and led to the consideration of other parameters (e.g. hypoxia and metabolic switch) that can have a role in cancer immunity.

A novel treatment combining PRO and PD-(L)1 inhibitor was tested in an *in vivo* model ovarian cancer. This experimental model showed that the combined therapy can reduce the tumour burden and metastasis and promote immune cell infiltration and activation.

1. Weiderpass, E. and J.E. Tyczynski, *Epidemiology of Patients with Ovarian Cancer with and Without a BRCA1/2 Mutation*. Mol Diagn Ther, 2015. **19**(6): p. 351-64.
2. Sankaranarayanan, R. and J. Ferlay, *Worldwide burden of gynaecological cancer: the size of the problem*. Best Pract Res Clin Obstet Gynaecol, 2006. **20**(2): p. 207-25.
3. Bankhead, C.R., et al., *Identifying symptoms of ovarian cancer: a qualitative and quantitative study*. BJOG, 2008. **115**(8): p. 1008-14.
4. Foley, O.W., J.A. Rauh-Hain, and M.G. del Carmen, *Recurrent epithelial ovarian cancer: an update on treatment*. Oncology (Williston Park), 2013. **27**(4): p. 288-94, 298.
5. Foote, J., et al., *ASCO Value Framework Highlights the Relative Value of Treatment Options in Ovarian Cancer*. J Oncol Pract, 2017. **13**(12): p. e1030-e1039.
6. Garcia, A. and H. Singh, *Bevacizumab and ovarian cancer*. Ther Adv Med Oncol, 2013. **5**(2): p. 133-41.
7. Evans, T. and U. Matulonis, *PARP inhibitors in ovarian cancer: evidence, experience and clinical potential*. Ther Adv Med Oncol, 2017. **9**(4): p. 253-267.
8. Goff, B.A., et al., *Ovarian carcinoma diagnosis*. Cancer, 2000. **89**(10): p. 2068-75.
9. Rice, L.W., et al., *Clinicopathologic variables, operative characteristics, and DNA ploidy in predicting outcome in ovarian epithelial carcinoma*. Obstet Gynecol, 1995. **86**(3): p. 379-85.
10. Karst, A.M. and R. Drapkin, *Ovarian cancer pathogenesis: a model in evolution*. J Oncol, 2010. **2010**: p. 932371.
11. Karnezis, A.N., et al., *The disparate origins of ovarian cancers: pathogenesis and prevention strategies*. Nat Rev Cancer, 2017. **17**(1): p. 65-74.
12. Karnezis, A.N. and K.R. Cho, *Of mice and women - Non-ovarian origins of "ovarian" cancer*. Gynecol Oncol, 2017. **144**(1): p. 5-7.
13. Kindelberger, D.W., et al., *Intraepithelial carcinoma of the fimbria and pelvic serous carcinoma: Evidence for a causal relationship*. Am J Surg Pathol, 2007. **31**(2): p. 161-9.
14. Kurman, R.J. and M. Shih Ie, *The origin and pathogenesis of epithelial ovarian cancer: a proposed unifying theory*. Am J Surg Pathol, 2010. **34**(3): p. 433-43.
15. Dubeau, L., *The cell of origin of ovarian epithelial tumours*. Lancet Oncol, 2008. **9**(12): p. 1191-7.
16. Shih Ie, M. and R.J. Kurman, *Ovarian tumorigenesis: a proposed model based on morphological and molecular genetic analysis*. Am J Pathol, 2004. **164**(5): p. 1511-8.
17. Neff, R.T., L. Senter, and R. Salani, *BRCA mutation in ovarian cancer: testing, implications and treatment considerations*. Ther Adv Med Oncol, 2017. **9**(8): p. 519-531.
18. Savage, K.I., et al., *BRCA1 deficiency exacerbates estrogen-induced DNA damage and genomic instability*. Cancer Res, 2014. **74**(10): p. 2773-2784.
19. Risch, H.A., et al., *Prevalence and penetrance of germline BRCA1 and BRCA2 mutations in a population series of 649 women with ovarian cancer*. Am J Hum Genet, 2001. **68**(3): p. 700-10.
20. Meinhold-Heerlein, I., et al., *The new WHO classification of ovarian, fallopian tube, and primary peritoneal cancer and its clinical implications*. Arch Gynecol Obstet, 2016. **293**(4): p. 695-700.
21. Selye, H., *The stress of life*. 1956, New York.: McGraw-Hill. 324 p.
22. Selye, H., *Selye's guide to stress research*. 1980, Van Nostrand Reinhold: New York. p. 3 volumes.
23. Chrousos, G.P. and P.W. Gold, *The concepts of stress and stress system disorders. Overview of physical and behavioral homeostasis*. JAMA, 1992. **267**(9): p. 1244-52.

24. Habib, K.E., P.W. Gold, and G.P. Chrousos, *Neuroendocrinology of stress*. Endocrinol Metab Clin North Am, 2001. **30**(3): p. 695-728; vii-viii.
25. Chrousos, G.P., *Stress and disorders of the stress system*. Nat Rev Endocrinol, 2009. **5**(7): p. 374-81.
26. Black, P.H., *Central nervous system-immune system interactions: psychoneuroendocrinology of stress and its immune consequences*. Antimicrob Agents Chemother, 1994. **38**(1): p. 1-6.
27. Bremner, J.D., *Does stress damage the brain?* Biol Psychiatry, 1999. **45**(7): p. 797-805.
28. Cook, S.C. and C.L. Wellman, *Chronic stress alters dendritic morphology in rat medial prefrontal cortex*. J Neurobiol, 2004. **60**(2): p. 236-48.
29. Gold, P.W., R. Machado-Vieira, and M.G. Pavlatou, *Clinical and biochemical manifestations of depression: relation to the neurobiology of stress*. Neural Plast, 2015. **2015**: p. 581976.
30. Ahlquist, R.P., *A study of the adrenotropic receptors*. Am J Physiol, 1948. **153**(3): p. 586-600.
31. Dunser, M.W. and W.R. Hasibeder, *Sympathetic overstimulation during critical illness: adverse effects of adrenergic stress*. J Intensive Care Med, 2009. **24**(5): p. 293-316.
32. McEwen, B.S. and E. Stellar, *Stress and the individual. Mechanisms leading to disease*. Arch Intern Med, 1993. **153**(18): p. 2093-101.
33. Kufe, D.W., et al., *Cancer medicine 6*. 6th ed. 2003, Hamilton, Ont. ; Lewiston, NY: BC Decker.
34. Andersson, K., K. Fuxe, and L.F. Agnati, *Determinations of catecholamine half-lives and turnover rates in discrete catecholamine nerve terminal systems of the hypothalamus, the preoptic region and the forebrain by quantitative histofluorimetry*. Acta Physiol Scand, 1985. **123**(4): p. 411-26.
35. Fischer, A., A. Ziogas, and H. Anton-Culver, *Perception matters: Stressful life events increase breast cancer risk*. J Psychosom Res, 2018. **110**: p. 46-53.
36. Kruk, J. and H.Y. Aboul-Enein, *Psychological stress and the risk of breast cancer: a case-control study*. Cancer Detect Prev, 2004. **28**(6): p. 399-408.
37. Surtees, P.G., et al., *No evidence that social stress is associated with breast cancer incidence*. Breast Cancer Res Treat, 2010. **120**(1): p. 169-74.
38. Heo, J., et al., *Psychiatric comorbidities among ovarian cancer survivors in South Korea: A nationwide population-based, longitudinal study*. Psychooncology, 2018. **27**(3): p. 1021-1026.
39. Antoni, M.H., et al., *The influence of bio-behavioural factors on tumour biology: pathways and mechanisms*. Nat Rev Cancer, 2006. **6**(3): p. 240-8.
40. Thaker, P.H., et al., *Chronic stress promotes tumor growth and angiogenesis in a mouse model of ovarian carcinoma*. Nat Med, 2006. **12**(8): p. 939-44.
41. Sood, A.K., et al., *Stress hormone-mediated invasion of ovarian cancer cells*. Clin Cancer Res, 2006. **12**(2): p. 369-75.
42. Saul, A.N., et al., *Chronic stress and susceptibility to skin cancer*. J Natl Cancer Inst, 2005. **97**(23): p. 1760-7.
43. Lee, J.W., et al., *Surgical stress promotes tumor growth in ovarian carcinoma*. Clin Cancer Res, 2009. **15**(8): p. 2695-702.
44. Lara, H.E., et al., *Release of norepinephrine from human ovary: coupling to steroidogenic response*. Endocrine, 2001. **15**(2): p. 187-92.
45. Merz, C., et al., *Expression of the beta-2 adrenergic receptor (ADRB-2) in human and monkey ovarian follicles: a marker of growing follicles?* J Ovarian Res, 2015. **8**: p. 8.

46. Lutgendorf, S.K., et al., *Stress-related mediators stimulate vascular endothelial growth factor secretion by two ovarian cancer cell lines*. Clin Cancer Res, 2003. **9**(12): p. 4514-21.
47. Yang, E.V., et al., *Norepinephrine up-regulates the expression of vascular endothelial growth factor, matrix metalloproteinase (MMP)-2, and MMP-9 in nasopharyngeal carcinoma tumor cells*. Cancer Res, 2006. **66**(21): p. 10357-64.
48. Baker, J.G., I.P. Hall, and S.J. Hill, *Agonist and inverse agonist actions of beta-blockers at the human beta 2-adrenoceptor provide evidence for agonist-directed signaling*. Mol Pharmacol, 2003. **64**(6): p. 1357-69.
49. Madden, K.S., M.J. Szpunar, and E.B. Brown, *beta-Adrenergic receptors (beta-AR) regulate VEGF and IL-6 production by divergent pathways in high beta-AR-expressing breast cancer cell lines*. Breast Cancer Res Treat, 2011. **130**(3): p. 747-58.
50. Wang, H.M., et al., *Improved survival outcomes with the incidental use of beta-blockers among patients with non-small-cell lung cancer treated with definitive radiation therapy*. Ann Oncol, 2013. **24**(5): p. 1312-9.
51. Lu, H., et al., *Impact of beta-blockers on prostate cancer mortality: a meta-analysis of 16,825 patients*. Onco Targets Ther, 2015. **8**: p. 985-90.
52. Diaz, E.S., B.Y. Karlan, and A.J. Li, *Impact of beta blockers on epithelial ovarian cancer survival*. Gynecol Oncol, 2012. **127**(2): p. 375-8.
53. Heitz, F., et al., *Impact of beta blocker medication in patients with platinum sensitive recurrent ovarian cancer-a combined analysis of 2 prospective multicenter trials by the AGO Study Group, NCIC-CTG and EORTC-GCG*. Gynecol Oncol, 2013. **129**(3): p. 463-6.
54. Watkins, J.L., et al., *Clinical impact of selective and nonselective beta-blockers on survival in patients with ovarian cancer*. Cancer, 2015. **121**(19): p. 3444-51.
55. Buck, M.D., D. O'Sullivan, and E.L. Pearce, *T cell metabolism drives immunity*. J Exp Med, 2015. **212**(9): p. 1345-60.
56. Palmer, C.S., et al., *Glucose metabolism regulates T cell activation, differentiation, and functions*. Front Immunol, 2015. **6**: p. 1.
57. Krawczyk, C.M., et al., *Toll-like receptor-induced changes in glycolytic metabolism regulate dendritic cell activation*. Blood, 2010. **115**(23): p. 4742-9.
58. Michalek, R.D., et al., *Cutting edge: distinct glycolytic and lipid oxidative metabolic programs are essential for effector and regulatory CD4+ T cell subsets*. J Immunol, 2011. **186**(6): p. 3299-303.
59. Dashty, M., *A quick look at biochemistry: carbohydrate metabolism*. Clin Biochem, 2013. **46**(15): p. 1339-52.
60. Naifeh, J. and M. Varacallo, *Biochemistry, Aerobic Glycolysis*, in StatPearls. 2019: Treasure Island (FL).
61. Kopf, H., et al., *Rapamycin inhibits differentiation of Th17 cells and promotes generation of FoxP3+ T regulatory cells*. Int Immunopharmacol, 2007. **7**(13): p. 1819-24.
62. Palmer, C.S., et al., *Regulators of Glucose Metabolism in CD4(+) and CD8(+) T Cells*. Int Rev Immunol, 2016. **35**(6): p. 477-488.
63. Frauwirth, K.A. and C.B. Thompson, *Regulation of T lymphocyte metabolism*. J Immunol, 2004. **172**(8): p. 4661-5.
64. Qiao, G., et al., *beta-Adrenergic signaling blocks murine CD8(+) T-cell metabolic reprogramming during activation: a mechanism for immunosuppression by adrenergic stress*. Cancer Immunol Immunother, 2019. **68**(1): p. 11-22.
65. Kokolus, K.M., et al., *Baseline tumor growth and immune control in laboratory mice are significantly influenced by subthermoneutral housing temperature*. Proc Natl Acad Sci U S A, 2013. **110**(50): p. 20176-81.

66. Delves, P.J. and I.M. Roitt, *The immune system. First of two parts*. N Engl J Med, 2000. **343**(1): p. 37-49.
67. Abbas, A.K., A.H. Lichtman, and S. Pillai, *The basics of the basic and clinical immunology*. Actualites Pharmaceutiques, 2016. **55**(560): p. 9-9.
68. Abbas, A.K., A.H. Lichtman, and S. Pillai, *Basic immunology : functions and disorders of the immune system*. Fifth edition. ed. 2016, St. Louis, Missouri: Elsevier. x, 335 pages.
69. Abbas, A.K., et al., *Cellular and molecular immunology*. Ninth edition. ed. 2018, Philadelphia, PA: Elsevier. x, 565 pages.
70. Pang, B., et al., *Direct antigen presentation and gap junction mediated cross-presentation during apoptosis*. J Immunol, 2009. **183**(2): p. 1083-90.
71. Stockinger, B. and M. Veldhoen, *Differentiation and function of Th17 T cells*. Curr Opin Immunol, 2007. **19**(3): p. 281-6.
72. Burnet, F.M., *The concept of immunological surveillance*. Prog Exp Tumor Res, 1970. **13**: p. 1-27.
73. Dighe, A.S., et al., *Enhanced in vivo growth and resistance to rejection of tumor cells expressing dominant negative IFN gamma receptors*. Immunity, 1994. **1**(6): p. 447-56.
74. Shankaran, V., et al., *IFNgamma and lymphocytes prevent primary tumour development and shape tumour immunogenicity*. Nature, 2001. **410**(6832): p. 1107-11.
75. Smyth, M.J., et al., *Differential tumor surveillance by natural killer (NK) and NKT cells*. J Exp Med, 2000. **191**(4): p. 661-8.
76. Old, L.J. and E.A. Boyse, *Immunology of Experimental Tumors*. Annu Rev Med, 1964. **15**: p. 167-86.
77. Cheever, M.A., et al., *The prioritization of cancer antigens: a national cancer institute pilot project for the acceleration of translational research*. Clin Cancer Res, 2009. **15**(17): p. 5323-37.
78. Schreiber, R.D., L.J. Old, and M.J. Smyth, *Cancer immunoediting: integrating immunity's roles in cancer suppression and promotion*. Science, 2011. **331**(6024): p. 1565-70.
79. Koebel, C.M., et al., *Adaptive immunity maintains occult cancer in an equilibrium state*. Nature, 2007. **450**(7171): p. 903-7.
80. Bingle, L., N.J. Brown, and C.E. Lewis, *The role of tumour-associated macrophages in tumour progression: implications for new anticancer therapies*. J Pathol, 2002. **196**(3): p. 254-65.
81. Gentles, A.J., et al., *The prognostic landscape of genes and infiltrating immune cells across human cancers*. Nat Med, 2015. **21**(8): p. 938-945.
82. Hamanishi, J., et al., *Programmed cell death 1 ligand 1 and tumor-infiltrating CD8+ T lymphocytes are prognostic factors of human ovarian cancer*. Proc Natl Acad Sci U S A, 2007. **104**(9): p. 3360-5.
83. Lee, S.J., et al., *The clinical significance of tumor-infiltrating lymphocytes and microscopic satellites in acral melanoma in a korean population*. Ann Dermatol, 2013. **25**(1): p. 61-6.
84. Clemente, C.G., et al., *Prognostic value of tumor infiltrating lymphocytes in the vertical growth phase of primary cutaneous melanoma*. Cancer, 1996. **77**(7): p. 1303-10.
85. Clark, W.H., Jr., et al., *Model predicting survival in stage I melanoma based on tumor progression*. J Natl Cancer Inst, 1989. **81**(24): p. 1893-904.

86. Sato, E., et al., *Intraepithelial CD8+ tumor-infiltrating lymphocytes and a high CD8+/regulatory T cell ratio are associated with favorable prognosis in ovarian cancer*. Proc Natl Acad Sci U S A, 2005. **102**(51): p. 18538-43.
87. Agata, Y., et al., *Expression of the PD-1 antigen on the surface of stimulated mouse T and B lymphocytes*. Int Immunol, 1996. **8**(5): p. 765-72.
88. Day, C.L., et al., *PD-1 expression on HIV-specific T cells is associated with T-cell exhaustion and disease progression*. Nature, 2006. **443**(7109): p. 350-4.
89. Blank, C., T.F. Gajewski, and A. Mackensen, *Interaction of PD-L1 on tumor cells with PD-1 on tumor-specific T cells as a mechanism of immune evasion: implications for tumor immunotherapy*. Cancer Immunol Immunother, 2005. **54**(4): p. 307-14.
90. Gadiot, J., et al., *Overall survival and PD-L1 expression in metastasized malignant melanoma*. Cancer, 2011. **117**(10): p. 2192-201.
91. Yu, H., et al., *PD-L1 Expression in Lung Cancer*. J Thorac Oncol, 2016. **11**(7): p. 964-75.
92. Chen, B.J., et al., *PD-L1 expression is characteristic of a subset of aggressive B-cell lymphomas and virus-associated malignancies*. Clin Cancer Res, 2013. **19**(13): p. 3462-73.
93. Sheppard, K.A., et al., *PD-1 inhibits T-cell receptor induced phosphorylation of the ZAP70/CD3zeta signalosome and downstream signaling to PKCtheta*. FEBS Lett, 2004. **574**(1-3): p. 37-41.
94. Wintterle, S., et al., *Expression of the B7-related molecule B7-H1 by glioma cells: a potential mechanism of immune paralysis*. Cancer Res, 2003. **63**(21): p. 7462-7.
95. Dong, H., et al., *Tumor-associated B7-H1 promotes T-cell apoptosis: a potential mechanism of immune evasion*. Nat Med, 2002. **8**(8): p. 793-800.
96. Wherry, E.J., *T cell exhaustion*. Nat Immunol, 2011. **12**(6): p. 492-9.
97. Sun, C., R. Mezzadra, and T.N. Schumacher, *Regulation and Function of the PD-L1 Checkpoint*. Immunity, 2018. **48**(3): p. 434-452.
98. Chen, L. and X. Han, *Anti-PD-1/PD-L1 therapy of human cancer: past, present, and future*. J Clin Invest, 2015. **125**(9): p. 3384-91.
99. Abiko, K., et al., *IFN-gamma from lymphocytes induces PD-L1 expression and promotes progression of ovarian cancer*. Br J Cancer, 2015. **112**(9): p. 1501-9.
100. Sunshine, J. and J.M. Taube, *PD-1/PD-L1 inhibitors*. Curr Opin Pharmacol, 2015. **23**: p. 32-8.
101. Patel, S.P. and R. Kurzrock, *PD-L1 Expression as a Predictive Biomarker in Cancer Immunotherapy*. Mol Cancer Ther, 2015. **14**(4): p. 847-56.
102. Blank, C.U., et al., *CANCER IMMUNOLOGY. The "cancer immunogram"*. Science, 2016. **352**(6286): p. 658-60.
103. Kraft, S., et al., *PDL1 expression in desmoplastic melanoma is associated with tumor aggressiveness and progression*. J Am Acad Dermatol, 2017. **77**(3): p. 534-542.
104. Sabatier, R., et al., *Prognostic and predictive value of PDL1 expression in breast cancer*. Oncotarget, 2015. **6**(7): p. 5449-64.
105. Herbst, R.S., et al., *Predictive correlates of response to the anti-PD-L1 antibody MPDL3280A in cancer patients*. Nature, 2014. **515**(7528): p. 563-7.
106. Maleki Vareki, S., C. Garrigos, and I. Duran, *Biomarkers of response to PD-1/PD-L1 inhibition*. Crit Rev Oncol Hematol, 2017. **116**: p. 116-124.
107. Vesely, M.D. and R.D. Schreiber, *Cancer immunoediting: antigens, mechanisms, and implications to cancer immunotherapy*. Ann N Y Acad Sci, 2013. **1284**: p. 1-5.
108. Zaidi, M.R. and G. Merlino, *The two faces of interferon-gamma in cancer*. Clin Cancer Res, 2011. **17**(19): p. 6118-24.
109. Ayers, M., et al., *IFN-gamma-related mRNA profile predicts clinical response to PD-1 blockade*. J Clin Invest, 2017. **127**(8): p. 2930-2940.

110. Brahmer, J.R., et al., *Phase I study of single-agent anti-programmed death-1 (MDX-1106) in refractory solid tumors: safety, clinical activity, pharmacodynamics, and immunologic correlates*. J Clin Oncol, 2010. **28**(19): p. 3167-75.
111. Long, G.V., et al., *Nivolumab for Patients With Advanced Melanoma Treated Beyond Progression: Analysis of 2 Phase 3 Clinical Trials*. JAMA Oncol, 2017. **3**(11): p. 1511-1519.
112. Hamanishi, J., et al., *PD-1/PD-L1 blockade in cancer treatment: perspectives and issues*. Int J Clin Oncol, 2016. **21**(3): p. 462-73.
113. Patnaik, A., et al., *Phase I Study of Pembrolizumab (MK-3475; Anti-PD-1 Monoclonal Antibody) in Patients with Advanced Solid Tumors*. Clin Cancer Res, 2015. **21**(19): p. 4286-93.
114. Wong, R.M., et al., *Programmed death-1 blockade enhances expansion and functional capacity of human melanoma antigen-specific CTLs*. Int Immunol, 2007. **19**(10): p. 1223-34.
115. Brahmer, J.R., et al., *Safety and activity of anti-PD-L1 antibody in patients with advanced cancer*. N Engl J Med, 2012. **366**(26): p. 2455-65.
116. Powles, T., et al., *MPDL3280A (anti-PD-L1) treatment leads to clinical activity in metastatic bladder cancer*. Nature, 2014. **515**(7528): p. 558-62.
117. Smyth, M.J., et al., *Combination cancer immunotherapies tailored to the tumour microenvironment*. Nat Rev Clin Oncol, 2016. **13**(3): p. 143-58.
118. Melero, I., et al., *T-cell and NK-cell infiltration into solid tumors: a key limiting factor for efficacious cancer immunotherapy*. Cancer Discov, 2014. **4**(5): p. 522-6.
119. Zhang, L., et al., *Intratumoral T cells, recurrence, and survival in epithelial ovarian cancer*. N Engl J Med, 2003. **348**(3): p. 203-13.
120. Ohm, J.E., et al., *VEGF inhibits T-cell development and may contribute to tumor-induced immune suppression*. Blood, 2003. **101**(12): p. 4878-86.
121. Ziogas, A.C., et al., *VEGF directly suppresses activation of T cells from ovarian cancer patients and healthy individuals via VEGF receptor Type 2*. Int J Cancer, 2012. **130**(4): p. 857-64.
122. Gavalas, N.G., et al., *VEGF directly suppresses activation of T cells from ascites secondary to ovarian cancer via VEGF receptor type 2*. Br J Cancer, 2012. **107**(11): p. 1869-75.
123. Yang, J., J. Yan, and B. Liu, *Targeting VEGF/VEGFR to Modulate Antitumor Immunity*. Front Immunol, 2018. **9**: p. 978.
124. Manzoni, M., et al., *Immunological effects of bevacizumab-based treatment in metastatic colorectal cancer*. Oncology, 2010. **79**(3-4): p. 187-96.
125. Martino, E.C., et al., *Immune-modulating effects of bevacizumab in metastatic non-small-cell lung cancer patients*. Cell Death Discov, 2016. **2**: p. 16025.
126. Rini, B.I., et al., *Atezolizumab plus bevacizumab versus sunitinib in patients with previously untreated metastatic renal cell carcinoma (IMmotion151): a multicentre, open-label, phase 3, randomised controlled trial*. Lancet, 2019. **393**(10189): p. 2404-2415.
127. McDermott, D.F., et al., *Publisher Correction: Clinical activity and molecular correlates of response to atezolizumab alone or in combination with bevacizumab versus sunitinib in renal cell carcinoma*. Nat Med, 2018. **24**(12): p. 1941.
128. Kandalaft, L.E., K. Odunsi, and G. Coukos, *Immunotherapy in Ovarian Cancer: Are We There Yet?* J Clin Oncol, 2019. **37**(27): p. 2460-2471.
129. Zsiros, E., et al., *Immunotherapy for ovarian cancer: recent advances and perspectives*. Curr Opin Oncol, 2014. **26**(5): p. 492-500.
130. Mandai, M., et al., *Anti-PD-L1/PD-1 immune therapies in ovarian cancer: basic mechanism and future clinical application*. Int J Clin Oncol, 2016. **21**(3): p. 456-61.

131. Peng, J., et al., *Chemotherapy Induces Programmed Cell Death-Ligand 1 Overexpression via the Nuclear Factor-kappaB to Foster an Immunosuppressive Tumor Microenvironment in Ovarian Cancer*. *Cancer Res*, 2015. **75**(23): p. 5034-45.
132. Liu, J.F., et al., *A phase II trial of combination nivolumab and bevacizumab in recurrent ovarian cancer*. *Annals of Oncology*, 2018. **29**.
133. Naidoo, J., et al., *Toxicities of the anti-PD-1 and anti-PD-L1 immune checkpoint antibodies*. *Ann Oncol*, 2016. **27**(7): p. 1362.
134. Jenkins, R.W., D.A. Barbie, and K.T. Flaherty, *Mechanisms of resistance to immune checkpoint inhibitors*. *Br J Cancer*, 2018. **118**(1): p. 9-16.
135. Zhang, A.W., et al., *Interfaces of Malignant and Immunologic Clonal Dynamics in Ovarian Cancer*. *Cell*, 2018. **173**(7): p. 1755-1769 e22.
136. van Dijk, N., et al., *The Cancer Immunogram as a Framework for Personalized Immunotherapy in Urothelial Cancer*. *Eur Urol*, 2019. **75**(3): p. 435-444.
137. Yarchoan, M., A. Hopkins, and E.M. Jaffee, *Tumor Mutational Burden and Response Rate to PD-1 Inhibition*. *N Engl J Med*, 2017. **377**(25): p. 2500-2501.
138. Alexandrov, L.B., et al., *Signatures of mutational processes in human cancer*. *Nature*, 2013. **500**(7463): p. 415-21.
139. Cancer Genome Atlas Research, N., *Integrated genomic analyses of ovarian carcinoma*. *Nature*, 2011. **474**(7353): p. 609-15.
140. Gaillard, S.L., A.A. Secord, and B. Monk, *The role of immune checkpoint inhibition in the treatment of ovarian cancer*. *Gynecol Oncol Res Pract*, 2016. **3**: p. 11.
141. Webb, J.R., et al., *PD-L1 expression is associated with tumor-infiltrating T cells and favorable prognosis in high-grade serous ovarian cancer*. *Gynecol Oncol*, 2016. **141**(2): p. 293-302.
142. Binnewies, M., et al., *Understanding the tumor immune microenvironment (TIME) for effective therapy*. *Nat Med*, 2018. **24**(5): p. 541-550.
143. Joyce, J.A. and D.T. Fearon, *T cell exclusion, immune privilege, and the tumor microenvironment*. *Science*, 2015. **348**(6230): p. 74-80.
144. Chae, Y.K., et al., *Overexpression of adhesion molecules and barrier molecules is associated with differential infiltration of immune cells in non-small cell lung cancer*. *Sci Rep*, 2018. **8**(1): p. 1023.
145. Thurston, G. and J. Kitajewski, *VEGF and Delta-Notch: interacting signalling pathways in tumour angiogenesis*. *Br J Cancer*, 2008. **99**(8): p. 1204-9.
146. Martiny-Baron, G. and D. Marme, *VEGF-mediated tumour angiogenesis: a new target for cancer therapy*. *Curr Opin Biotechnol*, 1995. **6**(6): p. 675-80.
147. Huang, H., et al., *VEGF suppresses T-lymphocyte infiltration in the tumor microenvironment through inhibition of NF-kappaB-induced endothelial activation*. *FASEB J*, 2015. **29**(1): p. 227-38.
148. Vicari, A.P. and C. Caux, *Chemokines in cancer*. *Cytokine Growth Factor Rev*, 2002. **13**(2): p. 143-54.
149. Kelderman, S., et al., *Lactate dehydrogenase as a selection criterion for ipilimumab treatment in metastatic melanoma*. *Cancer Immunol Immunother*, 2014. **63**(5): p. 449-58.
150. Calcinotto, A., et al., *Modulation of microenvironment acidity reverses anergy in human and murine tumor-infiltrating T lymphocytes*. *Cancer Res*, 2012. **72**(11): p. 2746-56.
151. Alberts, B., *Molecular biology of the cell*. 4th ed. 2002, New York: Garland Science. xxxiv, 1548 p.
152. Benien, P. and A. Swami, *3D tumor models: history, advances and future perspectives*. *Future Oncol*, 2014. **10**(7): p. 1311-27.

153. Breslin, S. and L. O'Driscoll, *Three-dimensional cell culture: the missing link in drug discovery*. Drug Discov Today, 2013. **18**(5-6): p. 240-9.
154. Riffle, S. and R.S. Hegde, *Modeling tumor cell adaptations to hypoxia in multicellular tumor spheroids*. J Exp Clin Cancer Res, 2017. **36**(1): p. 102.
155. Hirt, C., et al., *"In vitro" 3D models of tumor-immune system interaction*. Adv Drug Deliv Rev, 2014. **79-80**: p. 145-54.
156. Zanoni, M., et al., *3D tumor spheroid models for in vitro therapeutic screening: a systematic approach to enhance the biological relevance of data obtained*. Sci Rep, 2016. **6**: p. 19103.
157. Duray, P.H., S.J. Hatfill, and N.R. Pellis, *Tissue culture in microgravity*. Sci Med (Phila), 1997. **4**(3): p. 46-55.
158. Andrade-Zaldivar, H., L. Santos, and A. De Leon Rodriguez, *Expansion of human hematopoietic stem cells for transplantation: trends and perspectives*. Cytotechnology, 2008. **56**(3): p. 151-60.
159. Freed, L.E., et al., *Advanced tools for tissue engineering: scaffolds, bioreactors, and signaling*. Tissue Eng, 2006. **12**(12): p. 3285-305.
160. Cowan, D.S., K.O. Hicks, and W.R. Wilson, *Multicellular membranes as an in vitro model for extravascular diffusion in tumours*. Br J Cancer Suppl, 1996. **27**: p. S28-31.
161. Elliott, N.T. and F. Yuan, *A review of three-dimensional in vitro tissue models for drug discovery and transport studies*. J Pharm Sci, 2011. **100**(1): p. 59-74.
162. Vaupel, P. and A. Mayer, *Hypoxia in cancer: significance and impact on clinical outcome*. Cancer and Metastasis Reviews, 2007. **26**(2): p. 225-239.
163. Nakayama, K., *Cellular signal transduction of the hypoxia response*. J Biochem, 2009. **146**(6): p. 757-65.
164. Chowdhury, R., et al., *Structural basis for oxygen degradation domain selectivity of the HIF prolyl hydroxylases*. Nat Commun, 2016. **7**: p. 12673.
165. Majmundar, A.J., W.J. Wong, and M.C. Simon, *Hypoxia-inducible factors and the response to hypoxic stress*. Mol Cell, 2010. **40**(2): p. 294-309.
166. Takagi, A., et al., *Three-dimensional cellular spheroid formation provides human prostate tumor cells with tissue-like features*. Anticancer Res, 2007. **27**(1A): p. 45-53.
167. Fischer, K., et al., *Inhibitory effect of tumor cell-derived lactic acid on human T cells*. Blood, 2007. **109**(9): p. 3812-3819.
168. Chang, C.H., et al., *Metabolic Competition in the Tumor Microenvironment Is a Driver of Cancer Progression*. Cell, 2015. **162**(6): p. 1229-1241.
169. *UKCCCR guidelines for the use of cell lines in cancer research*. Br J Cancer, 2000. **82**(9): p. 1495-509.
170. Flint, M.S., et al., *Restraint stress and stress hormones significantly impact T lymphocyte migration and function through specific alterations of the actin cytoskeleton*. Brain Behav Immun, 2011. **25**(6): p. 1187-96.
171. Abiko, K., et al., *PD-L1 on tumor cells is induced in ascites and promotes peritoneal dissemination of ovarian cancer through CTL dysfunction*. Clin Cancer Res, 2013. **19**(6): p. 1363-74.
172. Brignall, R., et al., *Integration of Kinase and Calcium Signaling at the Level of Chromatin Underlies Inducible Gene Activation in T Cells*. J Immunol, 2017. **199**(8): p. 2652-2667.
173. Ai, W., et al., *Optimal method to stimulate cytokine production and its use in immunotoxicity assessment*. Int J Environ Res Public Health, 2013. **10**(9): p. 3834-42.
174. Lamprecht, M.R., D.M. Sabatini, and A.E. Carpenter, *CellProfiler: free, versatile software for automated biological image analysis*. Biotechniques, 2007. **42**(1): p. 71-5.

175. McQuin, C., et al., *CellProfiler 3.0: Next-generation image processing for biology*. PLoS Biol, 2018. **16**(7): p. e2005970.
176. Carpenter, A.E., et al., *CellProfiler: image analysis software for identifying and quantifying cell phenotypes*. Genome Biol, 2006. **7**(10): p. R100.
177. Janat-Amsbury, M.M., et al., *Comparison of ID8 MOSE and VEGF-modified ID8 cell lines in an immunocompetent animal model for human ovarian cancer*. Anticancer Res, 2006. **26**(4B): p. 2785-9.
178. Bucsek, M.J., et al., *beta-Adrenergic Signaling in Mice Housed at Standard Temperatures Suppresses an Effector Phenotype in CD8(+) T Cells and Undermines Checkpoint Inhibitor Therapy*. Cancer Res, 2017. **77**(20): p. 5639-5651.
179. Workman, P., et al., *Guidelines for the welfare and use of animals in cancer research*. Br J Cancer, 2010. **102**(11): p. 1555-77.
180. Bleby, J., *Animals (Scientific Procedures) Act 1986*. Vet Rec, 1986. **119**(1): p. 22.
181. Whelan, G. and C. Trower, *Home Office consultation on changes to the Animals (Scientific Procedures) Act*. Vet Rec, 2011. **168**(25): p. 673-4.
182. Koppel, C., et al., *Optimization and validation of PD-L1 immunohistochemistry staining protocols using the antibody clone 28-8 on different staining platforms*. Mod Pathol, 2018. **31**(11): p. 1630-1644.
183. Arya, M., et al., *Basic principles of real-time quantitative PCR*. Expert Rev Mol Diagn, 2005. **5**(2): p. 209-19.
184. Nolan, T., R.E. Hands, and S.A. Bustin, *Quantification of mRNA using real-time RT-PCR*. Nat Protoc, 2006. **1**(3): p. 1559-82.
185. Walker, J.M. and R. Rapley, *Molecular biology and biotechnology*. 5th ed. 2009, Cambridge: Royal Society of Chemistry. xix, 604 p.
186. Kim, T.K. and J.H. Eberwine, *Mammalian cell transfection: the present and the future*. Anal Bioanal Chem, 2010. **397**(8): p. 3173-8.
187. Dalby, B., et al., *Advanced transfection with Lipofectamine 2000 reagent: primary neurons, siRNA, and high-throughput applications*. Methods, 2004. **33**(2): p. 95-103.
188. Adan, A., et al., *Flow cytometry: basic principles and applications*. Crit Rev Biotechnol, 2017. **37**(2): p. 163-176.
189. Wilkerson, M.J., *Principles and applications of flow cytometry and cell sorting in companion animal medicine*. Vet Clin North Am Small Anim Pract, 2012. **42**(1): p. 53-71.
190. Maggio, E.T., *Enzyme-immunoassay*. 1980, Boca Raton, Fla.: CRC Press. 295 p.
191. Crowther, J.R., *ELISA : theory and practice*. Methods in molecular biology. 1995, Totowa, N.J.: Humana Press. xi, 223 p.
192. Price, P., *Standard definitions of terms relating to mass spectrometry : A report from the committee on measurements and standards of the American society for mass spectrometry*. J Am Soc Mass Spectrom, 1991. **2**(4): p. 336-48.
193. Matthiesen, R. and J. Bunkenborg, *Introduction to mass spectrometry-based proteomics*. Methods Mol Biol, 2013. **1007**: p. 1-45.
194. Laemmli, U.K., *Cleavage of structural proteins during the assembly of the head of bacteriophage T4*. Nature, 1970. **227**(5259): p. 680-5.
195. Cole, S.W., et al., *Sympathetic nervous system regulation of the tumour microenvironment*. Nat Rev Cancer, 2015. **15**(9): p. 563-72.
196. Hara, M.R., et al., *A stress response pathway regulates DNA damage through beta2-adrenoreceptors and beta-arrestin-1*. Nature, 2011. **477**(7364): p. 349-53.
197. Lutgendorf, S.K., et al., *Social influences on clinical outcomes of patients with ovarian cancer*. J Clin Oncol, 2012. **30**(23): p. 2885-90.

198. Nilsson, M.B., et al., *Stress hormones regulate interleukin-6 expression by human ovarian carcinoma cells through a Src-dependent mechanism*. J Biol Chem, 2007. **282**(41): p. 29919-26.
199. Shahzad, M.M.K., et al., *Stress effects on FosB and interleukin-8 (IL8)-driven ovarian cancer growth and metastasis*. J Biol Chem, 2018. **293**(26): p. 10041.
200. Heidt, T., et al., *Chronic variable stress activates hematopoietic stem cells*. Nat Med, 2014. **20**(7): p. 754-758.
201. McKim, D.B., et al., *Social Stress Mobilizes Hematopoietic Stem Cells to Establish Persistent Splenic Myelopoiesis*. Cell Rep, 2018. **25**(9): p. 2552-2562 e3.
202. De Lorenzo, B.H., et al., *Sleep-deprivation reduces NK cell number and function mediated by beta-adrenergic signalling*. Psychoneuroendocrinology, 2015. **57**: p. 134-43.
203. Takenaka, M.C., et al., *Norepinephrine Controls Effector T Cell Differentiation through beta2-Adrenergic Receptor-Mediated Inhibition of NF-kappaB and AP-1 in Dendritic Cells*. J Immunol, 2016. **196**(2): p. 637-44.
204. Estrada, L.D., D. Agac, and J.D. Farrar, *Sympathetic neural signaling via the beta2-adrenergic receptor suppresses T-cell receptor-mediated human and mouse CD8(+) T-cell effector function*. Eur J Immunol, 2016. **46**(8): p. 1948-58.
205. Neubig, R.R., et al., *International Union of Pharmacology Committee on Receptor Nomenclature and Drug Classification. XXXVIII. Update on terms and symbols in quantitative pharmacology*. Pharmacol Rev, 2003. **55**(4): p. 597-606.
206. Chen, J., et al., *Regulation of PD-L1: a novel role of pro-survival signalling in cancer*. Ann Oncol, 2016. **27**(3): p. 409-16.
207. Swanson, M.A., W.T. Lee, and V.M. Sanders, *IFN-gamma production by Th1 cells generated from naive CD4+ T cells exposed to norepinephrine*. J Immunol, 2001. **166**(1): p. 232-40.
208. Torres, K.C., et al., *Norepinephrine, dopamine and dexamethasone modulate discrete leukocyte subpopulations and cytokine profiles from human PBMC*. J Neuroimmunol, 2005. **166**(1-2): p. 144-57.
209. Deighton, N.M., et al., *Regulation of adrenergic receptor number following chronic noradrenaline infusion in the rabbit*. Naunyn Schmiedebergs Arch Pharmacol, 1988. **338**(5): p. 517-22.
210. Schmitz, D., et al., *beta-Adrenergic blockade during systemic inflammation: impact on cellular immune functions and survival in a murine model of sepsis*. Resuscitation, 2007. **72**(2): p. 286-94.
211. Chen, G., et al., *Exosomal PD-L1 contributes to immunosuppression and is associated with anti-PD-1 response*. Nature, 2018. **560**(7718): p. 382-386.
212. Pinto, M.P., et al., *Patient inflammatory status and CD4+/CD8+ intraepithelial tumor lymphocyte infiltration are predictors of outcomes in high-grade serous ovarian cancer*. Gynecol Oncol, 2018. **151**(1): p. 10-17.
213. Fujita, K., et al., *Prolonged disease-free period in patients with advanced epithelial ovarian cancer after adoptive transfer of tumor-infiltrating lymphocytes*. Clin Cancer Res, 1995. **1**(5): p. 501-7.
214. Strasner, A. and M. Karin, *Immune infiltration and prostate cancer*. Frontiers in Oncology, 2015. **5**.
215. Nakakubo, Y., et al., *Clinical significance of immune cell infiltration within gallbladder cancer*. British Journal of Cancer, 2003. **89**(9): p. 1736-1742.
216. Menegaz, R.A., et al., *Peri- and intratumoral T and B lymphocytic infiltration in breast cancer*. European Journal of Gynaecological Oncology, 2008. **29**(4): p. 321-326.

217. Kawai, O., et al., *Predominant infiltration of macrophages and CD8(+) T cells in cancer nests is a significant predictor of survival in stage IV nonsmall cell lung cancer*. *Cancer*, 2008. **113**(6): p. 1387-1395.
218. Fridman, W.H., et al., *Immune infiltration in human cancer: prognostic significance and disease control*. *Curr Top Microbiol Immunol*, 2011. **344**: p. 1-24.
219. Sceneay, J., et al., *Primary tumor hypoxia recruits CD11b+/Ly6Cmed/Ly6G+ immune suppressor cells and compromises NK cell cytotoxicity in the premetastatic niche*. *Cancer Res*, 2012. **72**(16): p. 3906-11.
220. Disis, M.L., *Immune regulation of cancer*. *J Clin Oncol*, 2010. **28**(29): p. 4531-8.
221. Bauman, G.P., et al., *Induction of cAMP-dependent protein kinase (PKA) activity in T cells after stimulation of the prostaglandin E2 or the beta-adrenergic receptors: relationship between PKA activity and inhibition of anti-CD3 monoclonal antibody-induced T cell proliferation*. *Cell Immunol*, 1994. **158**(1): p. 182-94.
222. Kohm, A.P. and V.M. Sanders, *Norepinephrine and beta 2-adrenergic receptor stimulation regulate CD4+ T and B lymphocyte function in vitro and in vivo*. *Pharmacol Rev*, 2001. **53**(4): p. 487-525.
223. Kioi, M., et al., *Inhibition of vasculogenesis, but not angiogenesis, prevents the recurrence of glioblastoma after irradiation in mice*. *J Clin Invest*, 2010. **120**(3): p. 694-705.
224. Pennacchietti, S., et al., *Hypoxia promotes invasive growth by transcriptional activation of the met protooncogene*. *Cancer Cell*, 2003. **3**(4): p. 347-61.
225. Chang, Q., et al., *Hypoxia predicts aggressive growth and spontaneous metastasis formation from orthotopically grown primary xenografts of human pancreatic cancer*. *Cancer Res*, 2011. **71**(8): p. 3110-20.
226. Wilson, W.R. and M.P. Hay, *Targeting hypoxia in cancer therapy*. *Nat Rev Cancer*, 2011. **11**(6): p. 393-410.
227. Hu, H.T., et al., *HIF-1alpha links beta-adrenoceptor agonists and pancreatic cancer cells under normoxic condition*. *Acta Pharmacol Sin*, 2010. **31**(1): p. 102-10.
228. Shan, T., et al., *beta2-AR-HIF-1alpha: a novel regulatory axis for stress-induced pancreatic tumor growth and angiogenesis*. *Curr Mol Med*, 2013. **13**(6): p. 1023-34.
229. Ferruz, J., et al., *Release of norepinephrine from the rat ovary: local modulation of gonadotropins*. *Biol Reprod*, 1991. **45**(4): p. 592-7.
230. Mulholland, T., et al., *Drug screening of biopsy-derived spheroids using a self-generated microfluidic concentration gradient*. *Sci Rep*, 2018. **8**(1): p. 14672.
231. Foye, W.O., T.L. Lemke, and D.A. Williams, *Foye's principles of medicinal chemistry*. 7th ed. 2013, Philadelphia: Wolters Kluwer Health/Lippincott Williams & Wilkins. xviii, 1500 p. (some color).
232. Masson, N. and P.J. Ratcliffe, *Hypoxia signaling pathways in cancer metabolism: the importance of co-selecting interconnected physiological pathways*. *Cancer Metab*, 2014. **2**(1): p. 3.
233. Semenza, G.L., *HIF-1: upstream and downstream of cancer metabolism*. *Curr Opin Genet Dev*, 2010. **20**(1): p. 51-6.
234. Iyer, N.V., et al., *Cellular and developmental control of O2 homeostasis by hypoxia-inducible factor 1 alpha*. *Genes Dev*, 1998. **12**(2): p. 149-62.
235. UniProtKB - P52480 (KPYM_MOUSE). Available from: <https://www.oncologica.com/immunofocus/>.
236. Israelsen, W.J. and M.G. Vander Heiden, *Pyruvate kinase: Function, regulation and role in cancer*. *Semin Cell Dev Biol*, 2015. **43**: p. 43-51.
237. Gao, L., et al., *Induction of the glucose-6-phosphate dehydrogenase gene expression by chronic hypoxia in PC12 cells*. *FEBS Lett*, 2004. **569**(1-3): p. 256-60.

238. Langbein, S., et al., *Metastasis is promoted by a bioenergetic switch: new targets for progressive renal cell cancer*. *Int J Cancer*, 2008. **122**(11): p. 2422-8.
239. Patra, K.C. and N. Hay, *The pentose phosphate pathway and cancer*. *Trends Biochem Sci*, 2014. **39**(8): p. 347-54.
240. Flaherty, R.L., et al., *Glucocorticoids induce production of reactive oxygen species/reactive nitrogen species and DNA damage through an iNOS mediated pathway in breast cancer*. *Breast Cancer Res*, 2017. **19**(1): p. 35.
241. Iizuka, K. and Y. Horikawa, *ChREBP: a glucose-activated transcription factor involved in the development of metabolic syndrome*. *Endocr J*, 2008. **55**(4): p. 617-24.
242. Trepel, J., et al., *Targeting the dynamic HSP90 complex in cancer*. *Nat Rev Cancer*, 2010. **10**(8): p. 537-49.
243. Wegele, H., L. Muller, and J. Buchner, *Hsp70 and Hsp90--a relay team for protein folding*. *Rev Physiol Biochem Pharmacol*, 2004. **151**: p. 1-44.
244. Baker, J.D., et al., *Hsp90 Heterocomplexes Regulate Steroid Hormone Receptors: From Stress Response to Psychiatric Disease*. *Int J Mol Sci*, 2018. **20**(1).
245. Dreyfuss, G., M.S. Swanson, and S. Pinol-Roma, *Heterogeneous nuclear ribonucleoprotein particles and the pathway of mRNA formation*. *Trends Biochem Sci*, 1988. **13**(3): p. 86-91.
246. Loh, T.J., et al., *CD44 alternative splicing and hnRNP A1 expression are associated with the metastasis of breast cancer*. *Oncol Rep*, 2015. **34**(3): p. 1231-8.
247. Jean-Philippe, J., S. Paz, and M. Caputi, *hnRNP A1: the Swiss army knife of gene expression*. *Int J Mol Sci*, 2013. **14**(9): p. 18999-9024.
248. Carpenter, B., et al., *The roles of heterogeneous nuclear ribonucleoproteins in tumour development and progression*. *Biochim Biophys Acta*, 2006. **1765**(2): p. 85-100.
249. Griffin, M.E., et al., *Post-transcriptional regulation of glucose transporter-1 by an AU-rich element in the 3'UTR and by hnRNP A2*. *Biochem Biophys Res Commun*, 2004. **318**(4): p. 977-82.
250. Tauler, J. and J.L. Mulshine, *Lung cancer and inflammation: interaction of chemokines and hnRNPs*. *Curr Opin Pharmacol*, 2009. **9**(4): p. 384-8.
251. Mhaweche-Fauceglia, P., et al., *Intraepithelial T cells and tumor-associated macrophages in ovarian cancer patients*. *Cancer Immun*, 2013. **13**: p. 1.
252. Arias-Pulido, H., et al., *The combined presence of CD20 + B cells and PD-L1 + tumor-infiltrating lymphocytes in inflammatory breast cancer is prognostic of improved patient outcome*. *Breast Cancer Res Treat*, 2018. **171**(2): p. 273-282.
253. Cole, S.W. and A.K. Sood, *Molecular pathways: beta-adrenergic signaling in cancer*. *Clin Cancer Res*, 2012. **18**(5): p. 1201-6.
254. Phadke, S. and G. Clamon, *Beta blockade as adjunctive breast cancer therapy: A review*. *Crit Rev Oncol Hematol*, 2019. **138**: p. 173-177.
255. Jankovic, B.D., *Neuroimmunomodulation. From phenomenology to molecular evidence*. *Ann N Y Acad Sci*, 1994. **741**: p. 1-38.
256. De Santo, C., et al., *Nitroaspirin corrects immune dysfunction in tumor-bearing hosts and promotes tumor eradication by cancer vaccination*. *Proc Natl Acad Sci U S A*, 2005. **102**(11): p. 4185-90.
257. Chung, J.F., S.J. Lee, and A.K. Sood, *Immunological and pleiotropic effects of individual beta-blockers and their relevance in cancer therapies*. *Expert Opin Investig Drugs*, 2016. **25**(5): p. 501-5.
258. Haldar, R. and S. Ben-Eliyahu, *Reducing the risk of post-surgical cancer recurrence: a perioperative anti-inflammatory anti-stress approach*. *Future Oncol*, 2018. **14**(11): p. 1017-1021.

259. Greenfeld, K., et al., *Immune suppression while awaiting surgery and following it: dissociations between plasma cytokine levels, their induced production, and NK cell cytotoxicity*. Brain Behav Immun, 2007. **21**(4): p. 503-13.
260. Benish, M., et al., *Perioperative use of beta-blockers and COX-2 inhibitors may improve immune competence and reduce the risk of tumor metastasis*. Ann Surg Oncol, 2008. **15**(7): p. 2042-52.
261. Haldar, R., et al., *Perioperative inhibition of beta-adrenergic and COX2 signaling in a clinical trial in breast cancer patients improves tumor Ki-67 expression, serum cytokine levels, and PBMCs transcriptome*. Brain Behav Immun, 2018.
262. Ricon, I., et al., *Perioperative biobehavioral interventions to prevent cancer recurrence through combined inhibition of beta-adrenergic and cyclooxygenase 2 signaling*. Cancer, 2019. **125**(1): p. 45-56.
263. Gader, A.M., *The effects of beta adrenergic blockade on the responses of leucocyte counts to intravenous epinephrine in man*. Scand J Haematol, 1974. **13**(1): p. 11-6.
264. Ernstrom, U. and G. Sandberg, *Effects of adrenergic alpha- and beta-receptor stimulation on the release of lymphocytes and granulocytes from the spleen*. Scand J Haematol, 1973. **11**(4): p. 275-86.
265. Rogausch, H., et al., *Norepinephrine stimulates lymphoid cell mobilization from the perfused rat spleen via beta-adrenergic receptors*. Am J Physiol, 1999. **276**(3): p. R724-30.
266. Carlson, S.L., S. Fox, and K.M. Abell, *Catecholamine modulation of lymphocyte homing to lymphoid tissues*. Brain Behav Immun, 1997. **11**(4): p. 307-20.
267. Wang, L.P., et al., *Norepinephrine attenuates CXCR4 expression and the corresponding invasion of MDA-MB-231 breast cancer cells via beta2-adrenergic receptors*. Eur Rev Med Pharmacol Sci, 2015. **19**(7): p. 1170-81.
268. Datta, D., et al., *Ras-induced modulation of CXCL10 and its receptor splice variant CXCR3-B in MDA-MB-435 and MCF-7 cells: relevance for the development of human breast cancer*. Cancer Res, 2006. **66**(19): p. 9509-18.
269. Lo, B.K., et al., *CXCR3/ligands are significantly involved in the tumorigenesis of basal cell carcinomas*. Am J Pathol, 2010. **176**(5): p. 2435-46.
270. Maru, S.V., et al., *Chemokine production and chemokine receptor expression by human glioma cells: role of CXCL10 in tumour cell proliferation*. J Neuroimmunol, 2008. **199**(1-2): p. 35-45.
271. Liu, M., et al., *Targeting the IDO1 pathway in cancer: from bench to bedside*. Journal of Hematology & Oncology, 2018. **11**.
272. Avraham, R., et al., *Synergism between immunostimulation and prevention of surgery-induced immune suppression: an approach to reduce post-operative tumor progression*. Brain Behav Immun, 2010. **24**(6): p. 952-8.
273. Lutgendorf, S.K., et al., *Social isolation is associated with elevated tumor norepinephrine in ovarian carcinoma patients*. Brain Behav Immun, 2011. **25**(2): p. 250-5.
274. Angell, H. and J. Galon, *From the immune contexture to the Immunoscore: the role of prognostic and predictive immune markers in cancer*. Curr Opin Immunol, 2013. **25**(2): p. 261-7.
275. Iga, N., et al., *Variable indoleamine 2,3-dioxygenase expression in acral/mucosal melanoma and its possible link to immunotherapy*. Cancer Sci, 2019.
276. Khouri, C., et al., *Peripheral vasoconstriction induced by β -adrenoceptor blockers: a systematic review and a network meta-analysis*. Br J Clin Pharmacol, 2016. **82**(2): p. 549-60.
277. Viola, A., et al., *The pros and cons of chemokines in tumor immunology*. Trends Immunol, 2012. **33**(10): p. 496-504.

278. O'Hanlon, D.M., et al., *Soluble adhesion molecules (E-selectin, ICAM-1 and VCAM-1) in breast carcinoma*. Eur J Cancer, 2002. **38**(17): p. 2252-7.
279. Acerbi, I., et al., *Human breast cancer invasion and aggression correlates with ECM stiffening and immune cell infiltration*. Integr Biol (Camb), 2015. **7**(10): p. 1120-34.
280. Villalba, M., et al., *From tumor cell metabolism to tumor immune escape*. Int J Biochem Cell Biol, 2013. **45**(1): p. 106-13.
281. Freedman, L.P., et al., *Reproducibility: changing the policies and culture of cell line authentication*. Nat Methods, 2015. **12**(6): p. 493-7.
282. Hughes, P., et al., *The costs of using unauthenticated, over-passaged cell lines: how much more data do we need?* Biotechniques, 2007. **43**(5): p. 575, 577-8, 581-2 passim.
283. Korch, C., et al., *DNA profiling analysis of endometrial and ovarian cell lines reveals misidentification, redundancy and contamination*. Gynecol Oncol, 2012. **127**(1): p. 241-8.
284. Roby, K.F., et al., *Development of a syngeneic mouse model for events related to ovarian cancer*. Carcinogenesis, 2000. **21**(4): p. 585-91.
285. Goodspeed, A., et al., *Tumor-Derived Cell Lines as Molecular Models of Cancer Pharmacogenomics*. Mol Cancer Res, 2016. **14**(1): p. 3-13.
286. Domcke, S., et al., *Evaluating cell lines as tumour models by comparison of genomic profiles*. Nat Commun, 2013. **4**: p. 2126.
287. Kim, J.B., *Three-dimensional tissue culture models in cancer biology*. Semin Cancer Biol, 2005. **15**(5): p. 365-77.
288. Lee, J.M., et al., *A three-dimensional microenvironment alters protein expression and chemosensitivity of epithelial ovarian cancer cells in vitro*. Lab Invest, 2013. **93**(5): p. 528-42.
289. Cesarz, Z. and K. Tamama, *Spheroid Culture of Mesenchymal Stem Cells*. Stem Cells Int, 2016. **2016**: p. 9176357.
290. Ivanov, D.P. and A.M. Grabowska, *Spheroid arrays for high-throughput single-cell analysis of spatial patterns and biomarker expression in 3D*. Sci Rep, 2017. **7**: p. 41160.
291. Kerbel, R.S., *What is the optimal rodent model for anti-tumor drug testing?* Cancer Metastasis Rev, 1998. **17**(3): p. 301-4.
292. Talmadge, J.E., et al., *Murine models to evaluate novel and conventional therapeutic strategies for cancer*. Am J Pathol, 2007. **170**(3): p. 793-804.
293. Thaker, P.H., S.K. Lutgendorf, and A.K. Sood, *The neuroendocrine impact of chronic stress on cancer*. Cell Cycle, 2007. **6**(4): p. 430-3.
294. Jaggi, A.S., et al., *A review on animal models for screening potential anti-stress agents*. Neurol Sci, 2011. **32**(6): p. 993-1005.
295. Gesi, C., et al., *Post-traumatic Stress Disorder in patients with ovarian cancer*. Int Rev Psychiatry, 2017. **29**(5): p. 403-408.
296. Norton, T.R., et al., *Ovarian cancer patients' psychological distress: the role of physical impairment, perceived unsupportive family and friend behaviors, perceived control, and self-esteem*. Health Psychol, 2005. **24**(2): p. 143-52.